Frequency-explicit a posteriori error estimates for finite element discretizations of Maxwell's equations

Théophile Chaumont-Frelet, Patrick Vega

FREQUENCY-EXPLICIT A POSTERIORI ERROR ESTIMATES FOR FINITE ELEMENT DISCRETIZATIONS OF MAXWELL'S EQUATIONS

T. CHAUMONT-FRELET[⋆,†] AND P. VEGA[⋆,†]

Abstract. We consider residual-based *a posteriori* error estimators for Galerkin-type discretizations of time-harmonic Maxwell's equations. We focus on configurations where the frequency is high, or close to a resonance frequency, and derive reliability and efficiency estimates. In contrast to previous related works, our estimates are frequency-explicit. In particular, our key contribution is to show that even if the constants appearing in the reliability and efficiency estimates may blow up on coarse meshes, they become independent of the frequency for sufficiently refined meshes. Such results were previously known for the Helmholtz equation describing scalar wave propagation problems and we show that they naturally extend, at the price of many technicalities in the proofs, to Maxwell's equations. Our mathematical analysis is performed in the 3D case, and covers conforming Nédélec discretizations of the first and second family, as well as first-order (and hybridizable) discontinuous Galerkin schemes. We also present numerical experiments in the 2D case, where Maxwell's equations are discretized with Nédélec elements of the first family. These illustrating examples perfectly fit our key theoretical findings, and suggest that our estimates are sharp.

Key words. A posteriori error estimates, Discontinuous Galerkin methods, Finite element methods, High-frequency problems, Maxwell's equations.

1. Introduction

Maxwell's equations constitute the central model of electrodynamics [27]. They are ubiquitously employed to describe the propagation of electromagnetic fields, and encompass a wide range of applications, including radar imaging [19], telecommunications [40], and nanophotonics [25], just to cite a few. In realistic geometries, analytical solutions to Maxwell's equations are out of reach, which motivates the development of numerical schemes to compute approximate solutions. While several approaches, such as finite differences [44] or boundary elements [5], are available for the problem under consideration, we focus on finite element methods in this work [33]. The latter are especially suited in the case of heterogeneous media with complex geometries, due to the flexibility of unstructured meshes.

Current computer hardware enables the realization of three dimensional simulations that are of practical interest, but the associate computational costs are still important regarding power consumption and simulation time. As a result, not only do numerical schemes need to be accurate and robust, but they also have to be as efficient as possible. In the context of finite element methods, an attractive idea to limit the computational cost is to adapt the mesh size and/or the polynomial degree of the basis functions only locally in the areas of the domain where the solution exhibits a complicated behavior.

These local refinements may be carried out by an iterative refinement process that is driven by *a posteriori* error estimators. Besides, error estimators can also be employed to quantitatively estimate the discretization error, which enable practitioners to decide whether the numerical solution is sufficiently accurate for the application purposes. As a result, *a posteriori* error estimators have attracted an increasing attention over the last decades. We refer the reader to [2, 17, 42], and the references therein.

Early works on *a posteriori* error estimation have focused on scalar coercive problems [2, 42]. It turns out that there are two key properties an *a posteriori* estimator should satisfy. On the

[⋆]Inria, 2004 Route des Lucioles, 06902 Valbonne, France

[†]Laboratoire J.A. Dieudonné, Parc Valrose, 28 Avenue Valrose, 06108 Nice Cedex 02, 06000 Nice, France

one hand, "reliability" states that the estimator is an upper bound to the discretization error, i.e., there exists a constant $C_{\rm rel}$ such that

$$\|\!|e|\!\|_\Omega \leq C_{\rm rel}\eta \tag{1.1a}$$

where $\|\!|e|\!\|_\Omega$ is a measure of the error in the whole computational domain. On the other hand, "efficiency" refers to the fact that the estimator associated with each element K of the mesh is a lower bound for the error measured in a small region around K. Specifically, there exists a constant $C_{\rm eff}$ such that

$$\eta_K \leq C_{\rm eff}\|\!|e|\!\|_{\widetilde{K}} + \mathrm{osc}_{\mathcal{T}_{K,h}}, \tag{1.1b}$$

where $\|\!|e|\!\|_{\widetilde{K}}$ is a measure of the error in a small area $\widetilde{K} \supset K$, and $\mathrm{osc}_{\mathcal{T}_{K,h}}$ is a "data oscillation" term linked to the right-hand side (see Section 2.8).

In the context of scalar elliptic problems with constant coefficients, $C_{\rm rel}$ and $C_{\rm eff}$ only depend on the "shape-regularity" parameter of the discretization mesh (see Section 2.4 below). These results were subsequently extended to scalar time-harmonic wave propagation problems [11, 21, 41]. It is now well-known that in contrast to the elliptic case, the constants $C_{\rm rel}$ and $C_{\rm eff}$ not only depend on the shape-regularity parameter, but also on the frequency. Specifically, for a fixed mesh, the estimates of (1.1) deteriorate when the frequency increases.

Here, we focus on time-harmonic Maxwell's equations set in a Lipschitz polyhedral domain $\Omega \subset \mathbb{R}^3$. Namely, for a fixed frequency $\omega > 0$, and a given current density $\boldsymbol{J} : \Omega \to \mathbb{C}^3$, the (unknown) electric field $\boldsymbol{E} : \Omega \to \mathbb{C}^3$ satisfies

$$\left\{ \begin{array}{rcll} -\omega^2\boldsymbol{\varepsilon}\boldsymbol{E} + \boldsymbol{\nabla}\times(\boldsymbol{\mu}^{-1}\boldsymbol{\nabla}\times\boldsymbol{E}) &=& i\omega\boldsymbol{J} & \text{in } \Omega, \\ \boldsymbol{E}\times\boldsymbol{n} &=& \boldsymbol{o} & \text{on } \partial\Omega, \end{array} \right. \tag{1.2}$$

where $\partial\Omega$ is the boundary of Ω, and $\boldsymbol{n}$ is the outward normal unit vector to $\partial\Omega$. As we explain in detail in Section 2.1, the complex tensor-valued coefficients $\boldsymbol{\varepsilon}$ and $\boldsymbol{\mu}$ represent the electromagnetic properties of the materials contained in Ω. Notice than since $\boldsymbol{\varepsilon}$ and $\boldsymbol{\mu}$ are allowed to take complex values, our model problem (1.2) encompass a large number of scenarios, including the presence of conductive materials, as well as perfectly matched layers [6, 7, 33], that approximate a radiation condition in the context of scattering problems (see Remark 2.1).

Several works deal with *a posteriori* error estimation for Galerkin discretizations of (1.2), including reliability and efficiency proofs [4, 32, 37], as well as convergence analysis of adaptive strategies [45]. However, to the best of our knowledge, these results are not "frequency-explicit", in the sense that the reliability and efficiency constants implicitly depend on the frequency. As shown for instance in [11], the reliability constant may be surprisingly large in some cases, leading to important underestimation of the error (we also refer the reader to the numerical experiments presented in Section 5). This is especially problematic when the estimator is used as a stopping criterion. On the other hand, the convergence speed of adaptive schemes also depends on this constants. As a result, it is of interest to estimate the size of these constants, and to identify mesh sizes for which the estimator can be trusted.

In this work, we analyze the efficiency and reliability of residual estimators for time-harmonic Maxwell's equations (1.2) discretized with Nédélec finite elements and first-order discontinuous Galerkin (DG) methods. In particular, we provide a thorough inspection of the behaviour of the efficiency and reliability constants when the frequency is large and/or close to a resonance frequency. Our key contributions are twofold. On the one hand, we show that the efficiency constant is bounded independently of the frequency as soon as the number of degrees of freedom (dofs) per wavelength is bounded from below. On the other hand, we establish that the reliability constant may be bounded independently of the frequency, assuming the mesh is sufficiently refined, or the discretization order is sufficiently large. Specifically, for Nédélec discretizations, our findings are summarized by the estimates

$$\omega\|\boldsymbol{E}-\boldsymbol{E}_h\|_{\boldsymbol{\varepsilon},\Omega} + \|\boldsymbol{\nabla}\times(\boldsymbol{E}-\boldsymbol{E}_h)\|_{\boldsymbol{\mu}^{-1},\Omega} \leq C\,(1+\gamma_{\rm ba,E})\,\eta, \tag{1.3a}$$

and

$$\eta_K \leq C\left(1+\frac{\omega h_K}{c_{\min,\widetilde{K}}}\right)\left(\omega\|\boldsymbol{E}-\boldsymbol{E}_h\|_{\boldsymbol{\varepsilon},\widetilde{K}}+\|\boldsymbol{\nabla}\times(\boldsymbol{E}-\boldsymbol{E}_h)\|_{\boldsymbol{\mu}^{-1},\widetilde{K}}\right)+\operatorname{osc}_{\mathcal{T}_{K,h}}, \tag{1.3b}$$

where h_K is the diameter of the element K, $\boldsymbol{E}$ and $\boldsymbol{E}_h$ are the solution to (1.2) and its discrete approximation, $c_{\min,\widetilde{K}}$ is the minimum wavespeed in the patch around K, and $\gamma_{\mathrm{ba,E}}$ is the so-called "approximation factor" that measures the approximation properties of the finite element space, and that is properly introduced in Section 2.11 below. We refer the reader to Theorems 3.4 and 3.7. For first-order discontinuous Galerkin discretizations, we derive in Theorems 4.5 and 4.8 estimates similar to (1.3), but including both the error on the electric field $\boldsymbol{E}$, and on the magnetic field $\boldsymbol{H}$.

In (1.3), the frequency appears in the reliability and efficiency constants through the terms $\gamma_{\mathrm{ba,E}}$ and $\omega h_K/c_{\min,\widetilde{K}}$. On the one hand, the approximation factor $\gamma_{\mathrm{ba,E}}$ is now standardly used in the *a posteriori* error analysis of the Helmholtz equation, and we refer the reader to [11, 21, 41] where the notation σ stands for the approximation factor, as well as in the *a priori* error analysis of Helmholtz problems [13, 30] and Maxwell's equations [31, 38], where the symbol η is employed. In general, it is complicated to derive fully-explicit estimates for the approximation factor [11]. However, at least in the case of scalar wave propagation problems, qualitative upper bounds are available for several configurations of interest [12, 13, 30]. The analysis of the approximation factor for Maxwell's equations is very recent, so that less results are currently available [31, 38]. We also provide novel estimates in Appendix A.

On the other hand, since $\lambda_K := c_{\min,\widetilde{K}}/(2\pi\omega)$ denotes the minimal wavelength in a neighborhood of K, $(\omega h_K/c_{\min,\widetilde{K}})^{-1} \simeq \lambda_K/h_K$ is a measure of the number of dofs per wavelength, locally around K. In particular, the condition $\omega h_K/c_{\min,\widetilde{K}} \leq C$ means that there are "sufficiently many" dofs per wavelength. It is thus natural for this term to appear in (1.3). In addition, since it is required to have a sufficient number of dofs per wavelength for approximability reasons, it is expected that $\omega h_K/c_{\min,\widetilde{K}}$ is small in scenarios of interest.

Our main findings are almost identical to recently established results concerning scalar wave propagation problems modeled by the Helmholtz equation [11, 21, 41]. As a result, they appear as a natural extension of now well-established results for scalar wave propagation problems to Maxwell's equations. However, while the proofs are carried out in the same spirit, important complications arise due to the "$\boldsymbol{\mathcal{H}}(\mathbf{curl})$ context", justifying the present work.

The remainder of this work is organized as follow. Section 2 presents the model problem we consider, and gather notations as well as key preliminary results. In Section 3 we analyze the Nédélec discretization of the second-order variational formulation (1.2), while the analysis of first-order discontinuous Galerkin methods is presented in Section 4. We report numerical experiments that illustrate our key findings in Section 5, and draw our conclusions in Section 6. In Appendix A, we provide an upper bound for the approximation factor in the case of a smooth domain with constant real-valued coefficients, while in Appendix B, we revisit standard gradient extraction results which we believe, is of independent interest.

2. Settings

Here, we review key notations and preliminary results.

2.1. Domain and coefficients.

We consider Maxwell's equations (1.2) in a Lipschitz polyhedral domain $\Omega \subset \mathbb{R}^3$. We denote by $\ell_\Omega := \sup_{\boldsymbol{x},\boldsymbol{y}\in\Omega}|\boldsymbol{x}-\boldsymbol{y}|$ the diameter of Ω.

The electromagnetic properties of the materials contained inside Ω are described by two symmetric tensor-valued functions $\boldsymbol{\varepsilon},\boldsymbol{\mu} : \Omega \to \mathcal{S}(\mathbb{C}^3)$. For the sake of simplicity, we assume that we can partition Ω into a set $\mathscr{P}$ of non-overlapping polyhedral subdomains P such that $\boldsymbol{\varepsilon}|_P$ and $\boldsymbol{\mu}|_P$ are constant for all $P \in \mathscr{P}$. The short-hand notations $\boldsymbol{\zeta} := \boldsymbol{\varepsilon}^{-1}$ and $\boldsymbol{\chi} := \boldsymbol{\mu}^{-1}$ will also be useful. Notice that the above tensor fields are symmetric, but not self-adjoint.

If $\boldsymbol{\phi} \in \{\boldsymbol{\varepsilon}, \boldsymbol{\mu}, \boldsymbol{\zeta}, \boldsymbol{\chi}\}$ is any of the aforementioned tensor fields, we introduce the notations

$$\phi_{\min}(\boldsymbol{x}) := \min_{\substack{\boldsymbol{u}\in\mathbb{C}^3 \\ |\boldsymbol{u}|=1}} \operatorname{Re} \boldsymbol{\phi}(\boldsymbol{x})\boldsymbol{u}\cdot\overline{\boldsymbol{u}}, \qquad \phi_{\max}(\boldsymbol{x}) := \max_{\substack{\boldsymbol{u}\in\mathbb{C}^3 \\ |\boldsymbol{u}|=1}} \max_{\substack{\boldsymbol{v}\in\mathbb{C}^3 \\ |\boldsymbol{v}|=1}} \operatorname{Re} \boldsymbol{\phi}(\boldsymbol{x})\boldsymbol{u}\cdot\overline{\boldsymbol{v}},$$

as well as

$$\phi_{D,\min} := \operatorname*{ess\,inf}_{\boldsymbol{x}\in D} \phi_{\min}(\boldsymbol{x}), \qquad \phi_{D,\max} := \operatorname*{ess\,sup}_{\boldsymbol{x}\in D} \phi_{\max}(\boldsymbol{x})$$

for any open set $D \subset \Omega$. Additionally, we assume that $\phi_{\Omega,\min} > 0$.

Remark 2.1 (Conductive materials and perfectly matched layers)**.** *The coefficients $\boldsymbol{\varepsilon}$ and $\boldsymbol{\mu}$ are usually meant to represent the electric permittivity and the magnetic permeability of the materials contained inside the computational domain Ω (see, e.g., §4.4 and §6.4 of* [27]*). In this case, these tensors are real-valued. As mathematical convenience, we allow complex-valued tensors to treat additional physical effects in a unified framework.*

Since the frequency is fixed, we can for instance handle a material with (real-valued) permittivity $\widetilde{\boldsymbol{\varepsilon}}$, permeability $\widetilde{\boldsymbol{\mu}}$ and conductivity $\widetilde{\boldsymbol{\sigma}}$, by setting $\boldsymbol{\varepsilon} := \widetilde{\boldsymbol{\varepsilon}} - (1/i\omega)\widetilde{\boldsymbol{\sigma}}$ and $\boldsymbol{\mu} := \widetilde{\boldsymbol{\mu}}$, as done in [14] *for instance. One readily sees that the proposed framework covers this scenario.*

Another situation of importance is the case of perfectly matched layers (PML), that are widely employed to mimic the effect of Siver-Müller's radiation condition in unbounded media. Considering for the sake of simplicity the Cartesian PML approach [6, 7, 33]*, the physical coefficients $\widetilde{\boldsymbol{\varepsilon}}$ and $\widetilde{\boldsymbol{\mu}}$ are modified as follows. Assuming the region of interest Ω_0 is contained in the cube $(-L, L)^3$, the Cartesian PML approach consists in selecting a largest computational domain $\Omega_0 \subset (-L, L)^3 \subset \Omega$, and for $\boldsymbol{x} \in \Omega$ defining*

$$\boldsymbol{\varepsilon} := \boldsymbol{B}^{-1}\widetilde{\boldsymbol{\varepsilon}}\boldsymbol{A}^{-1} \qquad \text{and} \qquad \boldsymbol{\mu} := \boldsymbol{B}^{-1}\widetilde{\boldsymbol{\mu}}\boldsymbol{A}^{-1},$$

where $\boldsymbol{A}$ and $\boldsymbol{B}$ are defined as

$$\boldsymbol{A} := \begin{pmatrix} \frac{1}{d_2 d_3} & 0 & 0 \\ 0 & \frac{1}{d_1 d_3} & 0 \\ 0 & 0 & \frac{1}{d_1 d_2} \end{pmatrix} \qquad \text{and} \qquad \boldsymbol{B} := \begin{pmatrix} d_1 & 0 & 0 \\ 0 & d_2 & 0 \\ 0 & 0 & d_3 \end{pmatrix},$$

with $d_j(\boldsymbol{x}) := 1 - \sigma_j(\boldsymbol{x}_j)/(i\omega)$, $\sigma_j(\boldsymbol{x}_j) = 0$ for $\boldsymbol{x}_j \in (-L, L)$ and $\sigma_j(\boldsymbol{x}_j) > 0$ if $|\boldsymbol{x}_j| > L$. Assuming for the sake of simplicity that the physical coefficients are transverse isotropic (i.e. the tensors are diagonal), straightforward computations reveal that

$$\widetilde{\varepsilon}_{\Omega,\min} \geq \left(1 - \frac{\sigma^2}{\omega^2}\right) \varepsilon_{\Omega,\min} \qquad \text{and} \qquad \widetilde{\mu}_{\Omega,\min} \geq \left(1 - \frac{\sigma^2}{\omega^2}\right) \mu_{\Omega,\min},$$

so that this approach fits to our theoretical framework if $\sigma_j(\boldsymbol{x}_j) < \omega$ for $j \in \{1, 2, 3\}$.

2.2. **Functional spaces.** In the following, if $D \subset \Omega$, $\mathscr{L}^2(D)$ denotes the space of square-integrable complex-valued function over D, see e.g. [1], and $\boldsymbol{\mathscr{L}}^2(D) := \big(\mathscr{L}^2(D)\big)^3$. We equip $\boldsymbol{\mathscr{L}}^2(D)$ with the following (equivalent) norms

$$\|\boldsymbol{w}\|_D^2 := \int_D |\boldsymbol{w}|^2, \qquad \|\boldsymbol{w}\|_{\boldsymbol{\phi},D}^2 := \operatorname{Re} \int_D \boldsymbol{\phi}\boldsymbol{w}\cdot\overline{\boldsymbol{w}}, \qquad \boldsymbol{w} \in \boldsymbol{\mathscr{L}}^2(D)$$

with $\boldsymbol{\phi} \in \{\boldsymbol{\varepsilon}, \boldsymbol{\mu}, \boldsymbol{\zeta}, \boldsymbol{\chi}\}$. We denote by $(\cdot,\cdot)_D$ the inner-product of $\boldsymbol{\mathscr{L}}^2(D)$, and we drop the subscript when $D = \Omega$. If $F \subset \overline{\Omega}$ is a two-dimensional measurable planar subset, $\|\cdot\|_F$ and $\langle\cdot,\cdot\rangle_F$ respectively denote the natural norm and inner-product of both $\mathscr{L}^2(F)$ and $\boldsymbol{\mathscr{L}}^2(F) := (\mathscr{L}(F))^3$.

Classically [1], we employ the notation $\mathcal{H}^1(D)$ for the usual Sobolev space of functions $w \in \mathscr{L}^2(D)$ such that $\boldsymbol{\nabla} w \in \boldsymbol{\mathscr{L}}^2(D)$. We also set $\boldsymbol{\mathcal{H}}^1(D) := \big(\mathcal{H}^1(D)\big)^3$ and introduce the semi-norms

$$\|\boldsymbol{\nabla}\boldsymbol{w}\|_D^2 := \sum_{j,k=1}^3 \left|\frac{\partial \boldsymbol{w}_j}{\partial \boldsymbol{x}_k}\right|^2, \qquad \|\boldsymbol{\nabla}\boldsymbol{w}\|_{\boldsymbol{\phi},D}^2 := \sum_{j,k=1}^3 \int_D \phi_{\max} \left|\frac{\partial \boldsymbol{w}_j}{\partial \boldsymbol{x}_k}\right|^2,$$

for $\boldsymbol{w} \in \boldsymbol{\mathcal{H}}^1(\Omega)$ and $\boldsymbol{\phi} \in \{\boldsymbol{\varepsilon}, \boldsymbol{\mu}, \boldsymbol{\zeta}, \boldsymbol{\chi}\}$.

We shall also need Sobolev spaces of vector-valued functions with well-defined divergence and rotation [26]. Specifically, we denote by $\boldsymbol{\mathcal{H}}(\mathbf{curl}, D)$ the space of function $\boldsymbol{w} \in \boldsymbol{\mathscr{L}}^2(D)$ with $\boldsymbol{\nabla} \times \boldsymbol{w} \in \boldsymbol{\mathscr{L}}^2(D)$, that we equip with the "energy" norm

$$|||\boldsymbol{v}|||^2_{\mathbf{curl},\omega,\boldsymbol{\phi},\boldsymbol{\psi},D} := \omega^2 \|\boldsymbol{v}\|^2_{\boldsymbol{\phi},D} + \|\boldsymbol{\nabla} \times \boldsymbol{v}\|^2_{\boldsymbol{\psi},D}, \quad \boldsymbol{v} \in \boldsymbol{\mathcal{H}}(\mathbf{curl}, D),$$

for $\boldsymbol{\phi}, \boldsymbol{\psi} \in \{\boldsymbol{\varepsilon}, \boldsymbol{\mu}, \boldsymbol{\zeta}, \boldsymbol{\chi}\}$. For the analysis of first-order methods, we also introduce the norm

$$|||(\boldsymbol{e}, \boldsymbol{h})|||^2_{\mathbf{curl},\omega,D} := |||\boldsymbol{e}|||^2_{\mathbf{curl},\omega,\boldsymbol{\varepsilon},\boldsymbol{\chi},D} + |||\boldsymbol{h}|||^2_{\mathbf{curl},\omega,\boldsymbol{\mu},\boldsymbol{\zeta},D}, \qquad (\boldsymbol{e}, \boldsymbol{h}) \in \boldsymbol{\mathcal{H}}_0(\mathbf{curl}, D) \times \boldsymbol{\mathcal{H}}(\mathbf{curl}, D),$$

for the product space.

In addition, if $\boldsymbol{\xi} : D \to \mathbb{C}^3$ is a measurable tensor-valued function we will use the notation $\boldsymbol{\mathcal{H}}(\mathrm{div}, \boldsymbol{\xi}, D)$ for the set of functions $\boldsymbol{w} \in \boldsymbol{\mathscr{L}}^2(D)$ with $\boldsymbol{\nabla} \cdot (\boldsymbol{\xi}\boldsymbol{w}) \in L^2(D)$, and we will write $\boldsymbol{\mathcal{H}}(\mathrm{div}^0, \boldsymbol{\xi}, D)$ for the set of fields $\boldsymbol{w} \in \boldsymbol{\mathcal{H}}(\mathrm{div}, \boldsymbol{\xi}, D)$ such that $\boldsymbol{\nabla} \cdot (\boldsymbol{\xi}\boldsymbol{w}) = 0$ in D. When $\boldsymbol{\xi} = \mathbf{I}_3$, the identity tensor, we simply write $\boldsymbol{\mathcal{H}}(\mathrm{div}, D)$ and $\boldsymbol{\mathcal{H}}(\mathrm{div}^0, D)$.

For any of the aforementioned spaces $\mathscr{V}$, the notation $\mathscr{V}_0$ denotes the closure of smooth, compactly supported, functions into $\mathscr{L}^2(D)$ (or $\boldsymbol{\mathscr{L}}^2(D)$) with respect to the norm $\mathscr{V}$. These spaces also correspond to the kernel of the naturally associated trace operators [1, 26].

Finally, if $\mathscr{D}$ is a collection of disjoint sets $D \subset \Omega$ and $\mathscr{V}(D)$ is any of the aforementioned space, $\mathscr{V}(\mathscr{D})$ stands for the "broken" space of functions in $\boldsymbol{v} \in \boldsymbol{\mathscr{L}}^2(\Omega)$ (or $\mathscr{L}^2(\Omega)$) such that $\boldsymbol{v}|_D \in \mathscr{V}(D)$ for all $D \in \mathscr{D}$. We employ the same notation for the norms and semi-norms of $\mathscr{V}(\mathscr{D})$ and $\mathscr{V}(D)$, with the subscript $\mathscr{D}$ instead of D.

2.3. **Variational formulations.** In the remaining of this work, we assume that $\boldsymbol{J} \in \boldsymbol{\mathcal{H}}(\mathrm{div}, \Omega)$. Then, we may recast (1.2) into a weak formulation, which consists in looking for $\boldsymbol{E} \in \boldsymbol{\mathcal{H}}_0(\mathbf{curl}, \Omega)$ such that

$$b(\boldsymbol{E}, \boldsymbol{v}) = i\omega(\boldsymbol{J}, \boldsymbol{v}) \qquad \forall \boldsymbol{v} \in \boldsymbol{\mathcal{H}}_0(\mathbf{curl}, \Omega) \tag{2.1}$$

where

$$b(\boldsymbol{e}, \boldsymbol{v}) := -\omega^2(\boldsymbol{\varepsilon}\boldsymbol{e}, \boldsymbol{v}) + (\boldsymbol{\chi}\boldsymbol{\nabla} \times \boldsymbol{e}, \boldsymbol{\nabla} \times \boldsymbol{v}) \qquad \forall \boldsymbol{e}, \boldsymbol{v} \in \boldsymbol{\mathcal{H}}_0(\mathbf{curl}, \Omega).$$

It is easily seen that the sesquilinear form $b(\cdot, \cdot)$ satisfies the following "Gårding inequality"

$$|||\boldsymbol{e}|||^2_{\mathbf{curl},\omega,\boldsymbol{\varepsilon},\boldsymbol{\chi},\Omega} = \mathrm{Re}\, b(\boldsymbol{e}, \boldsymbol{e}) + 2\omega^2 \|\boldsymbol{e}\|^2_{\boldsymbol{\varepsilon},\Omega} \qquad \forall \boldsymbol{e} \in \boldsymbol{\mathcal{H}}_0(\mathbf{curl}, \Omega). \tag{2.2}$$

While Nédélec discretizations immediately build upon (2.1), first-order DG methods hinge on the first-order counterpart of (1.2), where we look for $\boldsymbol{E}, \boldsymbol{H} : \Omega \to \mathbb{C}^3$ such that

$$\left\{ \begin{array}{rcll} i\omega\boldsymbol{\varepsilon}\boldsymbol{E} - \boldsymbol{\nabla} \times \boldsymbol{H} & = & \boldsymbol{J} & \text{in } \Omega, \\ i\omega\boldsymbol{\mu}\boldsymbol{H} + \boldsymbol{\nabla} \times \boldsymbol{E} & = & \boldsymbol{o} & \text{in } \Omega, \\ \boldsymbol{E} \times \boldsymbol{n} & = & \boldsymbol{o} & \text{on } \partial\Omega, \\ \boldsymbol{\mu}\boldsymbol{H} \cdot \boldsymbol{n} & = & o & \text{on } \partial\Omega. \end{array} \right. \tag{2.3}$$

The associated variational formulation consists in finding a pair $(\boldsymbol{E}, \boldsymbol{H}) \in \boldsymbol{\mathscr{L}}^2(\Omega) \times \boldsymbol{\mathscr{L}}^2(\Omega)$ satisfying

$$b((\boldsymbol{E}, \boldsymbol{H}), (\boldsymbol{v}, \boldsymbol{w})) = i\omega(\boldsymbol{J}, \boldsymbol{v}) \qquad \forall (\boldsymbol{v}, \boldsymbol{w}) \in \boldsymbol{\mathcal{H}}_0(\mathbf{curl}, \Omega) \times \boldsymbol{\mathcal{H}}(\mathbf{curl}, \Omega) \tag{2.4}$$

where

$$b((\boldsymbol{e}, \boldsymbol{h}), (\boldsymbol{v}, \boldsymbol{w})) := -\omega^2 (\boldsymbol{\mu}\boldsymbol{h}, \boldsymbol{r}) + i\omega (\boldsymbol{e}, \boldsymbol{\nabla} \times \boldsymbol{r}) - i\omega (\boldsymbol{h}, \boldsymbol{\nabla} \times \boldsymbol{v}) - \omega^2 (\boldsymbol{\varepsilon}\boldsymbol{e}, \boldsymbol{v})$$

for all $\boldsymbol{e}, \boldsymbol{v} \in \boldsymbol{\mathscr{L}}^2(\Omega)$ and $(\boldsymbol{v}, \boldsymbol{w}) \in \boldsymbol{\mathcal{H}}_0(\mathbf{curl}, \Omega) \times \boldsymbol{\mathcal{H}}(\mathbf{curl}, \Omega)$.

We finally note that we can equivalently rewrite (1.2) or (2.3) in terms of magnetic field as

$$\left\{ \begin{array}{rcll} -\omega^2\boldsymbol{\mu}\boldsymbol{H} + \boldsymbol{\nabla} \times (\boldsymbol{\zeta}\boldsymbol{\nabla} \times \boldsymbol{H}) & = & -\boldsymbol{\nabla} \times (\boldsymbol{\zeta}\boldsymbol{J}) & \text{in } \Omega, \\ \boldsymbol{\mu}\boldsymbol{H} \cdot \boldsymbol{n} & = & o & \text{on } \partial\Omega, \end{array} \right.$$

and the associated sesquilinear form

$$\widetilde{b}(\boldsymbol{h}, \boldsymbol{v}) := -\omega^2(\boldsymbol{\mu}\boldsymbol{h}, \boldsymbol{v}) + (\boldsymbol{\zeta}\boldsymbol{\nabla} \times \boldsymbol{h}, \boldsymbol{\nabla} \times \boldsymbol{v}) \qquad \forall \boldsymbol{h}, \boldsymbol{v} \in \boldsymbol{\mathcal{H}}(\mathbf{curl}, \Omega)$$

will be useful in the sequel.

2.4. **Computational mesh.** We consider a mesh $\mathcal{T}_h$ that partitions Ω into non-overlapping tetrahedral elements K. We assume that the mesh $\mathcal{T}_h$ is conforming in the sense of [15], which means that the intersection $\overline{K_+} \cap \overline{K_-}$ of two distinct elements $K_\pm \in \mathcal{T}_h$ is either empty, or a single vertex, edge, or face of both K_- and K_+. We further denote by $\mathcal{F}_h^{\mathrm{e}}$ the set of exterior faces lying on the boundary $\partial\Omega$ and by $\mathcal{F}_h^{\mathrm{i}}$ the remaining (interior) faces.

We also require that the mesh $\mathcal{T}_h$ is conforming with the physical partition $\mathscr{P}$. Specifically, we assume that for each $K \in \mathcal{T}_h$, there exists $P \in \mathscr{P}$ such that $K \subset P$. It equivalently means that the coefficients are constant over each element $K \in \mathcal{T}_h$, and that the interfaces of the partition $\mathscr{P}$ are covered by mesh faces $F \in \mathcal{F}_h := \mathcal{F}_h^{\mathrm{e}} \cup \mathcal{F}_h^{\mathrm{i}}$.

For $K \in \mathcal{T}_h$, $\mathcal{F}_K \subset \mathcal{F}_h$ denotes the faces of K, and the notations

$$h_K := \sup_{\boldsymbol{x},\boldsymbol{y}\in K} |\boldsymbol{x}-\boldsymbol{y}|, \qquad \rho_K := \sup\{r>0 \mid \exists \boldsymbol{x} \in K :\ B(\boldsymbol{x},r) \subset K\},$$

stand for the diameter of K and the radius of the largest ball contained in $\overline{K}$. We write $\beta_K := h_K/\rho_K$ for the "shape-regularity" parameter of K, and $\beta := \max_{K\in\mathcal{T}_h} \beta_K$ for the global shape-regularity parameter of the mesh. The (global) mesh size is defined as $h := \max_{K\in\mathcal{T}_h} h_K$.

Remark 2.2 (Hanging nodes)**.** *Discontinuous Galerkin methods allow for hanging nodes that violate the above assumption, and can be especially beneficial in the context of mesh adaptivity techniques* [9]*. We believe that the present analysis could extend to meshes featuring hanging nodes, but at the price of increased technicalities in the definition of the quasi-interpolation operators described in Section 2.6 below.*

We define the jump and average of $\boldsymbol{v} \in \boldsymbol{\mathcal{H}}^1(\mathcal{T}_h)$ through $F := \partial K_- \cap \partial K_+ \in \mathcal{F}_h^{\mathrm{i}}$ by

$$[\![\boldsymbol{v}]\!]|_F := \boldsymbol{v}_+(\boldsymbol{n}_+ \cdot \boldsymbol{n}_F) + \boldsymbol{v}_-(\boldsymbol{n}_- \cdot \boldsymbol{n}_F) \qquad \{\!\{\boldsymbol{v}\}\!\}|_F := \frac{1}{2}(\boldsymbol{v}_+ + \boldsymbol{v}_-)$$

where $\boldsymbol{v}_\pm$ is the trace of $\boldsymbol{v}$ on F from the interior of $K_\pm$ and $\boldsymbol{n}_\pm$ is the unit normal pointing outward of $K_\pm$. For exterior faces $F \in \mathcal{F}_h^{\mathrm{e}}$, it is convenient to define the jump and average as $[\![\boldsymbol{v}]\!]|_F := \{\!\{\boldsymbol{v}\}\!\}|_F := \boldsymbol{v}|_F$.

If $K \in \mathcal{T}_h$ and $F \in \mathcal{F}_h$, then

$$\mathcal{T}_{K,h} := \left\{K' \in \mathcal{T}_h \mid \overline{K} \cap \overline{K'} \neq \emptyset\right\}, \quad \mathcal{T}_{F,h} := \left\{K' \in \mathcal{T}_h \mid F \subset \partial K'\right\},$$

denote the mesh patches associated with K and F, and we use the symbols

$$\widetilde{K} := \mathrm{Int}\left(\bigcup_{K'\in\mathcal{T}_{K,h}} \overline{K'}\right), \quad \widetilde{F} := \mathrm{Int}\left(\bigcup_{K\in\mathcal{T}_{F,h}} \overline{K}\right),$$

for the associated open domains.

For any tensor fields $\boldsymbol{\phi} \in \{\boldsymbol{\varepsilon}, \boldsymbol{\mu}, \boldsymbol{\zeta}, \boldsymbol{\chi}\}$ representing the electromagnetic properties of Ω, we employ the notation $\phi_{F,\max} := \max_{K\in\mathcal{T}_{F,h}} \phi_{K,\max}$ for any $F \in \mathcal{F}_h$.

Finally, if $\mathcal{T} \subset \mathcal{T}_h$ and $\mathcal{F} \subset \mathcal{F}_h$ are collections of elements and faces, we write

$$(\cdot,\cdot)_{\mathcal{T}} := \sum_{K\in\mathcal{T}} (\cdot,\cdot)_K, \quad \langle\cdot,\cdot\rangle_{\partial\mathcal{T}} := \sum_{K\in\mathcal{T}} \langle\cdot,\cdot\rangle_{\partial K}, \quad \langle\cdot,\cdot\rangle_{\mathcal{F}} := \sum_{F\in\mathcal{F}} \langle\cdot,\cdot\rangle_F.$$

2.5. **Polynomial spaces.** In the following, for all $K \in \mathcal{T}_h$ and for $q \geq 0$, $\mathcal{P}_q(K)$ stands for the space of (complex-valued) polynomials defined over K and $\boldsymbol{\mathcal{P}}_q(K) := (\mathcal{P}_q(K))^3$. We shall also require the Nédélec polynomial space $\boldsymbol{\mathcal{N}}_q(K) := \boldsymbol{\mathcal{P}}_q(K) + \boldsymbol{x} \times \boldsymbol{\mathcal{P}}_q(K)$. The inclusions $\boldsymbol{\nabla}(\mathcal{P}_{q+1}(K)) \subset \boldsymbol{\mathcal{N}}_q(K) \subset \boldsymbol{\mathcal{P}}_{q+1}(K)$ hold true.

If $\mathcal{T} \subset \mathcal{T}_h$, $\mathcal{P}_q(\mathcal{T})$, $\boldsymbol{\mathcal{P}}_q(\mathcal{T})$ and $\boldsymbol{\mathcal{N}}_q(\mathcal{T})$ respectively stand for the space of functions that are piecewise in $\mathcal{P}_q(K)$, $\boldsymbol{\mathcal{P}}_q(K)$ and $\boldsymbol{\mathcal{N}}_q(K)$ for all $K \in \mathcal{T}$.

In the remaining we fix an integer $k \geq 0$ representing the polynomial degree we will consider for the analyzed discretization schemes. Of particular importance,

$$V_h := \mathcal{P}_{k+1}(\mathcal{T}_h) \cap H_0^1(\Omega), \qquad \widetilde{V}_h := \mathcal{P}_{k+1}(\mathcal{T}_h) \cap H^1(\Omega)$$

are the usual Lagrange finite element spaces (with and without essential boundary conditions) and

$$\boldsymbol{W}_h := \boldsymbol{\mathcal{N}}_k(\mathcal{T}_h) \cap \boldsymbol{\mathcal{H}}_0(\mathbf{curl},\Omega), \qquad \widetilde{\boldsymbol{W}}_h := \boldsymbol{\mathcal{N}}_k(\mathcal{T}_h) \cap \boldsymbol{\mathcal{H}}(\mathbf{curl},\Omega)$$

are the usual Nédélec spaces of the first-family [34]. Remark that we have $\boldsymbol{\nabla} V_h \subset \boldsymbol{W}_h$ and $\boldsymbol{\nabla}\widetilde{V}_h \subset \widetilde{\boldsymbol{W}}_h$. We also recall that $\boldsymbol{\mathcal{P}}_{k+1}(\mathcal{T}_h) \cap \boldsymbol{\mathcal{H}}_0(\mathbf{curl},\Omega)$ and $\boldsymbol{\mathcal{P}}_{k+1}(\mathcal{T}_h) \cap \boldsymbol{\mathcal{H}}(\mathbf{curl},\Omega)$ are the second-family of Nédélec spaces [35].

2.6. **Quasi-interpolation.** There exists two operators $\mathcal{Q}_h : H^1_0(\Omega) \to V_h$ and $\mathcal{R}_h : \boldsymbol{\mathcal{H}}_0(\mathbf{curl},\Omega) \to \boldsymbol{W}_h$ and a constant $\mathscr{C}_{\mathrm{i}}$ that only depends on β such that

$$h_K^{-1}\|w - \mathcal{Q}_h w\|_K + h_K^{-1/2}\|w - \mathcal{Q}_h w\|_{\partial K} \le \mathscr{C}_{\mathrm{i}}\|\boldsymbol{\nabla} w\|_{\widetilde{K}} \tag{2.5}$$

for all $w \in H^1_0(\Omega)$ and

$$h_K^{-1}\|\boldsymbol{w} - \mathcal{R}_h \boldsymbol{w}\|_K + h_K^{-1/2}\|(\boldsymbol{w} - \mathcal{R}_h \boldsymbol{w}) \times \boldsymbol{n}\|_{\partial K} \le \mathscr{C}_{\mathrm{i}}\|\boldsymbol{\nabla} \boldsymbol{w}\|_{\mathcal{T}_{K,h}} \tag{2.6}$$

for all $\boldsymbol{w} \in \boldsymbol{\mathcal{H}}^1(\mathcal{T}_h) \cap \boldsymbol{\mathcal{H}}_0(\mathbf{curl},\Omega)$. We will also use quasi-interpolation operators that operate on spaces without essential boundary conditions, namely, $\widetilde{\mathcal{Q}}_h : H^1(\Omega) \to \widetilde{V}_h$ and $\widetilde{\mathcal{R}}_h : \boldsymbol{\mathcal{H}}(\mathbf{curl},\Omega) \to \widetilde{\boldsymbol{W}}_h$. These operators also satisfy (2.5) and (2.6) for all $w \in H^1(\Omega)$ and $\boldsymbol{w} \in \boldsymbol{\mathcal{H}}^1(\mathcal{T}_h) \cap \boldsymbol{\mathcal{H}}(\mathbf{curl},\Omega)$. We refer the reader to, e.g, [22] for the construction of these operators.

Remark 2.3 (Commutativity)**.** *In the derivation of a priori error estimates for Maxwell's equations, commuting quasi-interpolation operators are of paramount importance* [10, 14, 23, 46]*. Interestingly, this property is not required in the context of a posteriori error estimates.*

2.7. **Bubble functions, inverse inequalities and extension operator.** Bubble functions constitute a standard tool that we will be using to prove efficiency estimates [42]. For an element $K \in \mathcal{T}_h$ and a face $F \in \mathcal{F}_h$, we denote by b_K and b_F the usual element and face "bubble" functions respectively supported in K and $\widetilde{F}$. We have

$$\|w\|_K \le \mathscr{C}_{\mathrm{b}}\|b_K^{1/2} w\|_K, \qquad \|v\|_F \le \mathscr{C}_{\mathrm{b}}\|b_F^{1/2} v\|_F \tag{2.7a}$$

for all $w \in \mathcal{P}_{k+1}(K)$ and $v \in \mathcal{P}_{k+1}(F)$. Here, $\mathscr{C}_{\mathrm{b}} > 0$ is a constant depending on the polynomial degree k and the shape regularity parameter β. Standard inverse inequalities imply that

$$\|\boldsymbol{\nabla}(w b_K)\|_K \le \mathscr{C}_{\mathrm{b}} h_K^{-1}\|w\|_K \qquad \forall w \in \mathcal{P}_{k+1}(K). \tag{2.7b}$$

We also employ an extension operator $\mathrm{F}_{\mathrm{ext}} : \mathcal{P}_{k+1}(F) \to \mathcal{P}_{k+1}(\widetilde{F})$ such that $F_{\mathrm{ext}}(v)|_F = v$ and

$$\|F_{\mathrm{ext}}(v)\|_{\mathcal{T}_{F,h}} + h_F\|\boldsymbol{\nabla}(\mathrm{F}_{\mathrm{ext}}(v))\|_{\mathcal{T}_{F,h}} \le \mathscr{C}_{\mathrm{b}} h_F^{1/2}\|v\|_F, \qquad v \in \mathcal{P}_{k+1}(F). \tag{2.7c}$$

Identical estimates hold for vectorial functions, applying the above estimates componentwise.

2.8. **Data oscillation.** Classically, our *a posteriori* error estimates include "data-oscillation" terms. These terms include a "projected source term" $\boldsymbol{J}_h \in \boldsymbol{\mathcal{P}}_{k+1}(\mathcal{T}_h)$, that is defined elementwise, for each $K \in \mathcal{T}_h$, as the unique polynomial $\boldsymbol{J}_h \in \boldsymbol{\mathcal{P}}_{k+1}(K)$ such that

$$\frac{\omega^2 h_K^2}{c^2_{\widetilde{K},\min}}(\boldsymbol{J}_h, \boldsymbol{v}_h)_K + h_K^2(\boldsymbol{\nabla}\cdot\boldsymbol{J}_h, \boldsymbol{\nabla}\cdot\boldsymbol{v}_h)_K = \frac{\omega^2 h_K^2}{c^2_{\widetilde{K},\min}}(\boldsymbol{J}, \boldsymbol{v}_h)_K + h_K^2(\boldsymbol{\nabla}\cdot\boldsymbol{J}, \boldsymbol{\nabla}\cdot\boldsymbol{v}_h)_K$$

for all $\boldsymbol{v}_h \in \boldsymbol{\mathcal{P}}_{k+1}(K)$. Notice that while other "traditional" projections or quasi-interpolation operators could be employed, we select this particular definition as it minimizes the terms appearing in the final error bounds.

We are now ready to introduce the elementwise oscillation terms

$$\mathrm{osc}_{0,K} := \sqrt{\mu_{\widetilde{K},\max}}\,\omega h_K\|\boldsymbol{J} - \boldsymbol{J}_h\|_K, \qquad \mathrm{osc}_{\mathrm{div},K} := \frac{h_K}{\sqrt{\varepsilon_{\widetilde{K},\min}}}\|\boldsymbol{\nabla}\cdot(\boldsymbol{J} - \boldsymbol{J}_h)\|_K$$

for all $K \in \mathcal{T}_h$, as well as their "patchwise" counterparts

$$\mathrm{osc}^2_{0,\mathcal{T}} := \sum_{K\in\mathcal{T}} \mathrm{osc}^2_{0,K}, \quad \mathrm{osc}^2_{\mathrm{div},\mathcal{T}} := \sum_{K\in\mathcal{T}} \mathrm{osc}^2_{\mathrm{div},K}, \quad \mathrm{osc}^2_{\mathcal{T}} := \mathrm{osc}^2_{0,\mathcal{T}} + \mathrm{osc}^2_{\mathrm{div},\mathcal{T}}$$

for $\mathcal{T} \subset \mathcal{T}_h$. If $\boldsymbol{J}$ is piecewise smooth, this oscillation term decreases faster than the discretization error to zero. Specifically, for $\mathcal{T} \subset \mathcal{T}_h$, if $\boldsymbol{J} \in \boldsymbol{\mathcal{H}}^{k+1}(\mathcal{T})$ and $\boldsymbol{\nabla}\cdot\boldsymbol{J} \in \mathcal{H}^{k+1}(\mathcal{T})$, then $\mathrm{osc}_{\mathcal{T}} = o(h^{k+1})$.

2.9. **Gradient extraction.** The extraction of gradients is a central tool in *a posteriori* error estimation for Maxwell's equations [4, 37]. Standard results may be found in [16] or [26], but unfortunately, they are not perfectly suited for our needs. As a result, we revisited the proofs from [26] in Appendix B to establish the results stated below.

For all $\boldsymbol{\theta} \in \boldsymbol{\mathcal{H}}_0(\mathbf{curl},\Omega)$, there exist $\boldsymbol{\phi} \in \boldsymbol{\mathcal{H}}^1(\mathscr{P}) \cap \boldsymbol{\mathcal{H}}_0(\mathbf{curl},\Omega)$ and $r \in \mathcal{H}^1_0(\Omega)$ such that $\boldsymbol{\theta} = \boldsymbol{\phi} + \boldsymbol{\nabla} r$ with

$$\|\boldsymbol{\nabla}\boldsymbol{\phi}\|_{\boldsymbol{\chi},\mathscr{P}} \leq \mathscr{C}_{\mathrm{r}} \|\boldsymbol{\nabla}\times\boldsymbol{\theta}\|_{\boldsymbol{\chi},\Omega}, \qquad \|\boldsymbol{\nabla} r\|_{\boldsymbol{\varepsilon},\Omega} \leq \mathscr{C}_{\mathrm{r}} \|\boldsymbol{\theta}\|_{\boldsymbol{\varepsilon},\Omega}, \tag{2.8}$$

where $\mathscr{C}_{\mathrm{r}}$ is a constant possibly depending on the geometry of Ω through the constants $\mathscr{C}_{\mathrm{e},\Omega}$ and $\widetilde{\mathscr{C}}_{\mathrm{e},\Omega}$ introduced in Appendix B, and the material contrasts $\varepsilon_{\Omega,\max}/\varepsilon_{\Omega,\min}$ and $\mu_{\Omega,\max}/\mu_{\Omega,\min}$.

Analogously, for all $\boldsymbol{\vartheta} \in \boldsymbol{\mathcal{H}}(\mathbf{curl},\Omega)$ there exist $\boldsymbol{\varphi} \in \boldsymbol{\mathcal{H}}^1(\mathscr{P}) \cap \boldsymbol{\mathcal{H}}(\mathbf{curl},\Omega)$ and $s \in \mathcal{H}^1(\Omega)$ such that $\boldsymbol{\vartheta} = \boldsymbol{\varphi} + \boldsymbol{\nabla} s$ with

$$\|\boldsymbol{\nabla}\boldsymbol{\varphi}\|_{\boldsymbol{\zeta},\mathscr{P}} \leq \mathscr{C}_{\mathrm{r}} \|\boldsymbol{\nabla}\times\boldsymbol{\vartheta}\|_{\boldsymbol{\zeta},\Omega}, \qquad \|\boldsymbol{\nabla} s\|_{\boldsymbol{\mu},\Omega} \leq \mathscr{C}_{\mathrm{r}} \|\boldsymbol{\vartheta}\|_{\boldsymbol{\mu},\Omega}. \tag{2.9}$$

Remark 2.4 (Novelty of our gradient extraction results)**.** *In contrast to standard results* [16, 26]*, the second estimates of* (2.8) *and* (2.9) *include the $\boldsymbol{\mathscr{L}}^2(\Omega)$-norm of $\boldsymbol{\theta}$ and $\boldsymbol{\vartheta}$ instead of their $\boldsymbol{\mathcal{H}}_0(\mathbf{curl},\Omega)$-norm. While this improvement only requires slight adaption in the standard proofs, it is of paramount importance to obtain correct scalings with respect to the frequency ω.*

2.10. **Well-posedness.** In the remaining of this document, we will work under the assumption that for the considered frequency, the (adjoint) problem under consideration is well-posed.

Assumption 2.5 (Well-posedness)**.** *For all $\boldsymbol{j} \in \boldsymbol{\mathscr{L}}^2(\Omega)$, there exists a unique $\boldsymbol{e}^\star(\boldsymbol{j}) \in \boldsymbol{\mathcal{H}}_0(\mathbf{curl},\Omega)$ such that*

$$b(\boldsymbol{w},\boldsymbol{e}^\star(\boldsymbol{j})) = \omega(\boldsymbol{w},\boldsymbol{\varepsilon}\boldsymbol{j}) \qquad \forall \boldsymbol{w} \in \boldsymbol{\mathcal{H}}_0(\mathbf{curl},\Omega). \tag{2.10}$$

Classically, we can infer from Assumption 2.5 that for all $\boldsymbol{l} \in \boldsymbol{\mathscr{L}}^2(\Omega)$, there exists a unique element $\boldsymbol{h}^\star(\boldsymbol{l}) \in \boldsymbol{\mathcal{H}}(\mathbf{curl},\Omega)$ such that

$$\widetilde{b}(\boldsymbol{w},\boldsymbol{h}^\star(\boldsymbol{l})) = \omega(\boldsymbol{w},\boldsymbol{\mu}\boldsymbol{l}) \qquad \forall \boldsymbol{w} \in \boldsymbol{\mathcal{H}}(\mathbf{curl}.\Omega), \tag{2.11}$$

We can then introduce the notations

$$\gamma_{\mathrm{s,E}} := \sup_{\substack{\boldsymbol{j}\in\boldsymbol{\mathcal{H}}(\mathrm{div}^0,\boldsymbol{\varepsilon},\Omega)\\ \|\boldsymbol{j}\|_{\boldsymbol{\varepsilon},\Omega}=1}} \|\!|\boldsymbol{e}^\star(\boldsymbol{j})|\!\|_{\mathbf{curl},\omega,\boldsymbol{\varepsilon},\boldsymbol{\chi},\Omega}, \qquad \gamma_{\mathrm{s,H}} := \sup_{\substack{\boldsymbol{l}\in\boldsymbol{\mathcal{H}}_0(\mathrm{div}^0,\boldsymbol{\mu},\Omega)\\ \|\boldsymbol{l}\|_{\boldsymbol{\varepsilon},\Omega}=1}} \|\!|\boldsymbol{h}^\star(\boldsymbol{j})|\!\|_{\mathbf{curl},\omega,\boldsymbol{\mu},\boldsymbol{\zeta},\Omega}. \tag{2.12}$$

2.11. **Approximation factor.** We shall also need two "approximation factors", that respectively describe the ability of the discrete spaces $\boldsymbol{W}_h$ and $\widetilde{\boldsymbol{W}}_h$ to approximate solutions to (2.10) and (2.11), and are defined by

$$\gamma_{\mathrm{ba,E}} := \sup_{\substack{\boldsymbol{j}\in\boldsymbol{\mathcal{H}}(\mathrm{div}^0,\boldsymbol{\varepsilon},\Omega)\\ \|\boldsymbol{j}\|_{\boldsymbol{\varepsilon},\Omega}=1}} \inf_{\boldsymbol{e}_h\in\boldsymbol{W}_h} \|\!|\boldsymbol{e}^\star(\boldsymbol{j}) - \boldsymbol{e}_h|\!\|_{\mathbf{curl},\omega,\boldsymbol{\varepsilon},\boldsymbol{\chi},\Omega} \tag{2.13a}$$

and

$$\gamma_{\mathrm{ba,H}} := \sup_{\substack{\boldsymbol{l}\in\boldsymbol{\mathcal{H}}_0(\mathrm{div}^0,\boldsymbol{\mu},\Omega)\\ \|\boldsymbol{h}\|_{\boldsymbol{\mu},\Omega}=1}} \inf_{\boldsymbol{h}_h\in\widetilde{\boldsymbol{W}}_h} \|\!|\boldsymbol{h}^\star(\boldsymbol{l}) - \boldsymbol{h}_h|\!\|_{\mathbf{curl},\omega,\boldsymbol{\mu},\boldsymbol{\zeta},\Omega}. \tag{2.13b}$$

Recalling (2.12), we clearly have $\gamma_{\mathrm{ba,E}} \leq \gamma_{\mathrm{s,E}}$, and $\gamma_{\mathrm{ba,H}} \leq \gamma_{\mathrm{s,H}}$, showing that the approximation factor is controlled independently of the mesh size h and the approximation order k. It does however, in general, depends on the wavenumber $\omega\ell_\Omega/c_{\min,\Omega}$, the geometry of $\widehat{\Omega}$, and the coefficients $\boldsymbol{\varepsilon}$ and $\boldsymbol{\mu}$.

The divergence-free conditions of the right-hand sides defining $\gamma_{\mathrm{ba,E}}$ and $\gamma_{\mathrm{ba,H}}$, show that $\boldsymbol{e}^\star(\boldsymbol{j}) \in \boldsymbol{\mathcal{H}}_0(\mathbf{curl},\Omega) \cap \boldsymbol{\mathcal{H}}(\mathrm{div}^0,\overline{\boldsymbol{\varepsilon}},\Omega)$ and $\boldsymbol{h}^\star(\boldsymbol{l}) \in \boldsymbol{\mathcal{H}}(\mathbf{curl},\Omega) \cap \boldsymbol{\mathcal{H}}_0(\mathrm{div}^0,\overline{\boldsymbol{\mu}},\Omega)$. Then, as long as Ω and the coefficients $\boldsymbol{\varepsilon}$ and $\boldsymbol{\mu}$ exhibit a regularity shift [8, 16], we have $\boldsymbol{e}^\star(\boldsymbol{j}), \boldsymbol{h}^\star(\boldsymbol{l}) \in \boldsymbol{\mathcal{H}}^s(\Omega)$ for some $0 < s \leq 1$, and standard approximation properties of Nédélec spaces (see e.g. [22]) imply that

$$\gamma_{\mathrm{ba,E}}, \gamma_{\mathrm{ba,H}} \leq C(\omega,\Omega,\boldsymbol{\varepsilon},\boldsymbol{\mu}) \left(\frac{h}{k}\right)^s. \tag{2.14}$$

As a result, the approximation factor may depend on the frequency (and more generally, on the geometry of the domain and the physical coefficients) for coarse meshes, but is asymptotically bounded independently of the frequency, the mesh size, and the approximation order.

In (2.14), the dependence on ω is not specified. In addition, the interest of high-order schemes is not obvious, as the convergence rate is limited to 1. For Helmholtz problems, several works giving a precise description of the behaviour of the approximation factor are available [13, 30]. We also refer the reader to [31, 38] for recent works on Maxwell's equations with transparent and impedance boundary conditions. In Appendix A, we analyze the case of constant real-valued coefficients $\boldsymbol{\varepsilon} = \varepsilon \mathbf{I}_3$ and $\boldsymbol{\mu} = \mu \mathbf{I}_3$ in a smooth domain, and we show that

$$\gamma_{\mathrm{ba,E}}, \gamma_{\mathrm{ba,H}} \leq C(\Omega, k) \left(\frac{\omega h}{c} + \frac{\omega}{\delta} \left(\frac{\omega h}{c} \right)^{k+1} \right),$$

where $c := 1/\sqrt{\varepsilon\mu}$ is the wavespeed and $\delta := |\omega - \omega_{\mathrm{r}}|$ is the distance between the forcing frequency ω and the closest resonance frequency ω_{r}. Thus, for a fixed number of dofs per wavelength ($\omega h/c$ is kept constant), the approximation factor increases if ω increases or δ decreases. On the other hand, the condition

$$\frac{\omega h}{c} \leq \left(\frac{\delta}{\omega} \right)^{1/(k+1)},$$

ensures that the approximation factors are bounded independently of the frequency. Thus, the number of dofs per wavelength must be increased when $\omega/\delta \to +\infty$, but this increase is less pronounced for high-order methods.

Remark 2.6 (Improved approximation factors)**.** *For the sake of simplicity, we employ Nédélec elements of the first family ($\boldsymbol{W}_h$ and $\widetilde{\boldsymbol{W}}_h$) to define the approximation factors. For some methods, we could, in principle, employ larger approximation spaces based on the second family of Nédélec elements. However, for the sake of simplicity, we do not include this possibility here, as the convergence orders are the same and since it permits a unified presentation.*

2.12. **Coefficient contrasts.** For $K \in \mathcal{T}_h$ and $\boldsymbol{\phi} \in \{\boldsymbol{\varepsilon}, \boldsymbol{\mu}, \boldsymbol{\zeta}, \boldsymbol{\chi}\}$, we employ the notation

$$\mathscr{C}_{\mathrm{c},\boldsymbol{\phi},K} := \frac{\max_{\widetilde{K}} \phi_{\max}}{\min_{\widetilde{K}} \phi_{\min}}$$

for the "contrast" of the coefficient $\boldsymbol{\phi}$ in the patch $\mathcal{T}_{K,h}$. We also set $\mathscr{C}_{\mathrm{c},\boldsymbol{\phi}} := \max_{K \in \mathcal{T}_h} \mathscr{C}_{\mathrm{c},\boldsymbol{\phi},K}$ and $\mathscr{C}_{\mathrm{c}} := \max_{\boldsymbol{\phi} \in \{\boldsymbol{\varepsilon},\boldsymbol{\mu},\boldsymbol{\zeta},\boldsymbol{\chi}\}} \mathscr{C}_{\mathrm{c},\boldsymbol{\phi}}$. Notice that these quantities are actually independent of the mesh $\mathcal{T}_h$, as long as it fits the partition $\mathscr{P}$, but is only affected by the definition of the coefficients $\boldsymbol{\varepsilon}$, $\boldsymbol{\mu}$.

2.13. **Notation for generic constants.** In the remaining of this document, if $A, B \geq 0$ are two positive real values, we employ the notation $A \lesssim B$ if there exists a constant C that only depends on $\mathscr{C}_{\mathrm{i}}$, $\mathscr{C}_{\mathrm{b}}$, $\mathscr{C}_{\mathrm{r}}$ and $\mathscr{C}_{\mathrm{c}}$ such that $A \leq CB$. Importantly, C is independent of ω and h. However C may depend on Ω and the global coefficient contrasts through $\mathscr{C}_{\mathrm{r}}$, and it may also depend on β through $\mathscr{C}_{\mathrm{i}}$ and $\mathscr{C}_{\mathrm{b}}$. We also employ the notation $A \gtrsim B$ if $B \lesssim A$ and $A \sim B$ if $A \lesssim B$ and $A \gtrsim B$.

3. Second-order schemes

In this section, we treat Nédélec finite element discretizations of second-order variational formulation (2.1).

3.1. **Numerical scheme.** We consider a discretization space $\boldsymbol{W}_h \subset \boldsymbol{X}_h \subset \boldsymbol{\mathcal{P}}_{k+1}(\Omega) \cap \boldsymbol{\mathcal{H}}_0(\mathbf{curl}, \Omega)$. In the case where $\boldsymbol{X}_h = \boldsymbol{W}_h$, the analyzed method corresponds to the usual first family of Nédélec finite elements, while if $\boldsymbol{X}_h = \boldsymbol{\mathcal{P}}_{k+1}(\Omega) \cap \boldsymbol{\mathcal{H}}_0(\mathbf{curl}, \Omega)$, the second family of Nédélec elements is covered. As it does not bring any additional complexity, our analysis actually also handles every situation "in between", where the first family of elements is used in some part of the mesh, while the second family is employed in the remaining areas.

The discrete method reads: find $\boldsymbol{E}_h \in \boldsymbol{X}_h$ such that

$$b(\boldsymbol{E}_h, \boldsymbol{v}_h) = i\omega(\boldsymbol{J}, \boldsymbol{v}_h) \tag{3.1}$$

for all $\boldsymbol{v}_h \in \boldsymbol{X}_h$. The existence and uniqueness of $\boldsymbol{E}_h$ are ensured provided that the mesh is sufficiently refined [10, 14, 23, 46]. For general meshes, to the best of our knowledge, the well-posedness of (3.1) is an open question.

In the remaining of this section, we will work under the assumption that a discrete solution $\boldsymbol{E}_h$ satisfying (3.1) has been computed. Notice that our analysis applies as soon as $\boldsymbol{E}_h \in \boldsymbol{X}_h$ satisfies (3.1) and in particular, unique solvability is not required. As a consequence of this assumption, we have

$$b(\boldsymbol{E} - \boldsymbol{E}_h, \boldsymbol{v}_h) = 0 \tag{3.2}$$

for all $\boldsymbol{v}_h \in \boldsymbol{X}_h$.

3.2. **Error estimators.** The design of our estimator is "classical". We largely follow [4, 37], but take special care to weight in each term of the estimator correctly in terms of frequency and electromagnetic coefficients. Our estimator splits into two parts, namely, for $K \in \mathcal{T}_h$

$$\eta_K^2 := \eta_{\mathrm{div},K}^2 + \eta_{\mathbf{curl},K}^2$$

with

$$\eta_{\mathrm{div},K} := \frac{1}{\sqrt{\underline{\varepsilon}_{\widetilde{K},\min}}} \left(h_K \|\boldsymbol{\nabla} \cdot (\boldsymbol{J} - i\omega\boldsymbol{\varepsilon}\boldsymbol{E}_h)\|_K + \omega h_K^{1/2} \| [\![\boldsymbol{\varepsilon}\boldsymbol{E}_h]\!] \cdot \boldsymbol{n}\|_{\partial K \setminus \partial\Omega} \right) \tag{3.3}$$

and

$$\eta_{\mathbf{curl},K} := \sqrt{\mu_{\widetilde{K},\max}} \Bigg(h_K \|i\omega\boldsymbol{J} + \omega^2 \boldsymbol{\varepsilon}\boldsymbol{E}_h - \boldsymbol{\nabla} \times (\boldsymbol{\chi}\boldsymbol{\nabla} \times \boldsymbol{E}_h)\|_K + h_K^{1/2} \| [\![\boldsymbol{\chi}\boldsymbol{\nabla} \times \boldsymbol{E}_h]\!] \times \boldsymbol{n}\|_{\partial K \setminus \partial\Omega} \Bigg). \tag{3.4}$$

We also set

$$\eta^2 := \sum_{K \in \mathcal{T}_h} \eta_K^2, \qquad \eta_{\mathrm{div}}^2 := \sum_{K \in \mathcal{T}_h} \eta_{\mathrm{div},K}^2, \qquad \eta_{\mathbf{curl}}^2 := \sum_{K \in \mathcal{T}_h} \eta_{\mathbf{curl},K}^2.$$

3.3. **Reliability.** This section is devoted to reliability estimates. The first step consists in controlling "residual terms", that is, the sesquilinear form applied to the error and an arbitrary test function. This is carried out in Lemma 3.1 and 3.2 below.

Lemma 3.1 (Control of the residual)**.** *The estimates*

$$|b(\boldsymbol{E} - \boldsymbol{E}_h, \boldsymbol{\nabla} q)| \lesssim \omega \eta_{\mathrm{div}} \|\boldsymbol{\nabla} q\|_{\boldsymbol{\varepsilon},\Omega} \tag{3.5}$$

and

$$|b(\boldsymbol{E} - \boldsymbol{E}_h, \boldsymbol{\phi})| \lesssim \eta_{\mathbf{curl}} \|\boldsymbol{\nabla}\boldsymbol{\phi}\|_{\boldsymbol{\chi},\mathcal{T}_h} \tag{3.6}$$

hold true for all $q \in \mathcal{H}_0^1(\Omega)$ *and* $\boldsymbol{\phi} \in \boldsymbol{\mathcal{H}}^1(\mathcal{T}_h) \cap \boldsymbol{\mathcal{H}}_0(\mathbf{curl}, \Omega)$.

Proof. We first establish (3.5). We observe that for any $w \in H_0^1(\Omega)$, we have

$$b(\boldsymbol{E} - \boldsymbol{E}_h, \boldsymbol{\nabla} w) = (i\omega\boldsymbol{J} + \omega^2\boldsymbol{\varepsilon}\boldsymbol{E}_h, \boldsymbol{\nabla} w) = i\omega(\boldsymbol{J} - i\omega\boldsymbol{\varepsilon}\boldsymbol{E}_h, \boldsymbol{\nabla} w)$$

so that

$$\begin{aligned} \frac{1}{i\omega} b(\boldsymbol{E} - \boldsymbol{E}_h, \boldsymbol{\nabla} w) &= i\omega \langle \boldsymbol{\varepsilon}\boldsymbol{E}_h \cdot \boldsymbol{n}, w \rangle_{\partial\mathcal{T}_h} - (\boldsymbol{\nabla} \cdot (\boldsymbol{J} - i\omega\boldsymbol{\varepsilon}\boldsymbol{E}_h), w)_{\mathcal{T}_h} \\ &= i\omega \langle [\![\boldsymbol{\varepsilon}\boldsymbol{E}_h]\!] \cdot \boldsymbol{n}, w \rangle_{\mathcal{F}_h^{\mathrm{i}}} - (\boldsymbol{\nabla} \cdot (\boldsymbol{J} - i\omega\boldsymbol{E}_h), w)_{\mathcal{T}_h}, \end{aligned}$$

and therefore

$$\begin{aligned} \frac{1}{\omega} |b(\boldsymbol{E} - \boldsymbol{E}_h, \boldsymbol{\nabla} w)| &\le \omega \sum_{F \in \mathcal{F}_h^{\mathrm{i}}} \| [\![\boldsymbol{\varepsilon}\boldsymbol{E}_h]\!] \cdot \boldsymbol{n}\|_F \|w\|_F + \sum_{K \in \mathcal{T}_h} \|\boldsymbol{\nabla} \cdot (\boldsymbol{J} - i\omega\boldsymbol{\varepsilon}\boldsymbol{E}_h)\|_K \|w\|_K \\ &\lesssim \sum_{K \in \mathcal{T}_h} \sqrt{\underline{\varepsilon}_{\widetilde{K},\min}} \eta_{\mathrm{div},K} \left(h_K^{-1} \|w\|_K + h_K^{-1/2} \|w\|_{\partial K \setminus \partial\Omega} \right). \end{aligned} \tag{3.7}$$

Let now $q \in H^1_0(\Omega)$. Since $\boldsymbol{\nabla}(\mathcal{Q}_h q) \in \boldsymbol{W}_h$, by Galerkin orthogonality (3.2), we can apply (3.7) with $w = q - \mathcal{Q}_h q$ to show that

$$\begin{aligned}\frac{1}{\omega}|b(\boldsymbol{E}-\boldsymbol{E}_h,\boldsymbol{\nabla}q)| &= \frac{1}{\omega}|b(\boldsymbol{E}-\boldsymbol{E}_h,\boldsymbol{\nabla}(q-\mathcal{Q}_h q))|\\ &\lesssim \sum_{K\in\mathcal{T}_h}\sqrt{\varepsilon_{\widetilde{K},\min}}\eta_{\mathrm{div},K}\left(h_K^{-1}\|q-\mathcal{Q}_h q\|_K + h_K^{-1/2}\|q-\mathcal{Q}_h q\|_{\partial K\setminus\partial\Omega}\right)\\ &\lesssim \sum_{K\in\mathcal{T}_h}\sqrt{\varepsilon_{\widetilde{K},\min}}\eta_{\mathrm{div},K}\|\boldsymbol{\nabla}q\|_{\widetilde{K}} \lesssim \eta_{\mathrm{div}}\|\boldsymbol{\nabla}q\|_{\boldsymbol{\varepsilon},\Omega},\end{aligned}$$

where we additionally employed (2.5). This shows (3.5).

We now focus on (3.6). Similarly, we start with an arbitrary element $\boldsymbol{w} \in \boldsymbol{\mathcal{H}}^1(\mathcal{T}_h)\cap\boldsymbol{\mathcal{H}}_0(\mathbf{curl},\Omega)$. We have

$$\begin{aligned}b(\boldsymbol{E}-\boldsymbol{E}_h,\boldsymbol{w}) &= i\omega(\boldsymbol{J},\boldsymbol{w}) + \omega^2(\boldsymbol{\varepsilon}\boldsymbol{E}_h,\boldsymbol{w}) - (\boldsymbol{\chi}\boldsymbol{\nabla}\times\boldsymbol{E}_h,\boldsymbol{\nabla}\times\boldsymbol{w})\\ &= (i\omega\boldsymbol{J}+\omega^2\boldsymbol{E}_h - \boldsymbol{\nabla}\times(\boldsymbol{\chi}\boldsymbol{\nabla}\times\boldsymbol{E}_h),\boldsymbol{w})_{\mathcal{T}_h} + \langle\boldsymbol{\chi}\boldsymbol{\nabla}\times\boldsymbol{E}_h\times\boldsymbol{n},\boldsymbol{w}\rangle_{\partial\mathcal{T}_h}\\ &= (i\omega\boldsymbol{J}+\omega^2\boldsymbol{E}_h - \boldsymbol{\nabla}\times(\boldsymbol{\chi}\boldsymbol{\nabla}\times\boldsymbol{E}_h),\boldsymbol{w})_{\mathcal{T}_h} + \langle[\![\boldsymbol{\chi}\boldsymbol{\nabla}\times\boldsymbol{E}_h]\!]\times\boldsymbol{n},\boldsymbol{w}\rangle_{\mathcal{F}_h^{\mathrm{i}}}\end{aligned}$$

and

$$\begin{aligned}|b(\boldsymbol{E}-\boldsymbol{E}_h,\boldsymbol{w})| &\le \sum_{K\in\mathcal{T}_h}\|i\omega\boldsymbol{J}+\omega^2\boldsymbol{E}_h-\boldsymbol{\nabla}\times(\boldsymbol{\chi}\boldsymbol{\nabla}\times\boldsymbol{E}_h)\|_K\|\boldsymbol{w}\|_K\\ &\quad+\sum_{F\in\mathcal{F}_h^{\mathrm{i}}}\|[\![\boldsymbol{\chi}\boldsymbol{\nabla}\times\boldsymbol{E}_h]\!]\times\boldsymbol{n}\|_F\|\boldsymbol{w}\times\boldsymbol{n}\|_F\\ &\lesssim \sum_{K\in\mathcal{T}_h}\frac{1}{\sqrt{\mu_{\widetilde{K},\max}}}\eta_{\mathbf{curl},K}\left(h_K^{-1}\|\boldsymbol{w}\|_K + h_K^{-1/2}\|\boldsymbol{w}\times\boldsymbol{n}\|_{\partial K}\right).\end{aligned}\tag{3.8}$$

Then, if $\boldsymbol{\phi} \in \boldsymbol{\mathcal{H}}^1(\mathcal{T}_h)\cap\boldsymbol{\mathcal{H}}_0(\mathbf{curl},\Omega)$, since $\mathcal{R}_h\boldsymbol{\phi}\in\boldsymbol{W}_h$, we can employ Galerkin orthogonality (3.2), (3.8) with $\boldsymbol{w}=\boldsymbol{\phi}-\mathcal{R}_h\boldsymbol{\phi}$ and (2.6), showing that

$$\begin{aligned}|b(\boldsymbol{E}-\boldsymbol{E}_h,\boldsymbol{\phi})| &= |b(\boldsymbol{E}-\boldsymbol{E}_h,\boldsymbol{\phi}-\mathcal{R}_h\boldsymbol{\phi})|\\ &\lesssim \sum_{K\in\mathcal{T}_h}\frac{1}{\sqrt{\mu_{\widetilde{K},\max}}}\eta_{\mathbf{curl},K}\left(h_K^{-1}\|\boldsymbol{\phi}-\mathcal{R}_h\boldsymbol{\phi}\|_K + h_K^{-1/2}\|(\boldsymbol{\phi}-\mathcal{R}_h\boldsymbol{\phi})\times\boldsymbol{n}\|_{\partial K}\right)\\ &\lesssim \sum_{K\in\mathcal{T}_h}\frac{1}{\sqrt{\mu_{\widetilde{K},\max}}}\eta_{\mathbf{curl},K}\|\boldsymbol{\nabla}\boldsymbol{\phi}\|_{\widetilde{K}} \lesssim \sum_{K\in\mathcal{T}_h}\eta_{\mathbf{curl},K}\|\boldsymbol{\nabla}\boldsymbol{\phi}\|_{\boldsymbol{\chi},\widetilde{K}} \lesssim \eta_{\mathbf{curl}}\|\boldsymbol{\nabla}\boldsymbol{\phi}\|_{\boldsymbol{\chi},\mathcal{T}_h}.\end{aligned}$$

□

Lemma 3.2 (General control of the residual)**.** *We have*

$$|b(\boldsymbol{E}-\boldsymbol{E}_h,\boldsymbol{\theta})| \lesssim \eta|\!|\!|\boldsymbol{\theta}|\!|\!|_{\mathbf{curl},\omega,\boldsymbol{\varepsilon},\boldsymbol{\chi},\Omega}\tag{3.9}$$

for all $\boldsymbol{\theta}\in\boldsymbol{\mathcal{H}}_0(\mathbf{curl},\Omega)$.

Proof. We first invoke Section 2.9, which yields the existence of $r\in\mathcal{H}^1_0(\Omega)$ and $\boldsymbol{\phi}\in\boldsymbol{\mathcal{H}}^1(\mathscr{P})\cap\boldsymbol{\mathcal{H}}_0(\mathbf{curl},\Omega)$ such that $\boldsymbol{\theta}=\boldsymbol{\nabla}r+\boldsymbol{\phi}$. In particular, we have $\boldsymbol{\phi}\in\boldsymbol{\mathcal{H}}^1(\mathcal{T}_h)\cap\boldsymbol{\mathcal{H}}_0(\mathbf{curl},\Omega)$, and hence employing (3.5), (3.6) as well as (2.8), we have

$$\begin{aligned}|b(\boldsymbol{E}-\boldsymbol{E}_h,\boldsymbol{\theta})| &\le |b(\boldsymbol{E}-\boldsymbol{E}_h,\boldsymbol{\nabla}r)| + |b(\boldsymbol{E}-\boldsymbol{E}_h,\boldsymbol{\phi})| \lesssim \eta_{\mathrm{div}}\omega\|\boldsymbol{\nabla}r\|_{\boldsymbol{\varepsilon},\Omega} + \eta_{\mathbf{curl}}\|\boldsymbol{\nabla}\boldsymbol{\phi}\|_{\boldsymbol{\chi},\mathcal{T}_h}\\ &\lesssim \eta_{\mathrm{div}}\omega\|\boldsymbol{\theta}\|_{\boldsymbol{\varepsilon},\Omega} + \eta_{\mathbf{curl}}\|\boldsymbol{\nabla}\times\boldsymbol{\theta}\|_{\boldsymbol{\chi},\Omega} \lesssim (\eta_{\mathrm{div}}+\eta_{\mathbf{curl}})|\!|\!|\boldsymbol{\theta}|\!|\!|_{\mathbf{curl},\omega,\boldsymbol{\varepsilon},\boldsymbol{\chi},\Omega},\end{aligned}$$

and (3.9) follows recalling that $\eta^2=\eta^2_{\mathrm{div}}+\eta^2_{\mathbf{curl}}$. □

The next step of the proof is an "Aubin-Nitsche" type result that we employ to estimate the error measured in the $\boldsymbol{\mathscr{L}}^2(\Omega)$-norm. This step is required to make up for the lack of coercivity of the sesquilinear form b.

Lemma 3.3 (Aubin-Nitsche)**.** *We have*

$$\omega\|\boldsymbol{E}-\boldsymbol{E}_h\|_{\boldsymbol{\varepsilon},\Omega} \lesssim (1+\gamma_{\mathrm{ba,E}})\eta.\tag{3.10}$$

Proof. We first introduce the Helmholtz decomposition of the error. Namely, we define p as the unique element of $H^1_0(\Omega)$ such that

$$(\boldsymbol{\varepsilon}\boldsymbol{\nabla} p, \boldsymbol{\nabla} v) = (\boldsymbol{\varepsilon}(\boldsymbol{E} - \boldsymbol{E}_h), \boldsymbol{\nabla} v) \qquad \forall v \in H^1_0(\Omega),$$

so that $\boldsymbol{E} - \boldsymbol{E}_h = \boldsymbol{\nabla} p + \boldsymbol{\theta}$, with $p \in H^1_0(\Omega)$ and $\boldsymbol{\theta} \in \boldsymbol{\mathcal{H}}(\mathrm{div}^0, \boldsymbol{\varepsilon}, \Omega)$. For the gradient part, we have

$$\omega^2 \|\boldsymbol{\nabla} p\|^2_{\boldsymbol{\varepsilon},\Omega} = \omega^2 \operatorname{Re}(\boldsymbol{\varepsilon}(\boldsymbol{E} - \boldsymbol{E}_h), \boldsymbol{\nabla} p) = -\operatorname{Re} b(\boldsymbol{E} - \boldsymbol{E}_h, \boldsymbol{\nabla} p) \lesssim \omega \eta_{\mathrm{div}} \|\boldsymbol{\nabla} p\|_{\boldsymbol{\varepsilon},\Omega},$$

so that $\omega \|\boldsymbol{\nabla} p\|_{\boldsymbol{\varepsilon},\Omega} \lesssim \eta_{\mathrm{div}}$.

For the divergence-free part, letting $\boldsymbol{\xi}$ be the unique element of $\boldsymbol{\mathcal{H}}_0(\mathbf{curl}, \Omega)$ such that $b(\boldsymbol{w}, \boldsymbol{\xi}) = \omega(\boldsymbol{w}, \boldsymbol{\varepsilon}\boldsymbol{\theta})$ for all $\boldsymbol{w} \in \boldsymbol{\mathcal{H}}_0(\mathbf{curl}, \Omega)$, we have

$$\begin{aligned}\omega \operatorname{Re}(\boldsymbol{\theta}, \boldsymbol{\varepsilon}\boldsymbol{\theta}) &= \omega \operatorname{Re}((\boldsymbol{E} - \boldsymbol{E}_h), \boldsymbol{\varepsilon}\boldsymbol{\theta}) - \omega \operatorname{Re}(\boldsymbol{\nabla} p, \boldsymbol{\varepsilon}\boldsymbol{\theta}) = \operatorname{Re} b(\boldsymbol{E} - \boldsymbol{E}_h, \boldsymbol{\xi}) - \omega \operatorname{Re}(\boldsymbol{\nabla} p, \boldsymbol{\varepsilon}\boldsymbol{\theta}) \\ &= \operatorname{Re} b(\boldsymbol{E} - \boldsymbol{E}_h, \boldsymbol{\xi} - \boldsymbol{\xi}_h) - \omega \operatorname{Re}(\boldsymbol{\nabla} p, \boldsymbol{\varepsilon}\boldsymbol{\theta}) \lesssim \eta |\!|\!| \boldsymbol{\xi} - \boldsymbol{\xi}_h |\!|\!|_{\mathbf{curl},\omega,\boldsymbol{\varepsilon},\boldsymbol{\chi},\Omega} + \omega \|\boldsymbol{\nabla} p\|_{\boldsymbol{\varepsilon},\Omega} \|\boldsymbol{\theta}\|_{\boldsymbol{\varepsilon},\Omega}\end{aligned}$$

for all $\boldsymbol{\xi}_h \in \boldsymbol{X}_h$. As $\boldsymbol{\theta} \in \boldsymbol{\mathcal{H}}(\mathrm{div}^0, \boldsymbol{\varepsilon}, \Omega)$, recalling definition (2.13a) of the approximation factor, it holds that

$$\omega \|\boldsymbol{\theta}\|^2_{\boldsymbol{\varepsilon},\Omega} \lesssim \omega \operatorname{Re}(\boldsymbol{\theta}, \boldsymbol{\varepsilon}\boldsymbol{\theta}) \lesssim (\gamma_{\mathrm{ba,E}} \eta + \omega \|\boldsymbol{\nabla} p\|_{\boldsymbol{\varepsilon},\Omega}) \|\boldsymbol{\theta}\|_{\boldsymbol{\varepsilon},\Omega},$$

and (3.10) follows. □

We close this section with the reliability estimate, that uses Gårding inequality (2.2).

Theorem 3.4 (Reliability)**.** *The following estimate holds true*

$$|\!|\!| \boldsymbol{E} - \boldsymbol{E}_h |\!|\!|_{\mathbf{curl},\omega,\boldsymbol{\varepsilon},\boldsymbol{\chi},\Omega} \lesssim (1 + \gamma_{\mathrm{ba,E}}) \eta.$$

Proof. Using (3.9), we have

$$\operatorname{Re} b(\boldsymbol{E} - \boldsymbol{E}_h, \boldsymbol{E} - \boldsymbol{E}_h) \lesssim \eta |\!|\!| \boldsymbol{E} - \boldsymbol{E}_h |\!|\!|_{\mathbf{curl},\omega,\boldsymbol{\varepsilon},\boldsymbol{\chi},\Omega}. \tag{3.11}$$

On the other hand, by using Gårding inequality (2.2), we have

$$|\!|\!| \boldsymbol{E} - \boldsymbol{E}_h |\!|\!|^2_{\mathbf{curl},\omega,\boldsymbol{\varepsilon},\boldsymbol{\chi},\Omega} \lesssim \operatorname{Re} b(\boldsymbol{E} - \boldsymbol{E}_h, \boldsymbol{E} - \boldsymbol{E}_h) + \omega^2 \|\boldsymbol{E} - \boldsymbol{E}_h\|^2_{\boldsymbol{\varepsilon},\Omega}, \tag{3.12}$$

and the result follows from (3.11), (3.12), Lemma 3.3 and the Young's inequality. □

3.4. **Efficiency.** In this section, we focus on efficiency estimates. Classically, the proofs rely on "bubble functions" and their key properties introduced in Section 2.7.

Lemma 3.5. *We have*

$$\eta_{\mathrm{div},K} \lesssim \omega \|\boldsymbol{E} - \boldsymbol{E}_h\|_{\boldsymbol{\varepsilon},\widetilde{K}} + \mathrm{osc}_{\mathrm{div},\mathcal{T}_{K,h}} \qquad \forall K \in \mathcal{T}_h. \tag{3.13}$$

Proof. Let $K \in \mathcal{T}_h$. We first notice that

$$\boldsymbol{\nabla} \cdot (\boldsymbol{J}_h - i\omega\boldsymbol{\varepsilon}\boldsymbol{E}_h) = \boldsymbol{\nabla} \cdot (\boldsymbol{J} - \boldsymbol{J}_h) - i\omega \boldsymbol{\nabla} \cdot (\boldsymbol{\varepsilon}(\boldsymbol{E} - \boldsymbol{E}_h)).$$

Recalling (2.7a) and (2.7b), after integration by parts, we have

$$\begin{aligned}\|\boldsymbol{\nabla} \cdot (\boldsymbol{J}_h - i\omega\boldsymbol{\varepsilon}\boldsymbol{E}_h)\|^2_K &\lesssim (b_K \boldsymbol{\nabla} \cdot (\boldsymbol{J}_h - i\omega\boldsymbol{\varepsilon}\boldsymbol{E}_h), \boldsymbol{\nabla} \cdot (\boldsymbol{J}_h - i\omega\boldsymbol{\varepsilon}\boldsymbol{E}_h))_K \\ &= (\boldsymbol{\nabla}(b_K \boldsymbol{\nabla} \cdot (\boldsymbol{J}_h - i\omega\boldsymbol{\varepsilon}\boldsymbol{E}_h)), i\omega\boldsymbol{\varepsilon}(\boldsymbol{E} - \boldsymbol{E}_h))_K + (b_K \boldsymbol{\nabla} \cdot (\boldsymbol{J}_h - i\omega\boldsymbol{\varepsilon}\boldsymbol{E}_h), \boldsymbol{\nabla} \cdot (\boldsymbol{J} - \boldsymbol{J}_h))_K \\ &\lesssim \sqrt{\varepsilon_{\widetilde{K},\max}} (\omega \|\boldsymbol{E} - \boldsymbol{E}_h\|_{\boldsymbol{\varepsilon},K} + \mathrm{osc}_{\mathrm{div},K}) h_K^{-1} \|\boldsymbol{\nabla} \cdot (\boldsymbol{J}_h - i\omega\boldsymbol{\varepsilon}\boldsymbol{E}_h)\|_K,\end{aligned}$$

so that

$$\frac{1}{\sqrt{\varepsilon_{\widetilde{K},\min}}} h_K \|\boldsymbol{\nabla} \cdot (\boldsymbol{J} - i\omega\boldsymbol{\varepsilon}\boldsymbol{E}_h)\|_K \lesssim \omega \|\boldsymbol{E} - \boldsymbol{E}_h\|_{\boldsymbol{\varepsilon},K} + \mathrm{osc}_{\mathrm{div},K}. \tag{3.14}$$

On the other hand, for $F \in \mathcal{F}_h^{\mathrm{i}} \cap \mathcal{F}_K$, we set $w_F := F_{\mathrm{ext}}(\,[\![\boldsymbol{\varepsilon}\boldsymbol{E}_h]\!]\cdot\boldsymbol{n}_F)b_F$. Then, recalling (2.7a) and that $b_F = 0$ on $\partial\widetilde{F}$, we have

$$\omega\|\,[\![\boldsymbol{\varepsilon}\boldsymbol{E}_h]\!]\cdot\boldsymbol{n}_F\|_F^2 \lesssim \omega|\langle\,[\![\boldsymbol{\varepsilon}\boldsymbol{E}_h]\!]\cdot\boldsymbol{n}_F, w_F\rangle_F| = \omega\left|\sum_{K'\in\mathcal{T}_{F,h}}\langle\boldsymbol{\varepsilon}\boldsymbol{E}_h\cdot\boldsymbol{n}_{K'}, w_F\rangle_{\partial K'}\right|$$
$$= \left|\sum_{K'\in\mathcal{T}_{F,h}}\left((i\omega\boldsymbol{\nabla}\cdot(\boldsymbol{\varepsilon}\boldsymbol{E}_h), w_F)_{K'} + i\omega(\boldsymbol{\varepsilon}\boldsymbol{E}_h, \boldsymbol{\nabla}w_F)_{K'}\right)\right|.$$

Recalling that $i\omega\boldsymbol{\nabla}\cdot(\boldsymbol{\varepsilon}\boldsymbol{E}) = \boldsymbol{J}$, we have

$$\omega\|\boldsymbol{\varepsilon}\,[\![\boldsymbol{E}_h]\!]\cdot\boldsymbol{n}_F\|_F^2 \lesssim \left|\sum_{K'\in\mathcal{T}_{F,h}}\left((\boldsymbol{\nabla}\cdot(\boldsymbol{J}-i\omega\boldsymbol{\varepsilon}\boldsymbol{E}_h), w_F)_{K'} + i\omega(\boldsymbol{\varepsilon}(\boldsymbol{E}-\boldsymbol{E}_h), \boldsymbol{\nabla}w_F)_{K'}\right)\right|,$$

and it follows from (2.7c) that

$$\frac{\omega h_F^{1/2}}{\sqrt{\varepsilon_{\widetilde{K},\min}}}\|\,[\![\boldsymbol{\varepsilon}\boldsymbol{E}_h]\!]\cdot\boldsymbol{n}_F\|_F \lesssim \frac{h_F}{\sqrt{\varepsilon_{\widetilde{K},\min}}}\|\boldsymbol{\nabla}\cdot(\boldsymbol{J}-i\omega\boldsymbol{\varepsilon}\boldsymbol{E}_h)\|_{\mathcal{T}_{F,h}} + \omega\|\boldsymbol{E}-\boldsymbol{E}_h\|_{\boldsymbol{\varepsilon},\widetilde{F}}. \tag{3.15}$$

Then, as $h_F \sim h_K$, (3.13) follows from definition (3.3) of η_{div}, (3.14) and (3.15). □

Lemma 3.6. *We have*

$$\eta_{\mathbf{curl},K} \lesssim \left(1+\frac{\omega h_K}{c_{\widetilde{K},\min}}\right)|\!|\!|\boldsymbol{E}-\boldsymbol{E}_h|\!|\!|_{\mathbf{curl},\omega,\boldsymbol{\varepsilon},\boldsymbol{\chi},\widetilde{K}} + \mathrm{osc}_{0,\mathcal{T}_{K,h}} \qquad \forall K\in\mathcal{T}_h. \tag{3.16}$$

Proof. For $K\in\mathcal{T}_h$, we set $\boldsymbol{r}_K := i\omega\boldsymbol{J}_h - \boldsymbol{\nabla}\times(\boldsymbol{\chi}\boldsymbol{\nabla}\times\boldsymbol{E}_h) + \omega^2\boldsymbol{\varepsilon}\boldsymbol{E}_h$. Thanks to (1.2), (2.7a), (2.7b) and after integrating by parts, we have

$$\begin{aligned}\|\boldsymbol{r}_K\|_K^2 &\lesssim (b_K\boldsymbol{r}_K, \boldsymbol{r}_K)_K = (\boldsymbol{r}_K, b_K\boldsymbol{r}_K)\\ &= (\boldsymbol{\chi}\boldsymbol{\nabla}\times(\boldsymbol{E}-\boldsymbol{E}_h), \boldsymbol{\nabla}\times(b_K\boldsymbol{r}_K))_K - \omega^2(\boldsymbol{\varepsilon}(\boldsymbol{E}-\boldsymbol{E}_h), b_K\boldsymbol{r}_K)_K - i\omega(\boldsymbol{J}-\boldsymbol{J}_h, b_K\boldsymbol{r}_K)_K\\ &\lesssim \left(\left(\frac{1}{\sqrt{\mu_{\widetilde{K},\min}}} + \sqrt{\varepsilon_{\widetilde{K},\max}}\omega h_K\right)|\!|\!|\boldsymbol{E}-\boldsymbol{E}_h|\!|\!|_{\mathbf{curl},\omega,\boldsymbol{\varepsilon},\boldsymbol{\chi},K} + \frac{1}{\sqrt{\mu_{\widetilde{K},\max}}}\mathrm{osc}_{0,K}\right)h_K^{-1}\|\boldsymbol{r}_K\|_K\end{aligned}$$

and then

$$\sqrt{\mu_{\widetilde{K},\max}}h_K\|i\omega\boldsymbol{J} - \boldsymbol{\nabla}\times(\boldsymbol{\chi}\boldsymbol{\nabla}\times\boldsymbol{E}_h) + \omega^2\boldsymbol{\varepsilon}\boldsymbol{E}_h\|_K \lesssim \left(1+\frac{\omega h_K}{c_{\widetilde{K},\min}}\right)|\!|\!|\boldsymbol{E}-\boldsymbol{E}_h|\!|\!|_{\mathbf{curl},\omega,\boldsymbol{\varepsilon},\boldsymbol{\chi},K} + \mathrm{osc}_{0,K}. \tag{3.17}$$

On the other hand, for $F\in\mathcal{F}_h^{\mathrm{i}}\cap\mathcal{F}_K$, we set $\boldsymbol{w}_F := \mathrm{F}_{\mathrm{ext}}(\,[\![\boldsymbol{\chi}\boldsymbol{\nabla}\times\boldsymbol{E}_h]\!]\times\boldsymbol{n}_F)b_F$. Then,

$$\|\,[\![\boldsymbol{\chi}\boldsymbol{\nabla}\times\boldsymbol{E}_h]\!]\times\boldsymbol{n}_F\|_F^2 \lesssim \langle\,[\![\boldsymbol{\chi}\boldsymbol{\nabla}\times\boldsymbol{E}_h]\!]\times\boldsymbol{n}_F, \boldsymbol{w}_F\rangle_F = \sum_{K'\in\mathcal{T}_{F,h}}\langle(\boldsymbol{\chi}\boldsymbol{\nabla}\times\boldsymbol{E}_h)\times\boldsymbol{n}_F, \boldsymbol{w}_F\rangle_{\partial K'}$$
$$= \sum_{K'\in\mathcal{T}_{F,h}}((-\boldsymbol{\nabla}\times(\boldsymbol{\chi}\boldsymbol{\nabla}\times\boldsymbol{E}_h), \boldsymbol{w}_F)_{K'} + (\boldsymbol{\chi}\boldsymbol{\nabla}\times\boldsymbol{E}_h, \boldsymbol{\nabla}\times\boldsymbol{w}_F)_{K'}),$$

thanks to (2.7a) and the fact that $b_F = 0$ on $\partial\widetilde{F}$. Since $i\omega\boldsymbol{J} = -\omega^2\boldsymbol{\varepsilon}\boldsymbol{E} + \boldsymbol{\nabla}\times(\boldsymbol{\chi}\boldsymbol{\nabla}\times\boldsymbol{E})$, we have

$$\|\,[\![\boldsymbol{\chi}\boldsymbol{\nabla}\times\boldsymbol{E}_h]\!]\times\boldsymbol{n}_F\|_F^2 \lesssim \sum_{K'\in\mathcal{T}_{F,h}}(-(\boldsymbol{\chi}\boldsymbol{\nabla}\times(\boldsymbol{E}-\boldsymbol{E}_h), \boldsymbol{\nabla}\times\boldsymbol{w}_F)_{K'} + \omega^2(\boldsymbol{\varepsilon}(\boldsymbol{E}-\boldsymbol{E}_h), \boldsymbol{w}_F)_{K'}$$
$$+ (\boldsymbol{r}_{K'}, \boldsymbol{w}_F)_{K'} + i\omega(\boldsymbol{J}-\boldsymbol{J}_h, \boldsymbol{w}_F)_{K'})$$

and it follows from (2.7c) that

(3.18)

$$\sqrt{\mu_{\widetilde{K},\max}}h_F^{1/2}\|[\![\boldsymbol{\chi}\boldsymbol{\nabla}\times\boldsymbol{E}_h]\!]\times\boldsymbol{n}_F\|_F \lesssim \sqrt{\mu_{\widetilde{K},\min}}h_F\|i\omega\boldsymbol{J}-\boldsymbol{\nabla}\times(\boldsymbol{\chi}\boldsymbol{\nabla}\times\boldsymbol{E}_h)+\omega^2\boldsymbol{\varepsilon}\boldsymbol{E}_h\|_{\mathcal{T}_{F,h}} + \left(1+\frac{\omega h_F}{c_{\widetilde{K},\min}}\right)|\!|\!|\boldsymbol{E}-\boldsymbol{E}_h|\!|\!|_{\mathbf{curl},\omega,\boldsymbol{\varepsilon},\boldsymbol{\chi},\widetilde{F}}+\operatorname{osc}_{0,\mathcal{T}_{F,h}}.$$

Thus, (3.16) follows from definition (3.4) of $\eta_{\mathbf{curl}}$, (3.17), (3.18) and the fact that $h_F\sim h_K$. □

We now state our efficiency estimate, that is a direct consequence of Lemmas 3.5 and 3.6.

Theorem 3.7 (Efficiency)**.** *We have*

$$\eta_K \lesssim \left(1+\frac{\omega h_K}{c_{\widetilde{K},\min}}\right)|\!|\!|\boldsymbol{E}-\boldsymbol{E}_h|\!|\!|_{\mathbf{curl},\omega,\boldsymbol{\varepsilon},\boldsymbol{\chi},\widetilde{K}}+\operatorname{osc}_{\mathcal{T}_{K,h}} \qquad \forall K\in\mathcal{T}_h.$$

4. First-order schemes

In this section, we analyze a family of discontinuous Galerkin schemes based on first-order formulation (2.4) of Maxwell's equations. The proofs of efficiency and reliability roughly follow the same path than for the second order schemes.

4.1. **Numerical scheme.** Following [3, 29, 39], the discrete problem consists in finding $(\boldsymbol{E}_h,\boldsymbol{H}_h)\in\boldsymbol{\mathcal{P}}_{k+1}(\mathcal{T}_h)\times\boldsymbol{\mathcal{P}}_{k+1}(\mathcal{T}_h)$ such that

$$b_h((\boldsymbol{E}_h,\boldsymbol{H}_h),(\boldsymbol{v}_h,\boldsymbol{w}_h))=i\omega(\boldsymbol{J},\boldsymbol{v}_h) \tag{4.1}$$

for all $\boldsymbol{v}_h,\boldsymbol{w}_h\in\boldsymbol{\mathcal{P}}_{k+1}(\mathcal{T}_h)$, where

$$b_h((\boldsymbol{E}_h,\boldsymbol{H}_h),(\boldsymbol{v},\boldsymbol{r})):=b((\boldsymbol{E}_h,\boldsymbol{H}_h),(\boldsymbol{v},\boldsymbol{r}))+\beta_h((\boldsymbol{E}_h,\boldsymbol{H}_h),(\boldsymbol{v},\boldsymbol{r})),$$

and β_h is a sesquilinear form over $\boldsymbol{\mathcal{P}}_{k+1}(\mathcal{T}_h)\times\boldsymbol{\mathcal{P}}_{k+1}(\mathcal{T}_h)$ that we call the "flux" form. We assume that if $\boldsymbol{e}_h,\boldsymbol{h}_h,\boldsymbol{v}_h^\dagger,\boldsymbol{w}_h^\dagger\in\boldsymbol{\mathcal{P}}_{k+1}(\mathcal{T}_h)$, then

$$\beta_h((\boldsymbol{e}_h,\boldsymbol{h}_h),(\boldsymbol{v}_h^\dagger,\boldsymbol{w}_h^\dagger))=0 \tag{4.2}$$

whenever $\boldsymbol{v}_h^\dagger\in\boldsymbol{\mathcal{H}}_0(\mathbf{curl},\Omega)$ and $\boldsymbol{w}_h^\dagger\in\boldsymbol{\mathcal{H}}(\mathbf{curl},\Omega)$. Essentially, we ask for the flux form to vanish for conforming test functions.

In practice, the sesquilinear form $\beta_h(\cdot,\cdot)$ is only employed with discrete arguments, in order to assemble the linear system associated with (4.1). However, in the context of abstract mathematical analysis, it is very convenient to extend the domain of definition of $\beta_h(\cdot,\cdot)$ and to apply it to "continuous" arguments as well. To simplify the discussion, we employ the notation $\mathbf{U}:=\boldsymbol{\mathcal{H}}_0(\mathbf{curl},\Omega)\times\boldsymbol{\mathcal{H}}(\mathbf{curl},\Omega)$ for the "energy" space of "continuous" functions, $\mathbf{D}_h:=\boldsymbol{\mathcal{P}}_{k+1}(\mathcal{T}_h)\times\boldsymbol{\mathcal{P}}_{k+1}(\mathcal{T}_h)$ for the "discrete" space of piecewise polynomial functions, and $\mathbf{S}_h:=\mathbf{U}+\mathbf{D}_h$. Because of assumption (4.2), we can consistently extend the domain of definition of $\beta_h(\cdot,\cdot)$ to $\mathbf{D}_h\times\mathbf{D}_h+\mathbf{S}_h\times\mathbf{U}$ by simply setting

$$\beta_h((\boldsymbol{e},\boldsymbol{h}),(\boldsymbol{v}^\dagger,\boldsymbol{w}^\dagger))=0 \tag{4.3}$$

for all $(\boldsymbol{e},\boldsymbol{h})\in\mathbf{S}_h$ and $(\boldsymbol{v}^\dagger,\boldsymbol{w}^\dagger)\in\mathbf{U}$.

Then, an immediate consequence of (4.3) is that the discrete form is consistent in the sense that

$$b_h((\boldsymbol{e},\boldsymbol{h}),(\boldsymbol{v},\boldsymbol{w}))=b((\boldsymbol{e},\boldsymbol{h}),(\boldsymbol{v},\boldsymbol{w})) \tag{4.4}$$

for all $(\boldsymbol{e},\boldsymbol{h})\in\mathbf{S}_h$, and $(\boldsymbol{v},\boldsymbol{w})\in\mathbf{U}$. In particular, observing that $\boldsymbol{W}_h\times\widetilde{\boldsymbol{W}}_h\subset\mathbf{U}$, the Galerkin orthogonality property

$$b_h((\boldsymbol{E}-\boldsymbol{E}_h,\boldsymbol{H}-\boldsymbol{H}_h),(\boldsymbol{v}_h^\dagger,\boldsymbol{w}_h^\dagger))=0 \tag{4.5}$$

holds true for all $\boldsymbol{v}_h^\dagger\in\boldsymbol{W}_h$ and $\boldsymbol{w}_h^\dagger\in\widetilde{\boldsymbol{W}}_h$, assuming $(\boldsymbol{E}_h,\boldsymbol{H}_h)$ solves (4.1).

4.2. **Examples of flux form.** After formally multiplying (2.3) by tests function $i\omega\overline{\boldsymbol{v}}_h, i\omega\overline{\boldsymbol{w}}_h \in \boldsymbol{\mathcal{P}}_{k+1}(\mathcal{T}_h)$ and integrating by parts locally in each element K, one obtain the formulation

$$b((\boldsymbol{E}_h,\boldsymbol{H}_h),(\boldsymbol{v}_h,\boldsymbol{w}_h)) + \sum_{K\in\mathcal{T}_h}\int_{\partial K}\boldsymbol{H}_h\cdot\overline{\boldsymbol{v}}_h\times\boldsymbol{n}_K + \sum_{K\in\mathcal{T}_h}\int_{\partial K}\boldsymbol{E}_h\cdot\overline{\boldsymbol{w}}_h\times\boldsymbol{n}_K = i\omega(\boldsymbol{J},\boldsymbol{v}_h). \tag{4.6}$$

Obviously, (4.6) is not a satisfactory discrete formulation, since no communication between separate elements of the mesh occur, all the considered functions being discontinuous. Following [3], the solution consists in replacing the traces of $\boldsymbol{E}_h$ and $\boldsymbol{H}_h$ by numerical fluxes $\boldsymbol{E}_h^\star$ and $\boldsymbol{H}_h^\star$, computed from $\boldsymbol{E}_h$ and $\boldsymbol{H}_h$, leading to

$$b((\boldsymbol{E}_h,\boldsymbol{H}_h),(\boldsymbol{v}_h,\boldsymbol{w}_h)) + \sum_{K\in\mathcal{T}_h}\int_{\partial K}\boldsymbol{H}_h^\star\cdot\overline{\boldsymbol{v}}_h\times\boldsymbol{n}_K + \sum_{K\in\mathcal{T}_h}\int_{\partial K}\boldsymbol{E}_h^\star\cdot\overline{\boldsymbol{w}}_h\times\boldsymbol{n}_K = i\omega(\boldsymbol{J},\boldsymbol{v}_h). \tag{4.7}$$

If the fluxes are single-valued on every face of the mesh, and if $\boldsymbol{H}_h^\star = \boldsymbol{o}$ on $\partial\Omega$, we may rewrite (4.7) with face-by-face integrals as

$$b((\boldsymbol{E}_h,\boldsymbol{H}_h),(\boldsymbol{v}_h,\boldsymbol{w}_h)) + \beta_h((\boldsymbol{E}_h,\boldsymbol{H}_h),(\boldsymbol{v}_h,\boldsymbol{w}_h)) = i\omega(\boldsymbol{J},\boldsymbol{v}_h)$$

with

$$\beta_h((\boldsymbol{E}_h,\boldsymbol{H}_h),(\boldsymbol{v}_h,\boldsymbol{w}_h)) := \sum_{F\in\mathcal{F}_h^{\mathrm{i}}}\int_F \boldsymbol{H}_h^\star\cdot\,[\![\overline{\boldsymbol{v}}_h]\!]\times\boldsymbol{n}_F + \sum_{F\in\mathcal{F}_h}\int_F \boldsymbol{E}_h^\star\cdot\,[\![\overline{\boldsymbol{w}}_h]\!]\times\boldsymbol{n}_F. \tag{4.8}$$

One readily sees that for any single-valued flux, the stabilization form $\beta_h(\cdot,\cdot)$ of (4.8) satisfies (4.2). As a result, the forthcoming analysis applies to a variety of DG schemes.

In particular, a rather general family of fluxes we cover reads

$$\boldsymbol{E}_h^\star := \frac{1}{\{\!\{Y\}\!\}}\left(\{\!\{Y\boldsymbol{E}_h\}\!\} + \frac{\alpha}{2}\,[\![\boldsymbol{H}_h]\!]\times\boldsymbol{n}\right),\quad \boldsymbol{H}_h^\star := \frac{1}{\{\!\{Z\}\!\}}\left(\{\!\{Z\boldsymbol{H}_h\}\!\} - \frac{\alpha}{2}\,[\![\boldsymbol{E}_h]\!]\times\boldsymbol{n}\right), \tag{4.9}$$

where Y, Z are piecewise constants weights, and $0\le\alpha\le 1$, see [43, §3.1.3]. We also refer the reader to [28, 29, 39]. These numerical fluxes are called centered fluxes for $\alpha = 0$ and upwind fluxes for $\alpha = 1$.

4.3. **Hybridization.** One asset of the scheme associated with any of the fluxes defined by (4.9) is that it is "hybridizable", which means that it can be equivalently rewritten with a Lagrange multiplier living on the faces of the mesh [24, 29, 36]. Such hybridized form is usually called hybrid discontinuous Galerkin (HDG), and exhibits less degrees of freedom than the "naive" formulation (4.1). It is thus well suited to speed up the solve of the associated linear system. Here, for the sake of simplicity, we focus on formulation (4.1), in particular for symmetry reasons with respect to the analysis of second-order schemes. Notice however, that since the hybridized system is an equivalent reformulation of (4.1), the proposed estimators apply equally well to HDG discretizations.

4.4. **Numerical solution.** As with conforming second-order schemes, it is an open question whether discrete problem (4.1) is well-posed for general meshes. The following analysis applies to any pair $(\boldsymbol{E}_h,\boldsymbol{H}_h)\in\boldsymbol{\mathcal{P}}_{k+1}(\mathcal{T}_h)\cap\boldsymbol{\mathcal{P}}_{k+1}(\mathcal{T}_h)$ satisfying (4.1). Again, unique solvability is not required.

We nevertheless mention [24] where the authors analyze (the hybridized version of) the method with upwind fluxes ((4.9) with $\alpha = 1$). They focus on a homogeneous media enclosed by impedance boundary conditions. In this setting, a key feature of the scheme is that it is well-posed without any assumption on the mesh size. While we work under slightly different assumptions here, we believe that this stability result indicates that the method is interesting for adaptivity techniques, since a coarse mesh may be used to start the algorithm.

4.5. **Error estimators.** For each $K \in \mathcal{T}_h$, the estimator is split into four parts

$$\eta_K^2 := \eta_{\mathrm{div},\boldsymbol{\varepsilon},K}^2 + \eta_{\mathrm{div},\boldsymbol{\mu},K}^2 + \eta_{\mathbf{curl},\boldsymbol{\varepsilon},K}^2 + \eta_{\mathbf{curl},\boldsymbol{\mu},K}^2,$$

where

$$\begin{aligned}
\eta_{\mathrm{div},\boldsymbol{\varepsilon},K} &:= \frac{1}{\sqrt{\varepsilon_{\widetilde{K},\min}}}\big(h_K\|\boldsymbol{\nabla}\cdot(\boldsymbol{J}-i\omega\boldsymbol{\varepsilon}\boldsymbol{E}_h)\|_K + \omega h_K^{1/2}\|\,[\![\boldsymbol{\varepsilon}\boldsymbol{E}_h]\!]\cdot\boldsymbol{n}\|_{\partial K\setminus\partial\Omega}\big),\\
\eta_{\mathrm{div},\boldsymbol{\mu},K} &:= \frac{1}{\sqrt{\mu_{\widetilde{K},\min}}}\big(\omega h_K\|\boldsymbol{\nabla}\cdot(\boldsymbol{\mu}\boldsymbol{H}_h)\|_K + \omega h_K^{1/2}\|\,[\![\boldsymbol{\mu}\boldsymbol{H}_h]\!]\cdot\boldsymbol{n}\|_{\partial K}\big),\\
\eta_{\mathbf{curl},\boldsymbol{\varepsilon},K} &:= \frac{1}{\sqrt{\varepsilon_{\widetilde{K},\max}}}\|\boldsymbol{J}-i\omega\boldsymbol{\varepsilon}\boldsymbol{E}_h+\boldsymbol{\nabla}\times\boldsymbol{H}_h\|_K + \sqrt{\mu_{\widetilde{K},\max}}\omega h_K^{1/2}\|\,[\![\boldsymbol{H}_h]\!]\times\boldsymbol{n}\|_{\partial K\setminus\partial\Omega},\\
\eta_{\mathbf{curl},\boldsymbol{\mu},K} &:= \frac{1}{\sqrt{\mu_{\widetilde{K},\max}}}\|i\omega\boldsymbol{\mu}\boldsymbol{H}_h+\boldsymbol{\nabla}\times\boldsymbol{E}_h\|_K + \sqrt{\varepsilon_{\widetilde{K},\max}}\omega h_K^{1/2}\|\,[\![\boldsymbol{E}_h]\!]\times\boldsymbol{n}\|_{\partial K}.
\end{aligned}$$

We also set $\eta^2 := \eta_{\mathrm{div}}^2 + \eta_{\mathbf{curl}}^2$ with

$$\eta_{\mathrm{div}}^2 := \sum_{K\in\mathcal{T}_h}\left(\eta_{\mathrm{div},\boldsymbol{\varepsilon},K}^2 + \eta_{\mathrm{div},\boldsymbol{\mu},K}^2\right), \qquad \eta_{\mathbf{curl}}^2 := \sum_{K\in\mathcal{T}_h}\left(\eta_{\mathbf{curl},\boldsymbol{\varepsilon},K}^2 + \eta_{\mathbf{curl},\boldsymbol{\mu},K}^2\right).$$

4.6. **Reliability.** We start by two lemmas where we show that the residual is controlled by the estimator.

Lemma 4.1 (Control of the residual)**.** *The estimates*

$$|b_h((\boldsymbol{E}-\boldsymbol{E}_h,\boldsymbol{H}-\boldsymbol{H}_h),(\boldsymbol{\nabla}u,\boldsymbol{\nabla}q))| \lesssim \omega\eta_{\mathrm{div}}\left(\|\boldsymbol{\nabla}p\|_{\boldsymbol{\varepsilon},\Omega}+\|\boldsymbol{\nabla}q\|_{\boldsymbol{\mu},\Omega}\right) \tag{4.10}$$

and

$$|b_h((\boldsymbol{E}-\boldsymbol{E}_h,\boldsymbol{H}-\boldsymbol{H}_h),(\boldsymbol{\phi},\boldsymbol{\psi}))| \lesssim \left(1+\max_{K\in\mathcal{T}_h}\frac{\omega h_K}{c_{\widetilde{K},\min}}\right)\eta_{\mathbf{curl}}\left(\|\boldsymbol{\nabla}\boldsymbol{\phi}\|_{\boldsymbol{\chi},\mathcal{T}_h}+\|\boldsymbol{\nabla}\boldsymbol{\psi}\|_{\boldsymbol{\zeta},\mathcal{T}_h}\right) \tag{4.11}$$

hold true for all $p\in\mathcal{H}_0^1(\Omega)$, $q\in\mathcal{H}^1(\Omega)$, $\boldsymbol{\phi}\in\boldsymbol{\mathcal{H}}^1(\mathcal{T}_h)\cap\boldsymbol{\mathcal{H}}_0(\mathbf{curl},\Omega)$ and $\boldsymbol{\psi}\in\boldsymbol{\mathcal{H}}^1(\mathcal{T}_h)\cap\boldsymbol{\mathcal{H}}(\mathbf{curl},\Omega)$.

Proof. We first establish (4.10). We observe that for any $v\in\mathcal{H}_0^1(\Omega)$, $w\in\mathcal{H}^1(\Omega)$, we have

$$b_h((\boldsymbol{E}-\boldsymbol{E}_h,\boldsymbol{H}-\boldsymbol{H}_h),(\boldsymbol{\nabla}v,\boldsymbol{\nabla}w)) = i\omega(\boldsymbol{J}-i\omega\boldsymbol{\varepsilon}\boldsymbol{E}_h,\boldsymbol{\nabla}v) - i\omega(i\omega\boldsymbol{\mu}\boldsymbol{H}_h,\boldsymbol{\nabla}w)$$

so that

$$\begin{aligned}
&\frac{1}{i\omega}b_h((\boldsymbol{E}-\boldsymbol{E}_h,\boldsymbol{H}-\boldsymbol{H}_h),(\boldsymbol{\nabla}v,\boldsymbol{\nabla}w))\\
&= -i\omega\langle\boldsymbol{\varepsilon}\boldsymbol{E}_h\cdot\boldsymbol{n},v\rangle_{\partial\mathcal{T}_h} - (\boldsymbol{\nabla}\cdot(\boldsymbol{J}-i\omega\boldsymbol{\varepsilon}\boldsymbol{E}_h),v)_{\mathcal{T}_h} - i\omega\langle\boldsymbol{\mu}\boldsymbol{H}_h\cdot\boldsymbol{n},w\rangle_{\partial\mathcal{T}_h} + i\omega(\boldsymbol{\nabla}\cdot(\boldsymbol{\mu}\boldsymbol{H}_h),w)_{\mathcal{T}_h}\\
&= -i\omega\langle\,[\![\boldsymbol{\varepsilon}\boldsymbol{E}_h]\!]\cdot\boldsymbol{n},v\rangle_{\mathcal{F}_h^{\mathrm{i}}} - (\boldsymbol{\nabla}\cdot(\boldsymbol{J}-i\omega\boldsymbol{\varepsilon}\boldsymbol{E}_h),v)_{\mathcal{T}_h} - i\omega\langle\,[\![\boldsymbol{\mu}\boldsymbol{H}_h]\!]\cdot\boldsymbol{n},w\rangle_{\mathcal{F}_h} + i\omega(\boldsymbol{\nabla}\cdot(\boldsymbol{\mu}\boldsymbol{H}_h),w)_{\mathcal{T}_h},
\end{aligned}$$

and therefore

$$\begin{aligned}
&\frac{1}{\omega}|b_h((\boldsymbol{E}-\boldsymbol{E}_h,\boldsymbol{H}-\boldsymbol{H}_h),(\boldsymbol{\nabla}v,\boldsymbol{\nabla}w))|\\
&\le \omega\sum_{F\in\mathcal{F}_h^{\mathrm{i}}}\|\,[\![\boldsymbol{\varepsilon}\boldsymbol{E}_h]\!]\cdot\boldsymbol{n}\|_F\|v\|_F + \omega\sum_{F\in\mathcal{F}_h}\|\,[\![\boldsymbol{\mu}\boldsymbol{H}_h]\!]\cdot\boldsymbol{n}\|_F\|w\|_F\\
&\quad+\sum_{K\in\mathcal{T}_h}\left(\|\boldsymbol{\nabla}\cdot(\boldsymbol{J}-i\omega\boldsymbol{\varepsilon}\boldsymbol{E}_h)\|_K\|v\|_K+\omega\|\boldsymbol{\nabla}\cdot(\boldsymbol{\mu}\boldsymbol{H}_h)\|_K\|w\|_K\right)\\
&\lesssim \sum_{K\in\mathcal{T}_h}\Big(\sqrt{\varepsilon_{\widetilde{K},\min}}\eta_{\mathrm{div},\boldsymbol{\varepsilon},K}\left(h_K^{-1}\|v\|_K+h_K^{-1/2}\|v\|_{\partial K\setminus\partial\Omega}\right)\\
&\qquad\qquad+\sqrt{\mu_{\widetilde{K},\min}}\eta_{\mathrm{div},\boldsymbol{\mu},K}\left(h_K^{-1}\|w\|_K+h_K^{-1/2}\|w\|_{\partial K}\right)\Big).
\end{aligned} \tag{4.12}$$

Now, let $p\in H_0^1(\Omega)$ and $q\in H^1(\Omega)$. Since $\boldsymbol{\nabla}(\mathcal{Q}_hp)\in\boldsymbol{W}_h$ and $\boldsymbol{\nabla}(\widetilde{\mathcal{Q}}_hq)\in\widetilde{\boldsymbol{W}}_h$, by Galerkin orthogonality (4.5), we can apply (4.12) with $v=p-\mathcal{Q}_hp$ and $w=q-\widetilde{\mathcal{Q}}_hq$ to show that

$$\frac{1}{\omega}|b_h((\boldsymbol{E}-\boldsymbol{E}_h,\boldsymbol{H}-\boldsymbol{H}_h),(\boldsymbol{\nabla}p,\boldsymbol{\nabla}q))|$$

$$
\begin{aligned}
&= |b_h((\boldsymbol{E}-\boldsymbol{E}_h, \boldsymbol{H}-\boldsymbol{H}_h), (\boldsymbol{\nabla}(p-\mathcal{Q}_h p), \boldsymbol{\nabla}(q-\widetilde{\mathcal{Q}}_h q)))| \\
&\lesssim \sum_{K\in\mathcal{T}_h} \left(\sqrt{\varepsilon_{\widetilde{K},\min}}\eta_{\mathrm{div},\boldsymbol{\varepsilon},K} \left(h_K^{-1}\|p-\mathcal{Q}_h p\|_K + h_K^{-1/2}\|p-\mathcal{Q}_h p\|_{\partial K\setminus\partial\Omega} \right) \right. \\
&\qquad \left. + \sqrt{\mu_{\widetilde{K},\min}}\eta_{\mathrm{div},\boldsymbol{\mu},K} \left(h_K^{-1}\|q-\widetilde{\mathcal{Q}}_h q\|_K + h_K^{-1/2}\|q-\widetilde{\mathcal{Q}}_h q\|_{\partial K} \right) \right) \\
&\lesssim \sum_{K\in\mathcal{T}_h} \left(\sqrt{\varepsilon_{\widetilde{K},\min}}\eta_{\mathrm{div},\boldsymbol{\varepsilon},K}\|\boldsymbol{\nabla} p\|_{\widetilde{K}} + \sqrt{\mu_{\widetilde{K},\min}}\eta_{\mathrm{div},\boldsymbol{\mu},K}\|\boldsymbol{\nabla} q\|_{\widetilde{K}} \right) \\
&\lesssim \eta_{\mathrm{div}} \left(\|\boldsymbol{\nabla} p\|_{\boldsymbol{\varepsilon},\Omega} + \|\boldsymbol{\nabla} q\|_{\boldsymbol{\mu},\Omega} \right),
\end{aligned}
$$

where we additionally employed (2.5). This shows (4.10).

We now focus on (4.11). Similarly, we start with arbitrary elements $\boldsymbol{v}\in\boldsymbol{\mathcal{H}}^1(\mathcal{T}_h)\cap\boldsymbol{\mathcal{H}}_0(\mathbf{curl},\Omega)$ and $\boldsymbol{w}\in\boldsymbol{\mathcal{H}}^1(\mathcal{T}_h)\cap\boldsymbol{\mathcal{H}}(\mathbf{curl},\Omega)$. We have

$$
\begin{aligned}
&b_h((\boldsymbol{E}-\boldsymbol{E}_h, \boldsymbol{H}-\boldsymbol{H}_h), (\boldsymbol{v},\boldsymbol{w})) \\
&= (i\omega\boldsymbol{J},\boldsymbol{v}) + (\omega^2\boldsymbol{\varepsilon}\boldsymbol{E}_h,\boldsymbol{v}) + (i\omega\boldsymbol{H}_h, \boldsymbol{\nabla}\times\boldsymbol{v}) + (\omega^2\boldsymbol{\mu}\boldsymbol{H}_h,\boldsymbol{w}) - (i\omega\boldsymbol{E}_h, \boldsymbol{\nabla}\times\boldsymbol{w}) \\
&= (i\omega\boldsymbol{J} + \omega^2\boldsymbol{\varepsilon}\boldsymbol{E}_h + i\omega\boldsymbol{\nabla}\times\boldsymbol{H}_h, \boldsymbol{v})_{\mathcal{T}_h} - i\omega\langle \boldsymbol{H}_h\times\boldsymbol{n}, \boldsymbol{v}\rangle_{\partial\mathcal{T}_h} \\
&\quad - i\omega(i\omega\boldsymbol{\mu}\boldsymbol{H}_h + \boldsymbol{\nabla}\times\boldsymbol{E}_h, \boldsymbol{w}) + i\omega\langle \boldsymbol{E}_h\times\boldsymbol{n}, \boldsymbol{w}\rangle_{\partial\mathcal{T}_h} \\
&= i\omega(\boldsymbol{J} - i\omega\boldsymbol{\varepsilon}\boldsymbol{E}_h + \boldsymbol{\nabla}\times\boldsymbol{H}_h, \boldsymbol{v})_{\mathcal{T}_h} - i\omega\langle [\![\boldsymbol{H}_h]\!]\times\boldsymbol{n}, \boldsymbol{v}\rangle_{\mathcal{F}_h^{\mathrm{i}}} \\
&\quad - i\omega(i\omega\boldsymbol{\mu}\boldsymbol{H}_h + \boldsymbol{\nabla}\times\boldsymbol{E}_h, \boldsymbol{w}) + i\omega\langle [\![\boldsymbol{E}_h]\!]\times\boldsymbol{n}, \boldsymbol{w}\rangle_{\mathcal{F}_h}
\end{aligned}
$$

and therefore

$$
\begin{aligned}
&|b_h((\boldsymbol{E}-\boldsymbol{E}_h, \boldsymbol{H}-\boldsymbol{H}_h), (\boldsymbol{v},\boldsymbol{w}))| \\
&\quad\le \sum_{K\in\mathcal{T}_h} (\omega\|\boldsymbol{J} - i\omega\boldsymbol{\varepsilon}\boldsymbol{E}_h + \boldsymbol{\nabla}\times\boldsymbol{H}_h\|_K\|\boldsymbol{v}\|_K + \omega\|i\omega\boldsymbol{\mu}\boldsymbol{H}_h + \boldsymbol{\nabla}\times\boldsymbol{E}_h\|_K\|\boldsymbol{w}\|_K) \\
&\qquad + \omega\sum_{F\in\mathcal{F}_h^{\mathrm{i}}} \|[\![\boldsymbol{H}_h]\!]\times\boldsymbol{n}\|_F\|\boldsymbol{v}\times\boldsymbol{n}\|_F + \omega\sum_{F\in\mathcal{F}_h} \|[\![\boldsymbol{E}_h]\!]\times\boldsymbol{n}\|_F\|\boldsymbol{w}\times\boldsymbol{n}\|_F \\
&\quad\lesssim \sum_{K\in\mathcal{T}_h} \left(1 + \frac{\omega h_K}{c_{\widetilde{K},\min}}\right) \left(\frac{1}{\sqrt{\mu_{\widetilde{K},\max}}}\eta_{\mathbf{curl},\boldsymbol{\varepsilon},K} \left(h_K^{-1}\|\boldsymbol{v}\|_K + h_K^{-1/2}\|\boldsymbol{v}\times\boldsymbol{n}\|_{\partial K\setminus\partial\Omega} \right) \right. \\
&\qquad\qquad \left. + \frac{1}{\sqrt{\varepsilon_{\widetilde{K},\max}}}\eta_{\mathbf{curl},\boldsymbol{\mu},K} \left(h_K^{-1}\|\boldsymbol{w}\|_K + h_K^{-1/2}\|\boldsymbol{w}\times\boldsymbol{n}\|_{\partial K} \right) \right).
\end{aligned} \tag{4.13}
$$

Let now $\boldsymbol{\phi}\in\boldsymbol{\mathcal{H}}^1(\mathcal{T}_h)\cap\boldsymbol{\mathcal{H}}_0(\mathbf{curl},\Omega)$ and $\boldsymbol{\psi}\in\boldsymbol{\mathcal{H}}^1(\mathcal{T}_h)\cap\boldsymbol{\mathcal{H}}(\mathbf{curl},\Omega)$. Since $\mathcal{R}_h\boldsymbol{\phi}\in\boldsymbol{W}_h$ and $\widetilde{\mathcal{R}}_h\boldsymbol{\psi}\in\widetilde{\boldsymbol{W}}_h$, by Galerkin orthogonality (4.5), we may employ (4.13) with $\boldsymbol{v}=\boldsymbol{\phi}-\mathcal{R}_h\boldsymbol{\phi}$, $\boldsymbol{w}=\boldsymbol{\psi}-\widetilde{\mathcal{R}}_h\boldsymbol{\psi}$ and (2.6), showing that

$$
\begin{aligned}
&|b_h((\boldsymbol{E}-\boldsymbol{E}_h, \boldsymbol{H}-\boldsymbol{H}_h), (\boldsymbol{\phi},\boldsymbol{\psi}))| = |b_h((\boldsymbol{E}-\boldsymbol{E}_h, \boldsymbol{H}-\boldsymbol{H}_h), (\boldsymbol{\phi}-\mathcal{R}_h\boldsymbol{\phi}, \boldsymbol{\psi}-\widetilde{\mathcal{R}}_h\boldsymbol{\psi}))| \\
&\lesssim \sum_{K\in\mathcal{T}_h} \left(1 + \frac{\omega h_K}{c_{\widetilde{K},\min}}\right) \left(\frac{1}{\sqrt{\mu_{\widetilde{K},\max}}}\eta_{\mathbf{curl},\boldsymbol{\varepsilon},K} \left(h_K^{-1}\|\boldsymbol{\phi}-\mathcal{R}_h\boldsymbol{\phi}\|_K + h_K^{-1/2}\|(\boldsymbol{\phi}-\mathcal{R}_h\boldsymbol{\phi})\times\boldsymbol{n}\|_{\partial K\setminus\partial\Omega} \right) \right. \\
&\qquad\qquad \left. + \frac{1}{\sqrt{\varepsilon_{\widetilde{K},\max}}}\eta_{\mathbf{curl},\boldsymbol{\mu},K} \left(h_K^{-1}\|\boldsymbol{\psi}-\widetilde{\mathcal{R}}_h\boldsymbol{\psi}\|_K + h_K^{-1/2}\|(\boldsymbol{\psi}-\widetilde{\mathcal{R}}_h\boldsymbol{\psi})\times\boldsymbol{n}\|_{\partial K} \right) \right) \\
&\lesssim \sum_{K\in\mathcal{T}_h} \left(1 + \frac{\omega h_K}{c_{\widetilde{K},\min}}\right) \left(\eta_{\mathbf{curl},\boldsymbol{\varepsilon},K}\|\boldsymbol{\nabla}\boldsymbol{\phi}\|_{\boldsymbol{\chi},\widetilde{K}} + \eta_{\mathbf{curl},\boldsymbol{\mu},K}\|\boldsymbol{\nabla}\boldsymbol{\psi}\|_{\boldsymbol{\zeta},\widetilde{K}} \right) \\
&\lesssim \left(1 + \max_{K\in\mathcal{T}_h} \frac{\omega h_K}{c_{\widetilde{K},\min}}\right) \eta_{\mathbf{curl}} \left(\|\boldsymbol{\nabla}\boldsymbol{\phi}\|_{\boldsymbol{\chi},\mathcal{T}_h} + \|\boldsymbol{\nabla}\boldsymbol{\psi}\|_{\boldsymbol{\zeta},\mathcal{T}_h} \right).
\end{aligned}
$$

□

Lemma 4.2 (General control of the residual)**.** *We have*

$$|b_h((\boldsymbol{E}-\boldsymbol{E}_h,\boldsymbol{H}-\boldsymbol{H}_h),(\boldsymbol{\theta},\boldsymbol{\vartheta}))| \lesssim \left(1+\max_{K\in\mathcal{T}_h}\frac{\omega h_K}{c_{\widetilde{K},\min}}\right)\eta\vertiii{(\boldsymbol{\theta},\boldsymbol{\vartheta})}_{\mathbf{curl},\omega,\Omega} \tag{4.14}$$

for all $\boldsymbol{\theta}\in\boldsymbol{\mathcal{H}}_0(\mathbf{curl},\Omega)$ *and* $\boldsymbol{\vartheta}\in\boldsymbol{\mathcal{H}}(\mathbf{curl},\Omega)$.

Proof. The results stated in Section 2.9 ensure the existence of $r\in\mathcal{H}^1_0(\Omega)$, $s\in\mathcal{H}^1(\Omega)$, $\boldsymbol{\phi}\in\boldsymbol{\mathcal{H}}^1(\mathscr{P})\cap\boldsymbol{\mathcal{H}}_0(\mathbf{curl},\Omega)$ and $\boldsymbol{\psi}\in\boldsymbol{\mathcal{H}}^1(\mathscr{P})\cap\boldsymbol{\mathcal{H}}(\mathbf{curl},\Omega)$ such that $\boldsymbol{\theta}=\boldsymbol{\nabla}r+\boldsymbol{\phi}$ and $\boldsymbol{\vartheta}=\boldsymbol{\nabla}s+\boldsymbol{\psi}$. Hence employing (4.10) and (4.11) as well as (2.8), we have

$$\begin{aligned}
|b_h((\boldsymbol{E}-\boldsymbol{E}_h,\boldsymbol{H}-\boldsymbol{H}_h),(\boldsymbol{\theta},\boldsymbol{\vartheta}))| &\le |b_h((\boldsymbol{E}-\boldsymbol{E}_h,\boldsymbol{H}-\boldsymbol{H}_h),(\boldsymbol{\nabla}r,\boldsymbol{\nabla}s))| + |b_h((\boldsymbol{E}-\boldsymbol{E}_h,\boldsymbol{H}-\boldsymbol{H}_h),(\boldsymbol{\phi},\boldsymbol{\psi}))|\\
&\lesssim \omega\eta_{\mathrm{div}}\left(\|\boldsymbol{\nabla}r\|_{\boldsymbol{\varepsilon},\Omega}+\|\boldsymbol{\nabla}s\|_{\boldsymbol{\mu},\Omega}\right)+\eta_{\mathbf{curl}}\left(\|\boldsymbol{\nabla}\boldsymbol{\phi}\|_{\boldsymbol{\chi},\mathcal{T}_h}+\|\boldsymbol{\nabla}\boldsymbol{\psi}\|_{\boldsymbol{\zeta},\mathcal{T}_h}\right)\\
&\lesssim \eta_{\mathrm{div}}\omega\left(\|\boldsymbol{\theta}\|_{\boldsymbol{\varepsilon},\Omega}+\|\boldsymbol{\vartheta}\|_{\boldsymbol{\mu},\Omega}\right)+\eta_{\mathbf{curl}}\left(\|\boldsymbol{\nabla}\times\boldsymbol{\theta}\|_{\boldsymbol{\chi},\Omega}+\|\boldsymbol{\nabla}\times\boldsymbol{\vartheta}\|_{\boldsymbol{\zeta},\Omega}\right)\\
&\lesssim \left(\eta_{\mathrm{div}}+\left(1+\max_{K\in\mathcal{T}_h}\frac{\omega h_K}{c_{\widetilde{K},\min}}\right)\eta_{\mathbf{curl}}\right)\vertiii{(\boldsymbol{\theta},\boldsymbol{\vartheta})}_{\mathbf{curl},\omega,\Omega},
\end{aligned}$$

and (4.14) follows recalling that $\eta^2:=\eta^2_{\mathrm{div}}+\eta^2_{\mathbf{curl}}$. □

As for the second-order schemes, the next step is an Aubin-Nitsche type result, that controls the $\boldsymbol{\mathscr{L}}^2(\Omega)$-norm of the error. To this end, we first state a result concerning the approximation factor for first-order schemes.

Lemma 4.3 (Approximation factor)**.** *For all* $\boldsymbol{j},\boldsymbol{l}\in\boldsymbol{\mathscr{L}}^2(\Omega)$*, there exists a unique pair* $(\boldsymbol{e}^\star,\boldsymbol{h}^\star)(\boldsymbol{j},\boldsymbol{l})\in\boldsymbol{\mathcal{H}}_0(\mathbf{curl},\Omega)\cap\boldsymbol{\mathcal{H}}(\mathbf{curl},\Omega)$ *such that*

$$b((\boldsymbol{v},\boldsymbol{w}),(\boldsymbol{e}^\star,\boldsymbol{h}^\star)(\boldsymbol{j},\boldsymbol{l}))=\omega(\boldsymbol{v},\boldsymbol{\varepsilon}\boldsymbol{j})+\omega(\boldsymbol{w},\boldsymbol{\mu}\boldsymbol{l}).$$

In addition, if $\boldsymbol{j}\in\boldsymbol{\mathcal{H}}(\mathrm{div}^0,\boldsymbol{\varepsilon},\Omega)$ *and* $\boldsymbol{l}\in\boldsymbol{\mathcal{H}}_0(\mathrm{div}^0,\boldsymbol{\mu},\Omega)$*, we have*

$$\inf_{\substack{\boldsymbol{e}_h\in\boldsymbol{W}_h\\ \boldsymbol{h}_h\in\widetilde{\boldsymbol{W}}_h}}\vertiii{(\boldsymbol{e}^\star,\boldsymbol{h}^\star)(\boldsymbol{j},\boldsymbol{l})-(\boldsymbol{e}_h,\boldsymbol{h}_h)}_{\mathbf{curl},\omega,\Omega}\lesssim\left(1+\gamma_{\mathrm{ba,E}}+\gamma_{\mathrm{ba,H}}\right)\left(\|\boldsymbol{j}\|_{\boldsymbol{\varepsilon},\Omega}+\|\boldsymbol{l}\|_{\boldsymbol{\mu},\Omega}\right). \tag{4.15}$$

Proof. Let $\boldsymbol{j},\boldsymbol{l}\in\boldsymbol{\mathscr{L}}^2(\Omega)$ and set $(\boldsymbol{e},\boldsymbol{h}):=(\boldsymbol{e}^\star,\boldsymbol{h}^\star)(\boldsymbol{j},\boldsymbol{l})$. We first observe that

$$-i\omega\boldsymbol{\nabla}\times\boldsymbol{h}=\omega\boldsymbol{\varepsilon}\boldsymbol{j}+\omega^2\overline{\boldsymbol{\varepsilon}}\boldsymbol{e},\qquad i\omega\boldsymbol{\nabla}\times\boldsymbol{e}=\omega\boldsymbol{\mu}\boldsymbol{l}+\omega^2\overline{\boldsymbol{\mu}}\boldsymbol{h}.$$

Then, considering $\boldsymbol{\phi}\in\boldsymbol{\mathcal{H}}(\mathbf{curl},\Omega)$ and $\boldsymbol{\psi}\in\boldsymbol{\mathcal{H}}_0(\mathbf{curl},\Omega)$, selecting the test functions $\boldsymbol{v}:=\boldsymbol{\zeta}\boldsymbol{\nabla}\times\boldsymbol{\phi}$ and $\boldsymbol{w}:=\boldsymbol{\chi}\boldsymbol{\nabla}\times\boldsymbol{\psi}$ and integrating by parts, we show that

$$b(\boldsymbol{\psi},\boldsymbol{e})=\omega(\boldsymbol{\psi},\boldsymbol{\varepsilon}\boldsymbol{j})+i(\overline{\boldsymbol{\mu}}\boldsymbol{\chi}\boldsymbol{\nabla}\times\boldsymbol{\psi},\boldsymbol{l}),\qquad \widetilde{b}(\boldsymbol{\phi},\boldsymbol{h})=\omega(\boldsymbol{\phi},\boldsymbol{\mu}\boldsymbol{l})-i(\overline{\boldsymbol{\varepsilon}}\boldsymbol{\zeta}\boldsymbol{\nabla}\times\boldsymbol{\phi},\boldsymbol{j}),$$

for all $\boldsymbol{\psi}\in\boldsymbol{\mathcal{H}}_0(\mathbf{curl},\Omega)$ and $\boldsymbol{\phi}\in\boldsymbol{\mathcal{H}}(\mathbf{curl},\Omega)$. At this point, it is tempting to use the approximation factors $\gamma_{\mathrm{ba,E}}$ and $\gamma_{\mathrm{ba,H}}$. However recalling (2.13), it is not possible yet, since the right-hand sides are not in $\boldsymbol{\mathscr{L}}^2(\Omega)$. The key idea then consists in "lifting" the last term in the above identities. To do so, we introduce $\boldsymbol{e}_0$ and $\boldsymbol{h}_0$ as the unique elements of $\boldsymbol{\mathcal{H}}_0(\mathbf{curl},\Omega)$ and $\boldsymbol{\mathcal{H}}(\mathbf{curl},\Omega)$ such that

$$2\omega^2(\boldsymbol{\varepsilon}\boldsymbol{\psi},\boldsymbol{e}_0)+b(\boldsymbol{\psi},\boldsymbol{e}_0)=i(\overline{\boldsymbol{\mu}}\boldsymbol{\chi}\boldsymbol{\nabla}\times\boldsymbol{\psi},\boldsymbol{l}),\qquad 2\omega^2(\boldsymbol{\mu}\boldsymbol{\phi},\boldsymbol{h}_0)+\widetilde{b}(\boldsymbol{\phi},\boldsymbol{h}_0)=-i(\overline{\boldsymbol{\varepsilon}}\boldsymbol{\zeta}\boldsymbol{\nabla}\times\boldsymbol{\phi},\boldsymbol{j}),$$

for all $\boldsymbol{\psi}\in\boldsymbol{\mathcal{H}}_0(\mathbf{curl},\Omega)$ and $\boldsymbol{\phi}\in\boldsymbol{\mathcal{H}}(\mathbf{curl},\Omega)$. As can be seen from (2.2), the left-hand sides correspond to coercive sesquilinear forms, and we have

$$\begin{aligned}
\vertiii{\boldsymbol{e}_0}^2_{\mathbf{curl},\omega,\boldsymbol{\varepsilon},\boldsymbol{\chi},\Omega}=\mathrm{Re}\left(2\omega^2(\boldsymbol{\varepsilon}\boldsymbol{e}_0,\boldsymbol{e}_0)+b(\boldsymbol{e}_0,\boldsymbol{e}_0)\right)&=\mathrm{Re}\,i(\boldsymbol{\chi}\overline{\boldsymbol{\mu}}\boldsymbol{\nabla}\times\boldsymbol{e}_0,\boldsymbol{l}),\\
&\lesssim\|\boldsymbol{\nabla}\times\boldsymbol{e}_0\|_{\boldsymbol{\chi},\Omega}\|\boldsymbol{l}\|_{\boldsymbol{\mu},\Omega}\lesssim\|\boldsymbol{l}\|_{\boldsymbol{\mu},\Omega}\vertiii{\boldsymbol{e}_0}_{\mathbf{curl},\omega,\boldsymbol{\varepsilon},\boldsymbol{\chi},\Omega}.
\end{aligned}$$

As a result, we have $\vertiii{\boldsymbol{e}_0}_{\mathbf{curl},\omega,\boldsymbol{\varepsilon},\boldsymbol{\chi},\Omega}\lesssim\|\boldsymbol{l}\|_{\boldsymbol{\mu},\Omega}$. Similar arguments show that $\vertiii{\boldsymbol{h}_0}_{\mathbf{curl},\omega,\boldsymbol{\mu},\boldsymbol{\zeta},\Omega}\lesssim\|\boldsymbol{j}\|_{\boldsymbol{\varepsilon},\Omega}$, and therefore

$$\vertiii{(\boldsymbol{e}_0,\boldsymbol{h}_0)}^2_{\mathbf{curl},\omega,\Omega}\lesssim\left(\|\boldsymbol{j}\|^2_{\boldsymbol{\varepsilon},\Omega}+\|\boldsymbol{l}\|^2_{\boldsymbol{\mu},\Omega}\right).$$

On the other hand, we see that

$$b(\boldsymbol{\psi},\boldsymbol{e}_0)=i(\overline{\boldsymbol{\mu}}\boldsymbol{\chi}\boldsymbol{\nabla}\times\boldsymbol{\psi},\boldsymbol{l})-2\omega^2(\boldsymbol{\varepsilon}\boldsymbol{\psi},\boldsymbol{e}_0),\qquad \widetilde{b}(\boldsymbol{\phi},\boldsymbol{h}_0)=-i(\overline{\boldsymbol{\varepsilon}}\boldsymbol{\zeta}\boldsymbol{\nabla}\times\boldsymbol{\phi},\boldsymbol{j})-2\omega^2(\boldsymbol{\mu}\boldsymbol{\phi},\boldsymbol{h}_0),$$

and therefore, letting $(\widetilde{\boldsymbol{e}},\widetilde{\boldsymbol{h}}) := (\boldsymbol{e},\boldsymbol{h}) - (\boldsymbol{e}_0,\boldsymbol{h}_0)$, we have

$$b(\boldsymbol{\psi},\widetilde{\boldsymbol{e}}) = \omega(\boldsymbol{\psi},\boldsymbol{\varepsilon}\boldsymbol{j}) + 2\omega^2(\boldsymbol{\varepsilon}\boldsymbol{\psi},\boldsymbol{e}_0) = \omega(\boldsymbol{\psi},\boldsymbol{\varepsilon}\widetilde{\boldsymbol{j}}),$$
$$\widetilde{b}(\boldsymbol{\phi},\widetilde{\boldsymbol{h}}) = \omega(\boldsymbol{\phi},\boldsymbol{\mu}\boldsymbol{l}) + 2\omega^2(\boldsymbol{\mu}\boldsymbol{\phi},\boldsymbol{h}_0) = \omega(\boldsymbol{\phi},\boldsymbol{\mu}\widetilde{\boldsymbol{l}}),$$

with $(\widetilde{\boldsymbol{j}},\widetilde{\boldsymbol{l}}) := (\boldsymbol{j},\boldsymbol{l}) + 2\omega(\boldsymbol{\varepsilon}^{-1}\overline{\boldsymbol{\varepsilon}}\boldsymbol{e}_0,\boldsymbol{\mu}^{-1}\overline{\boldsymbol{\mu}}\boldsymbol{h}_0)$.

Now, we observe that picking a gradient as a test function in the definition of $\boldsymbol{e}_0$ and $\boldsymbol{h}_0$ reveals that $\boldsymbol{e}_0 \in \boldsymbol{\mathcal{H}}(\mathrm{div}^0,\overline{\boldsymbol{\varepsilon}},\Omega)$ and $\boldsymbol{h}_0 \in \boldsymbol{\mathcal{H}}_0(\mathrm{div}^0,\overline{\boldsymbol{\mu}},\Omega)$. Hence $\boldsymbol{\varepsilon}^{-1}\overline{\boldsymbol{\varepsilon}}\boldsymbol{e}_0 \in \boldsymbol{\mathcal{H}}(\mathrm{div}^0,\boldsymbol{\varepsilon},\Omega)$ and $\boldsymbol{\mu}^{-1}\overline{\boldsymbol{\mu}}\boldsymbol{h}_0 \in \boldsymbol{\mathcal{H}}(\mathrm{div}^0,\boldsymbol{\mu},\Omega)$. As a result, we have

$$\begin{aligned}\inf_{\boldsymbol{e}_h\in\boldsymbol{W}_h} |\!|\!|\widetilde{\boldsymbol{e}}-\boldsymbol{e}_h|\!|\!|_{\mathbf{curl},\omega,\boldsymbol{\varepsilon},\boldsymbol{\chi},\Omega} &\le \gamma_{\mathrm{ba,E}}\|\widetilde{\boldsymbol{j}}\|_{\boldsymbol{\varepsilon},\Omega} \lesssim \gamma_{\mathrm{ba,E}}\left(\|\boldsymbol{j}\|_{\boldsymbol{\varepsilon},\Omega} + 2|\!|\!|\boldsymbol{e}_0|\!|\!|_{\mathbf{curl},\omega,\boldsymbol{\varepsilon},\boldsymbol{\chi},\Omega}\right)\\ &\lesssim \gamma_{\mathrm{ba,E}}\left(\|\boldsymbol{j}\|_{\boldsymbol{\varepsilon},\Omega} + \|\boldsymbol{l}\|_{\boldsymbol{\mu},\Omega}\right),\end{aligned}$$

and similarly

$$\inf_{\boldsymbol{h}_h\in\widetilde{\boldsymbol{W}}_h} |\!|\!|\widetilde{\boldsymbol{h}}-\boldsymbol{h}_h|\!|\!|_{\mathbf{curl},\omega,\boldsymbol{\mu},\boldsymbol{\zeta},\Omega} \lesssim \gamma_{\mathrm{ba,H}}\left(\|\boldsymbol{j}\|_{\boldsymbol{\varepsilon},\Omega} + \|\boldsymbol{l}\|_{\boldsymbol{\mu},\Omega}\right).$$

Now, (4.15) follows since

$$\begin{aligned}&\inf_{\substack{\boldsymbol{e}_h\in\boldsymbol{W}_h\\ \boldsymbol{h}_h\in\widetilde{\boldsymbol{W}}_h}} |\!|\!|(\boldsymbol{e},\boldsymbol{h})-(\boldsymbol{e}_h,\boldsymbol{h}_h)|\!|\!|_{\mathbf{curl},\omega,\Omega} = \inf_{\substack{\boldsymbol{e}_h\in\boldsymbol{W}_h\\ \boldsymbol{h}_h\in\widetilde{\boldsymbol{W}}_h}} |\!|\!|(\boldsymbol{e}_0,\boldsymbol{h}_0)+(\widetilde{\boldsymbol{e}},\widetilde{\boldsymbol{h}})-(\boldsymbol{e}_h,\boldsymbol{h}_h)|\!|\!|_{\mathbf{curl},\omega,\Omega}\\ &\le |\!|\!|(\boldsymbol{e}_0,\boldsymbol{h}_0)|\!|\!|_{\mathbf{curl},\omega,\Omega} + \inf_{\substack{\boldsymbol{e}_h\in\boldsymbol{W}_h\\ \boldsymbol{h}_h\in\widetilde{\boldsymbol{W}}_h}} |\!|\!|(\widetilde{\boldsymbol{e}},\widetilde{\boldsymbol{h}})-(\boldsymbol{e}_h,\boldsymbol{h}_h)|\!|\!|_{\mathbf{curl},\omega,\Omega}\\ &= |\!|\!|(\boldsymbol{e}_0,\boldsymbol{h}_0)|\!|\!|_{\mathbf{curl},\omega,\Omega} + \inf_{\boldsymbol{e}_h\in\boldsymbol{W}_h} |\!|\!|\widetilde{\boldsymbol{e}}-\boldsymbol{e}_h|\!|\!|_{\mathbf{curl},\omega,\boldsymbol{\varepsilon},\boldsymbol{\chi},\Omega} + \inf_{\boldsymbol{h}_h\in\widetilde{\boldsymbol{W}}_h} |\!|\!|\widetilde{\boldsymbol{h}}-\boldsymbol{h}_h|\!|\!|_{\mathbf{curl},\omega,\boldsymbol{\mu},\boldsymbol{\zeta},\Omega}\\ &\lesssim (1+\gamma_{\mathrm{ba,E}}+\gamma_{\mathrm{ba,H}})\left(\|\boldsymbol{j}\|_{\boldsymbol{\varepsilon},\Omega}+\|\boldsymbol{l}\|_{\boldsymbol{\mu},\Omega}\right).\end{aligned}$$

□

Lemma 4.4 (Aubin-Nitsche)**.** *We have*

$$\omega\|\boldsymbol{E}-\boldsymbol{E}_h\|_{\boldsymbol{\varepsilon},\Omega} + \omega\|\boldsymbol{H}-\boldsymbol{H}_h\|_{\boldsymbol{\mu},\Omega} \lesssim \left(1+\max_{K\in\mathcal{T}_h}\frac{\omega h_K}{c_{\widetilde{K},\min}}\right)(1+\gamma_{\mathrm{ba,E}}+\gamma_{\mathrm{ba,H}})\,\eta.$$

Proof. As in the second-order case, the proof relies on the Helmholtz decomposition of the error. We thus define $p \in H^1_0(\Omega)$ and $q \in H^1(\Omega)$ such that

$$(\boldsymbol{\varepsilon}\boldsymbol{\nabla}p,\boldsymbol{\nabla}v) = (\boldsymbol{\varepsilon}(\boldsymbol{E}-\boldsymbol{E}_h),\boldsymbol{\nabla}v), \qquad (\boldsymbol{\mu}\boldsymbol{\nabla}q,\boldsymbol{\nabla}w) = (\boldsymbol{\mu}(\boldsymbol{H}-\boldsymbol{H}_h),\boldsymbol{\nabla}w),$$

for all $v \in H^1_0(\Omega)$ and $q \in H^1(\Omega)$. Notice that p is uniquely defined and that q is defined up to constant, that does not contribute to its gradient. Then, we have

$$\boldsymbol{E}-\boldsymbol{E}_h = \boldsymbol{\nabla}p+\boldsymbol{\theta}, \qquad \boldsymbol{H}-\boldsymbol{H}_h = \boldsymbol{\nabla}q+\boldsymbol{\vartheta},$$

with $p \in H^1_0(\Omega)$, $q \in H^1(\Omega)$, $\boldsymbol{\theta} \in \boldsymbol{\mathcal{H}}(\mathrm{div}^0,\boldsymbol{\varepsilon},\Omega)$ and $\boldsymbol{\vartheta} \in \boldsymbol{\mathcal{H}}_0(\mathrm{div}^0,\boldsymbol{\mu},\Omega)$. For the gradient terms, we have

$$\begin{aligned}\omega^2\|\boldsymbol{\nabla}p\|^2_{\boldsymbol{\varepsilon},\Omega} + \omega^2\|\boldsymbol{\nabla}q\|^2_{\boldsymbol{\mu},\Omega} &= \omega^2\,\mathrm{Re}(\boldsymbol{\varepsilon}(\boldsymbol{E}-\boldsymbol{E}_h),\boldsymbol{\nabla}p) + \omega^2\,\mathrm{Re}(\boldsymbol{\mu}(\boldsymbol{H}-\boldsymbol{H}_h),\boldsymbol{\nabla}q)\\ &= -\,\mathrm{Re}\,b_h((\boldsymbol{E}-\boldsymbol{E}_h,\boldsymbol{H}-\boldsymbol{H}_h),(\boldsymbol{\nabla}p,\boldsymbol{\nabla}q)) \lesssim \omega\eta_{\mathrm{div}}(\|\boldsymbol{\nabla}p\|_{\boldsymbol{\varepsilon},\Omega}+\|\boldsymbol{\nabla}q\|_{\boldsymbol{\mu},\Omega}),\end{aligned}$$

so that

$$\omega\|\boldsymbol{\nabla}p\|_{\boldsymbol{\varepsilon},\Omega} + \omega\|\boldsymbol{\nabla}q\|_{\boldsymbol{\mu},\Omega} \lesssim \eta_{\mathrm{div}}. \tag{4.16}$$

For the remaining terms, we observe that

$$\begin{aligned}\omega\|\boldsymbol{\theta}\|^2_{\boldsymbol{\varepsilon},\Omega} + \omega\|\boldsymbol{\vartheta}\|^2_{\boldsymbol{\mu},\Omega} &= \mathrm{Re}\left(\omega(\boldsymbol{\varepsilon}\boldsymbol{\theta},\boldsymbol{\theta}) + \omega(\boldsymbol{\mu}\boldsymbol{\vartheta},\boldsymbol{\vartheta})\right) \lesssim \mathrm{Re}\left(\omega(\boldsymbol{\theta},\boldsymbol{\varepsilon}\boldsymbol{\theta}) + \omega(\boldsymbol{\vartheta},\boldsymbol{\mu}\boldsymbol{\vartheta})\right)\\ &= \mathrm{Re}\left(\omega(\boldsymbol{E}-\boldsymbol{E}_h,\boldsymbol{\varepsilon}\boldsymbol{\theta}) + \omega(\boldsymbol{H}-\boldsymbol{H}_h,\boldsymbol{\mu}\boldsymbol{\vartheta}) - \omega(\boldsymbol{\nabla}p,\boldsymbol{\varepsilon}\boldsymbol{\theta}) - \omega(\boldsymbol{\nabla}q,\boldsymbol{\mu}\boldsymbol{\vartheta})\right).\end{aligned}$$

Then, by Lemma 4.3, we may define $(\boldsymbol{\xi},\boldsymbol{\zeta})$ as the unique element of $\boldsymbol{\mathcal{H}}_0(\mathbf{curl},\Omega)\times\boldsymbol{\mathcal{H}}(\mathbf{curl},\Omega)$ such that

$$b((\boldsymbol{w},\boldsymbol{v}),(\boldsymbol{\xi},\boldsymbol{\zeta})) = \omega(\boldsymbol{w},\boldsymbol{\varepsilon}\boldsymbol{\theta}) + \omega(\boldsymbol{v},\boldsymbol{\mu}\boldsymbol{\vartheta})$$

for all $\boldsymbol{w}, \boldsymbol{v} \in \boldsymbol{\mathscr{L}}^2(\Omega)$. Using consistency property (4.4), Galerkin orthogonality (4.5) and (4.14), we have

$$\begin{aligned}\operatorname{Re}(\omega((\boldsymbol{E}-\boldsymbol{E}_h),\boldsymbol{\varepsilon\theta})+\omega((\boldsymbol{H}-\boldsymbol{H}_h),\boldsymbol{\mu\vartheta})) &= \operatorname{Re} b((\boldsymbol{E}-\boldsymbol{E}_h,\boldsymbol{H}-\boldsymbol{H}_h),(\boldsymbol{\xi},\boldsymbol{\zeta}))\\ &= \operatorname{Re} b_h((\boldsymbol{E}-\boldsymbol{E}_h,\boldsymbol{H}-\boldsymbol{H}_h),(\boldsymbol{\xi},\boldsymbol{\zeta})) = \operatorname{Re} b_h((\boldsymbol{E}-\boldsymbol{E}_h,\boldsymbol{H}-\boldsymbol{H}_h),(\boldsymbol{\xi}-\boldsymbol{\xi}_h,\boldsymbol{\zeta}-\boldsymbol{\zeta}_h))\\ &\lesssim \left(1+\max_{K\in\mathcal{T}_h}\frac{\omega h_K}{c_{\widetilde{K},\min}}\right)\eta|\!|\!|(\boldsymbol{\xi}-\boldsymbol{\xi}_h,\boldsymbol{\zeta}-\boldsymbol{\zeta}_h)|\!|\!|_{\mathbf{curl},\omega,\Omega}\end{aligned}$$

for all $\boldsymbol{\xi}_h \in \boldsymbol{W}_h$ and $\boldsymbol{\zeta}_h \in \widetilde{\boldsymbol{W}}_h$. Then, recalling (4.15), we deduce that

$$\begin{aligned}&\operatorname{Re}(\omega((\boldsymbol{E}-\boldsymbol{E}_h),\boldsymbol{\varepsilon\theta})+\omega((\boldsymbol{H}-\boldsymbol{H}_h),\boldsymbol{\mu\vartheta}))\\ &\qquad\lesssim\left(1+\max_{K\in\mathcal{T}_h}\frac{\omega h_K}{c_{\widetilde{K},\min}}\right)(1+\gamma_{\mathrm{ba,E}}+\gamma_{\mathrm{ba,H}})\,\eta(\|\boldsymbol{\theta}\|_{\boldsymbol{\varepsilon},\Omega}+\|\boldsymbol{\vartheta}\|_{\boldsymbol{\mu},\Omega}).\end{aligned}$$

Hence,

$$\begin{aligned}\omega\|\boldsymbol{\theta}\|^2_{\boldsymbol{\varepsilon},\Omega}+\omega\|\boldsymbol{\vartheta}\|^2_{\boldsymbol{\mu},\Omega} \lesssim \left(\left(1+\max_{K\in\mathcal{T}_h}\frac{\omega h_K}{c_{\widetilde{K},\min}}\right)(1+\gamma_{\mathrm{ba,E}}+\gamma_{\mathrm{ba,H}})\,\eta+\omega\|\boldsymbol{\nabla}p\|_{\boldsymbol{\varepsilon},\Omega}+\omega\|\boldsymbol{\nabla}q\|_{\boldsymbol{\mu},\Omega}\right)\\ \times(\|\boldsymbol{\theta}\|_{\boldsymbol{\varepsilon},\Omega}+\|\boldsymbol{\vartheta}\|_{\boldsymbol{\mu},\Omega}),\end{aligned}$$

and the result follows from (4.16). □

We are now ready to establish the main result of this section. Notice that contrary to second-order schemes, the estimate does not stem from a continuous-level Gårding inequality. The "electric-magnetic mismatch" part of the estimator is employed instead.

Theorem 4.5 (Reliability)**.** *The estimate*

$$|\!|\!|(\boldsymbol{E}-\boldsymbol{E}_h,\boldsymbol{H}-\boldsymbol{H}_h)|\!|\!|_{\mathbf{curl},\omega,\mathcal{T}_h}\lesssim\left(1+\max_{K\in\mathcal{T}_h}\frac{\omega h_K}{c_{\widetilde{K},\min}}\right)(1+\gamma_{\mathrm{ba,E}}+\gamma_{\mathrm{ba,H}})\,\eta \tag{4.17}$$

holds true.

Proof. We start by the observation that

$$\begin{aligned}\boldsymbol{\nabla}\times(\boldsymbol{E}-\boldsymbol{E}_h) &= -i\omega\boldsymbol{\mu}(\boldsymbol{H}-\boldsymbol{H}_h)-(i\omega\boldsymbol{\mu}\boldsymbol{H}_h+\boldsymbol{\nabla}\times\boldsymbol{E}_h),\\ \boldsymbol{\nabla}\times(\boldsymbol{H}-\boldsymbol{H}_h) &= i\omega\boldsymbol{\varepsilon}(\boldsymbol{E}-\boldsymbol{E}_h)-(\boldsymbol{J}-i\omega\boldsymbol{\varepsilon}\boldsymbol{E}_h+\boldsymbol{\nabla}\times\boldsymbol{H}_h),\end{aligned}$$

which immediately yields the estimates

$$\begin{aligned}\|\boldsymbol{\nabla}\times(\boldsymbol{E}-\boldsymbol{E}_h)\|_{\boldsymbol{\chi},\Omega}&\lesssim\omega\|\boldsymbol{H}-\boldsymbol{H}_h\|_{\boldsymbol{\mu},\Omega}+\sum_{K\in\mathcal{T}_h}\frac{1}{\sqrt{\mu_{\widetilde{K},\max}}}\|i\omega\boldsymbol{\mu}\boldsymbol{H}_h+\boldsymbol{\nabla}\times\boldsymbol{E}_h\|_K,\\ \|\boldsymbol{\nabla}\times(\boldsymbol{H}-\boldsymbol{H}_h)\|_{\boldsymbol{\zeta},\Omega}&\lesssim\omega\|\boldsymbol{E}-\boldsymbol{E}_h\|_{\boldsymbol{\varepsilon},\Omega}+\sum_{K\in\mathcal{T}_h}\frac{1}{\sqrt{\varepsilon_{\widetilde{K},\max}}}\|\boldsymbol{J}-i\omega\boldsymbol{\varepsilon}\boldsymbol{E}_h+\boldsymbol{\nabla}\times\boldsymbol{H}_h\|_K.\end{aligned}$$

Adding the last two inequalities, we have

$$\|\boldsymbol{\nabla}\times(\boldsymbol{E}-\boldsymbol{E}_h)\|_{\boldsymbol{\chi},\Omega}+\|\boldsymbol{\nabla}\times(\boldsymbol{H}-\boldsymbol{H}_h)\|_{\boldsymbol{\zeta},\Omega}\lesssim\omega\|\boldsymbol{E}-\boldsymbol{E}_h\|_{\boldsymbol{\varepsilon},\Omega}+\omega\|\boldsymbol{H}-\boldsymbol{H}_h\|_{\boldsymbol{\mu},\Omega}+\eta_{\mathbf{curl}}.$$

and (4.17) follows since we already estimated the $\boldsymbol{\mathscr{L}}^2(\Omega)$ terms in Lemma 4.4. □

4.7. **Efficiency.** We now show that the estimator proposed for DG discretizations is efficient. Classically, the proofs of this section hinge on the "bubble" functions introduced at Section 2.7.

We start by showing an upper bound for the "divergence" parts of the estimator, namely $\eta_{\mathrm{div},\boldsymbol{\varepsilon},K}$ and $\eta_{\mathrm{div},\boldsymbol{\mu},K}$. Notice that the definitions of $\eta_{\mathrm{div},\boldsymbol{\varepsilon},K}$ and $\eta_{\mathrm{div},K}$ from Section 3 are identical. As a result, we omit the proof of Lemma 4.6, as it is identical to the proof of Lemma 3.5, for the case of $\eta_{\mathrm{div},\boldsymbol{\varepsilon},K}$, and follows the same arguments for the case of $\eta_{\mathrm{div},\boldsymbol{\mu},K}$.

Lemma 4.6. *We have*

$$\eta_{\mathrm{div},\boldsymbol{\varepsilon},K} \lesssim \omega\|\boldsymbol{E}-\boldsymbol{E}_h\|_{\boldsymbol{\varepsilon},\widetilde{K}} + \mathrm{osc}_{\mathrm{div},\mathcal{T}_{K,h}}, \qquad \eta_{\mathrm{div},\boldsymbol{\mu},K} \lesssim \omega\|\boldsymbol{H}-\boldsymbol{H}_h\|_{\boldsymbol{\mu},\widetilde{K}}$$

for all $K \in \mathcal{T}_h$.

We now turn to the "rotation" parts of the estimator, which require increased attention.

Lemma 4.7. *We have*

$$\eta_{\mathbf{curl},\boldsymbol{\varepsilon},K} \lesssim \omega\|\boldsymbol{E}-\boldsymbol{E}_h\|_{\boldsymbol{\varepsilon},K} + \left(1+\frac{\omega h_K}{c_{\widetilde{K},\min}}\right)|\!|\!|\boldsymbol{H}-\boldsymbol{H}_h|\!|\!|_{\mathbf{curl},\omega,\boldsymbol{\mu},\boldsymbol{\zeta},\mathcal{T}_{K,h}} \tag{4.18a}$$

and

$$\eta_{\mathbf{curl},\boldsymbol{\mu},K} \lesssim \left(1+\frac{\omega h_K}{c_{\widetilde{K},\min}}\right)|\!|\!|\boldsymbol{E}-\boldsymbol{E}_h|\!|\!|_{\mathbf{curl},\omega,\boldsymbol{\varepsilon},\boldsymbol{\chi},\mathcal{T}_{K,h}} + \omega\|\boldsymbol{H}-\boldsymbol{H}_h\|_{\boldsymbol{\mu},K} \tag{4.18b}$$

for all $K \in \mathcal{T}_h$.

Proof. We only detail the proof of (4.18b), since (4.18a) is established similarly, given the "symmetry" of the formulation with respect to the electric and magnetic fields. We have

$$i\omega\boldsymbol{\mu}\boldsymbol{H}_h + \boldsymbol{\nabla}\times\boldsymbol{E}_h = -i\omega\boldsymbol{\mu}(\boldsymbol{H}-\boldsymbol{H}_h) - \boldsymbol{\mu}\boldsymbol{\chi}\boldsymbol{\nabla}\times(\boldsymbol{E}-\boldsymbol{E}_h).$$

As a result, it holds that

$$\|i\omega\boldsymbol{\mu}\boldsymbol{H}_h + \boldsymbol{\nabla}\times\boldsymbol{E}_h\|_K \le \sqrt{\mu_{K,\max}}\omega\|\boldsymbol{H}-\boldsymbol{H}_h\|_{\boldsymbol{\mu},K} + \frac{\mu_{K,\max}}{\sqrt{\mu_{K,\min}}}\|\boldsymbol{\nabla}\times(\boldsymbol{E}-\boldsymbol{E}_h)\|_{\boldsymbol{\chi},K}$$

and

$$\frac{1}{\sqrt{\mu_{\widetilde{K},\max}}}\|i\omega\boldsymbol{\mu}\boldsymbol{H}_h + \boldsymbol{\nabla}\times\boldsymbol{E}_h\|_K \lesssim \omega\|\boldsymbol{H}-\boldsymbol{H}_h\|_{\boldsymbol{\mu},K} + \|\boldsymbol{\nabla}\times(\boldsymbol{E}-\boldsymbol{E}_h)\|_{\boldsymbol{\chi},K}. \tag{4.19}$$

Then, for a face $F \in \mathcal{F}_K$, we set $\boldsymbol{w}_F := \mathrm{F}_{\mathrm{ext}}(\omega\,[\![\boldsymbol{E}_h]\!]\times\boldsymbol{n}_F)b_F$. With this notation, using (2.7a), and since $b_F = 0$ on $\partial\widetilde{F}$ and $\boldsymbol{E} \in \boldsymbol{\mathcal{H}}_0(\mathbf{curl},\Omega)$, we have

$$\begin{aligned}\omega^2\|\,[\![\boldsymbol{E}_h]\!]\times\boldsymbol{n}_F\|_F^2 \lesssim \omega\langle\,[\![\boldsymbol{E}_h]\!]\times\boldsymbol{n}_F,\boldsymbol{w}_F\rangle_F &= \omega\left|\sum_{K'\in\mathcal{T}_{F,h}}\langle(\boldsymbol{E}-\boldsymbol{E}_h)\times\boldsymbol{n}_{K'},\boldsymbol{w}_F\rangle_{\partial K'}\right| \\ &= \left|\sum_{K'\in\mathcal{T}_{F,h}}((\boldsymbol{E}-\boldsymbol{E}_h,\boldsymbol{\nabla}\times\boldsymbol{w}_F)_{K'} + (\boldsymbol{\nabla}\times(\boldsymbol{E}-\boldsymbol{E}_h),\boldsymbol{w}_F)_{K'})\right|.\end{aligned}$$

Then, it follows from (2.7c) that

$$\begin{aligned}&\omega^2\|\,[\![\boldsymbol{E}_h]\!]\times\boldsymbol{n}_F\|_F^2 \\ &\qquad\lesssim \left(\frac{1}{\sqrt{\varepsilon_{\widetilde{K},\min}}} + \sqrt{\mu_{\widetilde{K},\max}}\omega h_F\right)|\!|\!|\boldsymbol{E}-\boldsymbol{E}_h|\!|\!|_{\mathbf{curl},\omega,\boldsymbol{\varepsilon},\boldsymbol{\chi},\mathcal{T}_{F,h}}\left(h_F^{-1/2}\omega\|\,[\![\boldsymbol{E}_h]\!]\times\boldsymbol{n}_F\|_F\right).\end{aligned}$$

Thus, since $h_F \sim h_K$, (4.18b) follows from the definition of $\eta_{\mathbf{curl},\mu,K}$, (4.19) and (**??**). □

Our key efficiency estimate is a direct consequence of Lemmas 4.6 and 4.7.

Theorem 4.8 (Efficiency)**.** *The estimate*

$$\eta_K \lesssim \left(1+\frac{\omega h_K}{c_{\widetilde{K},\min}}\right)|\!|\!|(\boldsymbol{E}-\boldsymbol{E}_h,\boldsymbol{H}-\boldsymbol{H}_h)|\!|\!|_{\mathbf{curl},\omega,\mathcal{T}_{K,h}} + \mathrm{osc}_{\mathcal{T}_{K,h}}$$

holds true for all $K \in \mathcal{T}_h$.

5. Numerical experiments

In this section, we present three numerical examples in 2D with conforming Nédélec elements that illustrate our main findings. While the previous analysis was rigorously carried out in 3D, the key results also apply in 2D with the usual modifications for the curl operator.

In Experiments 5.1 and 5.2, we employ structured meshes. If $\Omega := (-L, L)^2$, is a square of size L, and given $h := 2L/n$, these meshes are defined by first introducing a $n \times n$ Cartesian grid of the domain and then, splitting each square of the grid into four triangles by joining the barycenter of the square with each of its vertices. On the other hand, Experiment 5.3 relies on unstructured meshes that are generated using the `MMG` software package [18].

5.1. **Analytical solution in a PEC cavity.** We consider the square $\Omega := (-1, 1)^2$, with coefficients $\boldsymbol{\varepsilon} := \boldsymbol{I}$ and $\mu := 1$. The source term is $\boldsymbol{J} := \boldsymbol{e}_1$, and the corresponding solution to (1.2) reads

$$\boldsymbol{E}(\boldsymbol{x}) = \frac{1}{\omega}\left(\frac{\cos(\omega \boldsymbol{x}_2)}{\cos\omega} - 1\right)\boldsymbol{e}_1. \tag{5.1}$$

As the problem under consideration does not feature absorption, there are resonance frequencies for which it is not well-posed. These resonances are attained at $\omega = k\pi/2$, $k \in \mathbb{N}^\star$, which is in agreement with (5.1).

We consider two sequences of frequencies to illustrate the influence of the approximation factor $\gamma_{\mathrm{ba,E}}$. On the one hand, we consider a series of frequencies tending towards the resonance frequency $\omega_{\mathrm{r}} = 3\pi/2$. On the other hand, a sequence of increasing frequency uniformly separated from the resonance set.

The first sequence of frequencies takes the form $\omega_\delta := \omega_{\mathrm{r}} + \delta(\pi/2)$ with $\delta = 1/2, 1/4, 1/8, \ldots, 1/64$. Figure 1 presents the corresponding results. The second sequence of frequencies reads $\omega_\ell := (\ell + 3/10) \times 2\pi$, for $\ell := 1, 2, 4, 8, 16, 32$. The corresponding results are reproduced on Figure 2.

Considering a fixed polynomial degree k, in both cases, one sees that when the frequency gets closer to the resonance value or is increased, the reliability constant is larger for coarse meshes. Asymptotically, when $h \to 0$ as the mesh is refined, the same effectivity index is achieved for all frequencies. This highlight our key theoretical finding, stating that the reliability and stability constants are independent of the frequency if the mesh is sufficiently refined.

On the other hand, if we compare different values of k, we see that the effectivity index decreases when k increases. This is expected, since the residual-estimator are not "polynomial-degree-robust" (see e.g. [11]). We also observe that the "asymptotic" effectivity index is achieved faster for higher values of k. This is in perfect accordance with our analysis (see in particular (A.15)), since the approximation factor decreases when k is increased for a fixed mesh.

5.2. **Analytical solution in a PML medium.** For this experiment, we still consider the square $\Omega_0 := (-1, 1)^2$, that we surround with a PML of length $\ell := 1/4$. Hence, the domain is $\Omega := (-1 - \ell, 1 + \ell)^2$. Following [6, 7, 33], the coefficients are defined as

$$\boldsymbol{\varepsilon} = \begin{pmatrix} d_2/d_1 & 0 \\ 0 & d_1/d_2 \end{pmatrix} \qquad \mu = d_1 d_2,$$

where $d_j := d_j(\boldsymbol{x}_j) := 1 + \sigma/(i\omega)\mathbf{1}_{\boldsymbol{x}_j > 1}$ with $\sigma = (3/4)\omega$. Notice that $\boldsymbol{\varepsilon} = \mathbf{I}$ and $\mu = 1$ inside Ω_0 and are only modified inside the PML.

We consider a plane wave travelling in the direction $\boldsymbol{d} := (\cos\phi, \sin\phi)$ and polarized along $\boldsymbol{p} := (\sin\phi, -\cos\phi)$, with $\phi = \pi/12$. We thus let $\boldsymbol{\xi}_\phi(\boldsymbol{x}) := \boldsymbol{p} e^{-i\omega \boldsymbol{d}\cdot\boldsymbol{x}}$. Then, we separate the "total" and "scattered" field regions with a cut off function $\chi(\boldsymbol{x}) := \widehat{\chi}(|\boldsymbol{x}|)$, where $\widehat{\chi}$ is the unique element of $C^2(\mathbb{R})$ such that $\widehat{\chi}(t) = 1$ if $t < 0.8$, $\widehat{\chi}(t) = 0$ if $t > 0.9$, and $\widehat{\chi}|_{[0.8,0.9]}$ is a polynomial of degree 5. All in all, the solution reads $\boldsymbol{E} := \chi\boldsymbol{\xi}_\phi$. The corresponding right-hand side, $\boldsymbol{J} := -\omega^2\boldsymbol{E} + \boldsymbol{\nabla}\times\boldsymbol{\nabla}\times\boldsymbol{E}$, is supported in the ring $0.8 \le |\boldsymbol{x}| \le 0.9$.

The effectivity indices obtained for different frequencies ω, mesh sizes h and polynomial degree k are plotted on Figure 3. The conclusions are similar to the previous experiment and perfectly illustrate our analysis. In particular, for a fixed k, the asymptotic effectivity index is independent of the frequency ω. We observe a preasymptotic range where the effectivity index is higher, that

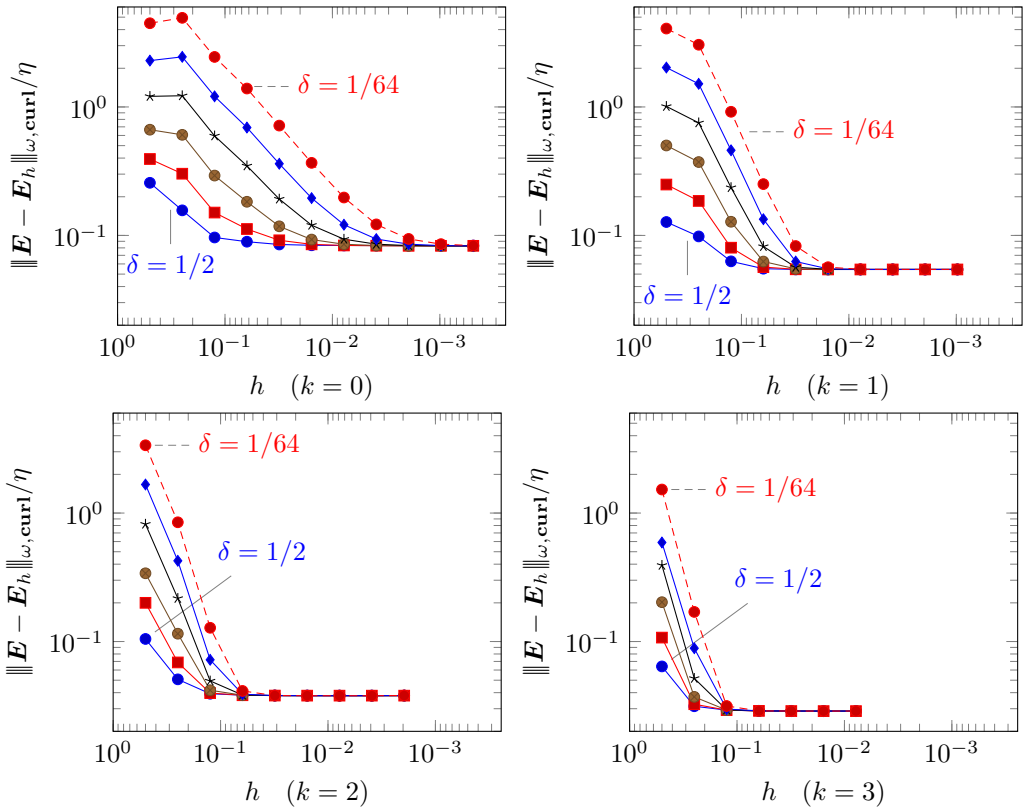

FIGURE 1. PEC cavity: near resonance example

corresponds to a large approximation factor $\gamma_{\mathrm{ba,E}}$. As expected, the asymptotic regime is achieved faster for higher values of k.

5.3. **Scattering by a penetrable obstacle.** We consider scattering by the penetrable obstacle $G := (-1/4, 1/4)^2$. We select Ω_0, the PMLs, and $\boldsymbol{J}$ as in Experiment 5.2, we also keep the definition of $\boldsymbol{\varepsilon}$ and μ in $\Omega \setminus G$, but set

$$\mu := \frac{1}{4} \qquad \boldsymbol{\varepsilon} := \begin{pmatrix} 8 & 0 \\ 0 & 32 \end{pmatrix}$$

in G. Here, the analytical solution is unavailable. Given $\boldsymbol{E}_h$ we then compute errors compared to $\widetilde{\boldsymbol{E}}$, where $\widetilde{\boldsymbol{E}}$ is computed on the same mesh than $\boldsymbol{E}_h$ with $k = 6$. Figure 4 presents the most accurate approximation of the solution computed for different frequencies.

The goal of this experiment is to analyze the ability of the proposed estimator to drive a mesh adaptive algorithm. In contrast to the previous experiments, we consider general unstructured meshes that are generated using the `MMG` software package [18]. This package takes as input an already existing mesh, and a set of maximal mesh sizes associated with each vertex of the input mesh. The output is a new mesh, locally refined in such way that the prescribed mesh sizes are respected. We use the `MMG` package, together with Dörfler's marking [20], to iteratively refine the mesh.

Algorithm 5.1 (Adaptive refinements)**.** *Specifically, our adaptive algorithm is as follows:*

- *Given a mesh $\mathcal{T}_h$, compute the associated discrete solution and estimators η_K.*
- *Order the elements K by decreasing values of η_K and constitute a set $\mathcal{M} \subset \mathcal{T}_h$ by adding the elements in the list until*

$$\sum_{K\in\mathcal{M}} \eta_K^2 \geq \theta \sum_{K\in\mathcal{T}_h} \eta_K^2$$

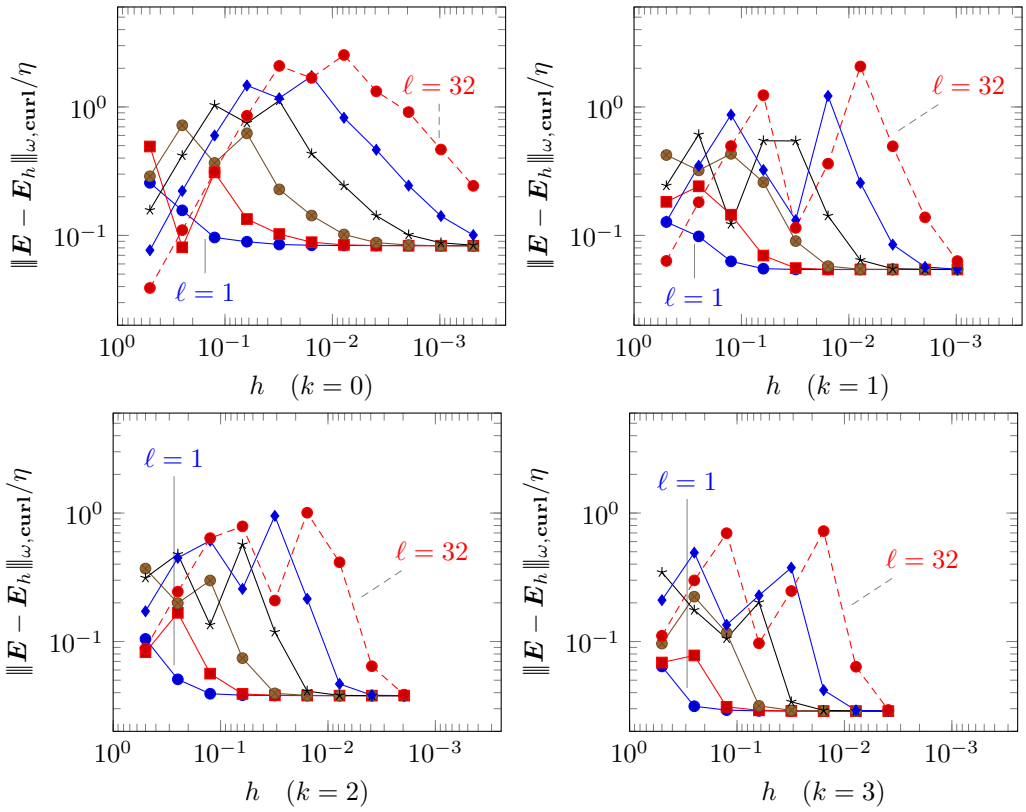

FIGURE 2. PEC cavity: high frequency example

where $\theta := 0.1$.

- *Associate with each element* $K \in \mathcal{T}_h$ *a "desired size"* $\widetilde{h}_K$. *This is done by setting* $\widetilde{h}_K := h_K/2$ *if* $K \in \mathcal{M}$, *and* $\widetilde{h}_K := h_K$ *otherwise.*
- *Associate with each vertex* $\boldsymbol{a} \in \mathcal{V}_h$ *a "desired size"* $\widetilde{h}_{\boldsymbol{a}}$ *that is the minimum of the desired size of the elements* $K \in \mathcal{T}_h$ *having* $\boldsymbol{a}$ *as a vertex.*
- *Use* `MMG` *with* $\mathcal{T}_h$ *and* $\{\widetilde{h}_{\boldsymbol{a}}\}_{\boldsymbol{a}\in\mathcal{V}_h}$ *to produce a new mesh* $\widetilde{\mathcal{T}}_h$.
- *Perform a new iteration with* $\mathcal{T}_h := \widetilde{\mathcal{T}}_h$.

On Figure 5, we present the initial mesh, as well as the meshes obtained after 10 iterations of Algorithm 5.1 for different values of k and ω. In all cases, the regions selected for refinements are understandable. On the top-left corner, the frequency is rather low, so that the cutoff function employed to inject the incident wave is the main source of fast oscillations. This area is clearly refined. Also, one clearly sees that the mesh is strongly refined in the vicinity of the corner of the scatterer, which is to be excepted, due to singularities [8, 16]. In the two bottom panels, we observe that the mesh is essentially refined inside the scatterer, and coarser inside the PML. On the one hand, it is perfectly suited for the mesh to be refined inside the scatterer, since the wavespeed is smaller (hence, the oscillation is more oscillatory) in this region. On the other hand, it is understandable that the mesh is coarse in the PML, as outgoing radiations are rapidly absorbed.

Figures 6 provides more quantitative results. On the one hand, we plot the relative error

$$\text{Error} := 100 \cdot \frac{\|\widetilde{\boldsymbol{E}} - \boldsymbol{E}_h\|_{\mathbf{curl},\omega,\boldsymbol{\varepsilon},\boldsymbol{\chi},\Omega}}{\|\widetilde{\boldsymbol{E}}\|_{\mathbf{curl},\omega,\boldsymbol{\varepsilon},\boldsymbol{\chi},\Omega}}$$

measured in percentage against the number of degrees of freedom N at each iteration. We see that asymptotically, the error behaves as $O(N^{-(k+1)/2})$, which is the optimal rate. This indicates that the produced meshes are optimal, and thus, adequately refined for all the frequencies and

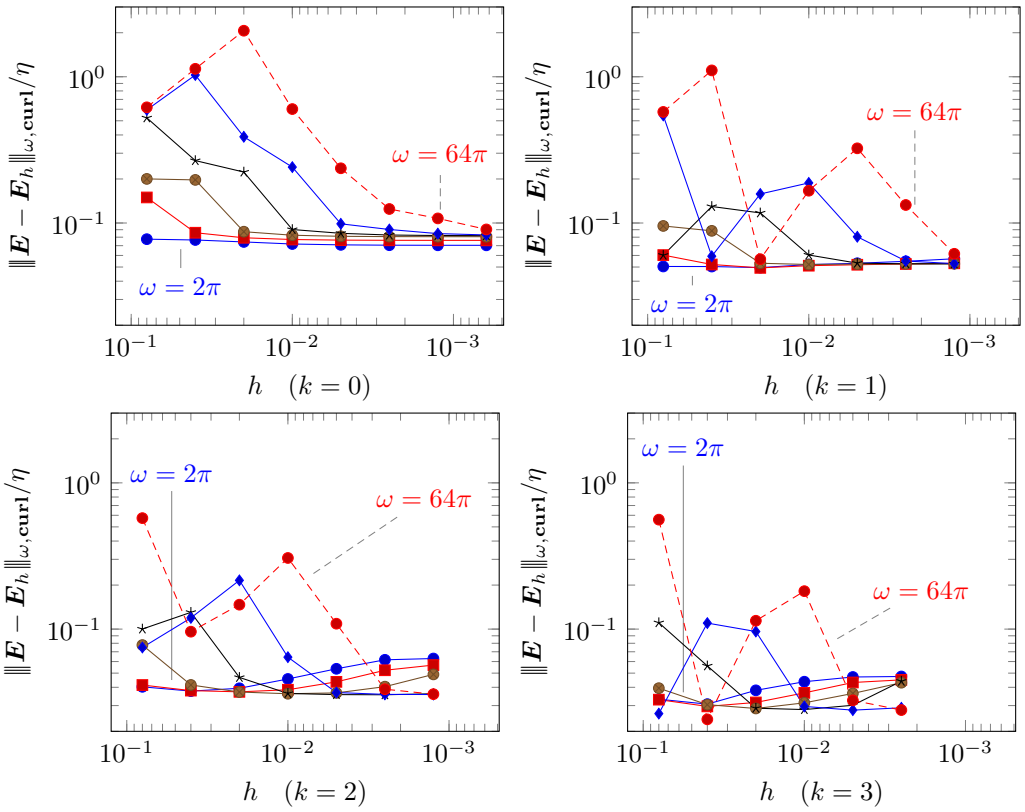

FIGURE 3. PML medium: plane wave in free space

polynomial degree considered. On the other hand, we also plot the effectivity index against the iteration number. The curves we obtain are similar to the one presented above for uniform meshes, and again comfort our key theoretical findings. Specifically, the error is underestimated on coarse meshes, and this under estimation is more pronounced for higher frequencies. Asymptotically however, the effectivity index becomes independent of the frequency.

6. Conclusion

We analyzed residual-based *a posteriori* error estimators for the discretization of time-harmonic Maxwell's equations in heterogeneous media. We have focused on (conforming) Nédélec finite element discretizations of the second-order formulation, and first-order discontinuous Galerkin methods. The novelty of our work is that we derive frequency-explicit reliability and efficiency estimates.

Our findings generalize previous results established for scalar wave propagation problems modeled by the Helmholtz equation. Specifically, we establish that the efficiency constant is independent of the frequency as soon as the number of degrees of freedom per wavelength is bounded from below. On the other hand, we show that the reliability constant is bounded independently of the frequency for sufficiently refined meshes, but can become large at high frequencies (or close to resonances) for coarse meshes and/or low polynomial degree.

We presented numerical experiments that highlight these key theoretical features. We produced three different test cases, including interior problems as well as scattering problems with perfectly matched layers. In all cases, the behavior of the estimator fits the theoretical predictions. Finally, the estimator has been employed to drive an adaptive refinement algorithm based on Dörfler marking. We obtained optimal convergence rates in terms of number of degrees of freedom, which indicate that the proposed estimator is perfectly suited for adaptivity purposes.

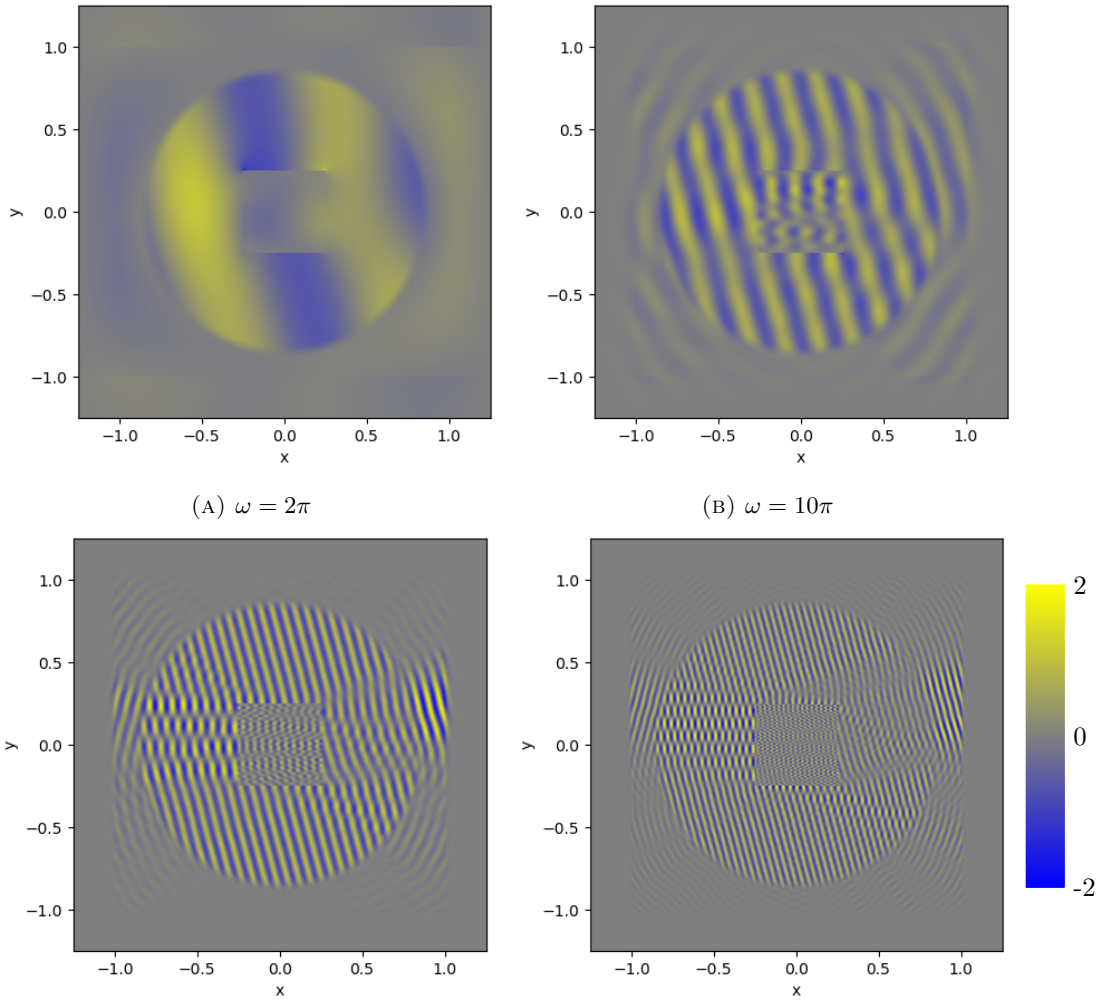

(A) $\omega = 2\pi$ (B) $\omega = 10\pi$

(C) $\omega = 30\pi$ (D) $\omega = 50\pi$

FIGURE 4. $\operatorname{Re} \widetilde{\boldsymbol{E}}_2$ computed at the last iteration of the adaptive algorithm

APPENDIX A. APPROXIMATION FACTOR

We consider the case where $\boldsymbol{\varepsilon} = \varepsilon \mathbf{I}_3$ and $\boldsymbol{\mu} = \mu \mathbf{I}_3$ for two real strictly positive constants $\varepsilon, \mu \in \mathbb{R}$, and Ω is of class $\mathcal{C}^{k+1,1}$. For the sake of shortness, we only consider the "electric" problem here, but the "magnetic" problem can be dealt with following the same procedure. In particular, notice that the shift-regularity results of Section A.3 below work for both types of boundary conditions.

A.1. **High-order Sobolev spaces.** In addition to the first-order Sobolev spaces introduced at Section 2.2. We will need, for $m \geq 0$, the high-order Sobolev space $\boldsymbol{\mathcal{H}}^m(\Omega)$ of functions $\boldsymbol{v} \in \boldsymbol{\mathscr{L}}^2(\Omega)$ such that $\partial^{|\alpha|}\boldsymbol{v}/\partial^\alpha \boldsymbol{x} \in \boldsymbol{\mathscr{L}}^2(\Omega)$ for all $|\alpha| \leq m$, see e.g. [1]. This space is equipped with the norm

$$\|\boldsymbol{v}\|_{\boldsymbol{\mathcal{H}}^m}^2 := \sum_{j=0}^{m} \left(\ell_\Omega^j \sum_{|\alpha|=j} \left\| \frac{\partial^{|\alpha|}\boldsymbol{v}}{\partial^\alpha \boldsymbol{x}} \right\|_\Omega^2 \right).$$

A.2. **High-order interpolation.** Following [22], and assuming that $0 \leq m \leq k$, we have

$$\|\boldsymbol{w} - \mathcal{R}_h \boldsymbol{w}\|_\Omega \leq \mathscr{C}_{\mathrm{i}} h^{m+1} \|\boldsymbol{w}\|_{\boldsymbol{\mathcal{H}}^{m+1}}, \qquad \|\boldsymbol{\nabla} \times (\boldsymbol{w} - \mathcal{R}_h \boldsymbol{w})\|_\Omega \leq \mathscr{C}_{\mathrm{i}} h^{m+1} \|\boldsymbol{\nabla} \times \boldsymbol{w}\|_{\boldsymbol{\mathcal{H}}^{m+1}}$$

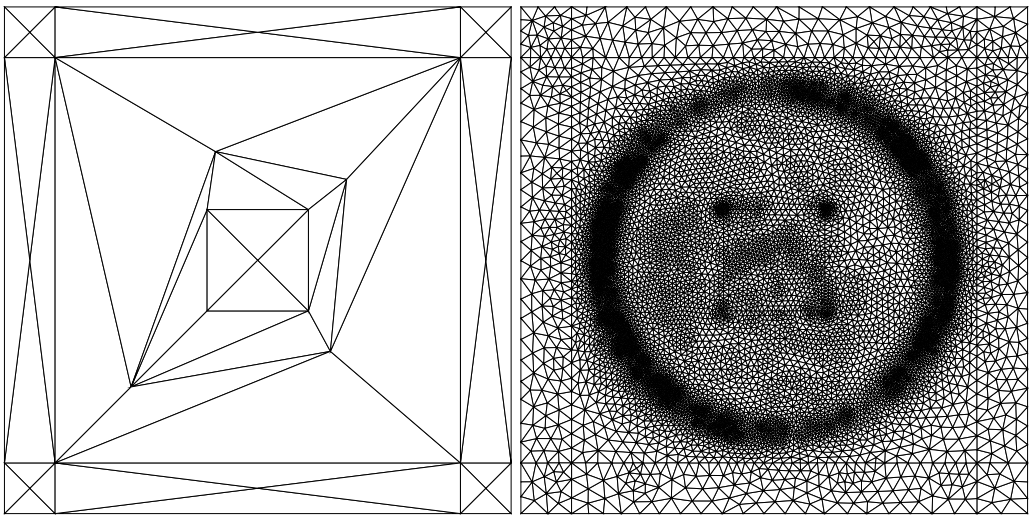

(A) Initial mesh (B) $k = 0$ and $\omega = 2\pi$

(C) $k = 1$ and $\omega = 30\pi$ (D) $k = 2$ and $\omega = 60\pi$

FIGURE 5. Initial mesh and mesh obtained at iteration 10 of the algorithm for different polynomial degrees and frequencies in Experiment 5.3

for all $\boldsymbol{w} \in \boldsymbol{\mathcal{H}}_0(\mathbf{curl}, \Omega) \cap \boldsymbol{\mathcal{H}}^{m+1}(\Omega)$, where the constant $\mathscr{C}_{\mathrm{i}}$ only depends on k and the shape-regularity parameter β.

A.3. **Regularity pick-up.** Let $\boldsymbol{v} \in \boldsymbol{\mathcal{H}}(\mathbf{curl}, \Omega) \cap \boldsymbol{\mathcal{H}}(\mathrm{div}^0, \Omega)$, with either $\boldsymbol{v} \times \boldsymbol{n} = \boldsymbol{o}$ or $\boldsymbol{v} \cdot \boldsymbol{n} = o$ on $\partial\Omega$. Then, for all $0 \le m \le k$, if $\boldsymbol{\nabla} \times \boldsymbol{v} \in \boldsymbol{\mathcal{H}}^m(\Omega)$, then we have $\boldsymbol{v} \in \boldsymbol{\mathcal{H}}^{m+1}(\Omega)$ with

$$\|\boldsymbol{v}\|_{\boldsymbol{\mathcal{H}}^{m+1}} \le \mathscr{C}_{\mathrm{shift}} \ell_\Omega \|\boldsymbol{\nabla} \times \boldsymbol{v}\|_{\boldsymbol{\mathcal{H}}^m}, \tag{A.1}$$

where the constant $\mathscr{C}_{\mathrm{shift}}$ only depends on Ω and k. We refer the reader to Corollary 3.7 of [26]. Notice in particular that if $m \le k-1$ and $\boldsymbol{u} \in \boldsymbol{\mathcal{H}}_0(\mathbf{curl}, \omega) \cap \boldsymbol{\mathcal{H}}(\mathrm{div}^0, \Omega)$ satisfies $\boldsymbol{\nabla} \times \boldsymbol{\nabla} \times \boldsymbol{u} \in \boldsymbol{\mathcal{H}}^m$, then

$$\|\boldsymbol{u}\|_{\boldsymbol{\mathcal{H}}^{m+2}} \le \mathscr{C}_{\mathrm{shift}}^2 \ell_\Omega^2 \|\boldsymbol{\nabla} \times \boldsymbol{\nabla} \times \boldsymbol{u}\|_{\boldsymbol{\mathcal{H}}^m}. \tag{A.2}$$

A.4. **Rescaling.** Let $\boldsymbol{j} \in \boldsymbol{\mathcal{H}}(\mathrm{div}^0, \Omega)$. Introducing $K := \omega \ell_\Omega / c$ and $\boldsymbol{g} := (\ell_\Omega / c)\boldsymbol{j}$, we may rewrite equation (2.10) defining $\boldsymbol{e} := \boldsymbol{e}^\star(\boldsymbol{j})$ as

$$-K^2 \boldsymbol{e} + \ell_\Omega^2 \boldsymbol{\nabla} \times \boldsymbol{\nabla} \times \boldsymbol{e} = K \boldsymbol{g}. \tag{A.3}$$

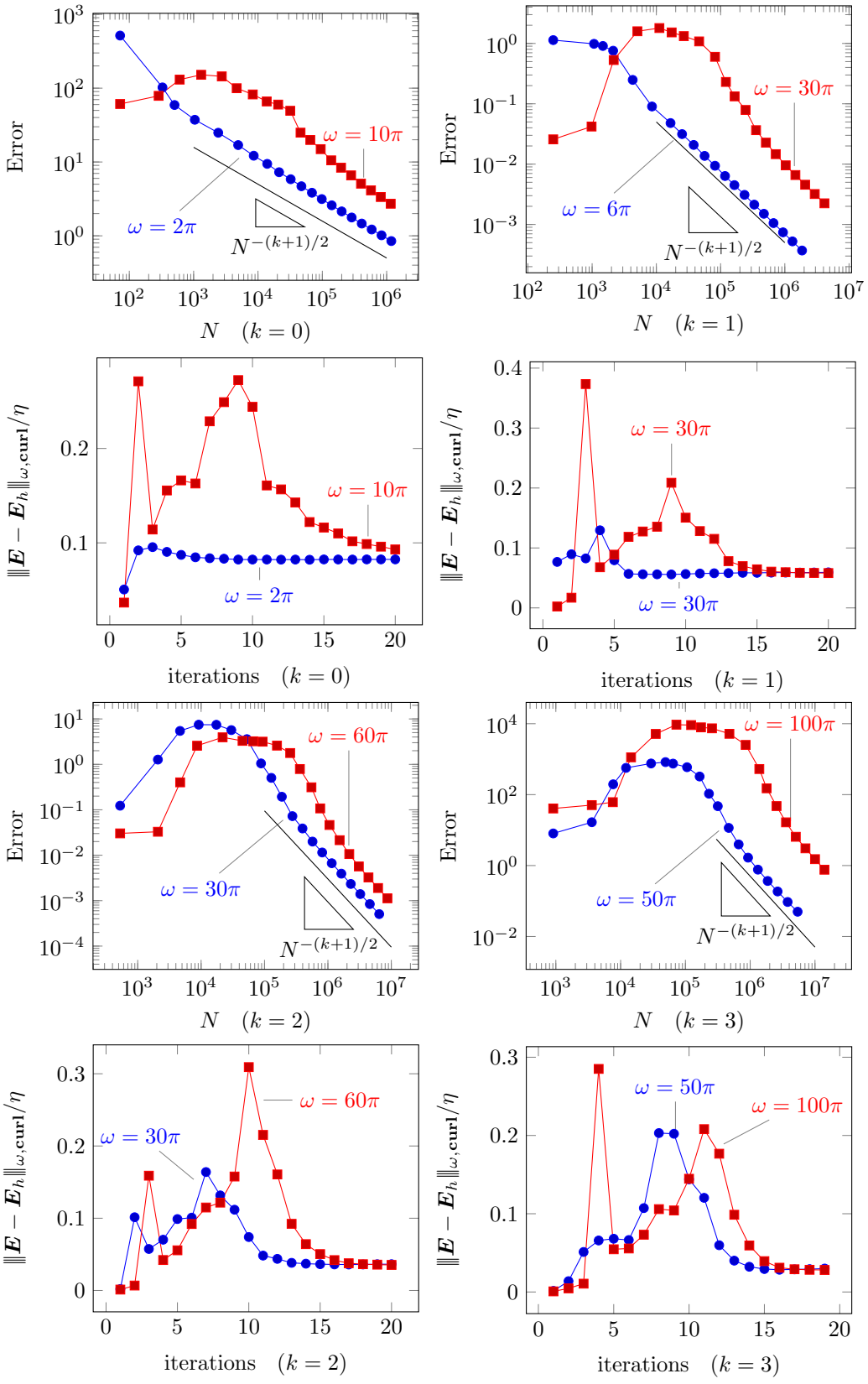

FIGURE 6. Scattering by a penetrable obstacle

In addition, it follows from (2.12) that

$$K^2\|\boldsymbol{e}\|_\Omega^2 + \ell_\Omega^2\|\boldsymbol{\nabla}\times\boldsymbol{e}\|_\Omega^2 \le \gamma_{\mathrm{s,E}}^2\|\boldsymbol{g}\|_\Omega^2. \tag{A.4}$$

A.5. **Stability.** The problem under consideration is self-adjoint, as we consider real-valued coefficients $\boldsymbol{\varepsilon}$ and $\boldsymbol{\mu}$. We may thus introduce a sequence of eigenpairs $\{(\lambda_j,\boldsymbol{\phi}_j)\}_{j\ge0}$ such that $\ell_\Omega^2\boldsymbol{\nabla}\times\boldsymbol{\nabla}\times\boldsymbol{\phi}_j = \lambda_j\boldsymbol{\phi}_j$. Classically, we chose the normalization $\|\boldsymbol{\phi}_j\|_\Omega = 1$, so that $\{\boldsymbol{\phi}_j\}_{j\ge0}$ and $\{\sqrt{\lambda_j}\boldsymbol{\phi}_j\}_{j\ge0}$ are orthonormal basis of $\boldsymbol{\mathcal{H}}(\mathrm{div}^0,\Omega)$ and $\boldsymbol{\mathcal{H}}_0(\mathbf{curl},\Omega)\cap\boldsymbol{\mathcal{H}}(\mathrm{div}^0,\Omega)$, respectively. We also introduce $D := \min_{j\ge0}|\sqrt{\lambda_j}-K|$, and $\delta := \min_{j\ge0}|\omega_j-\omega|$, with $\omega_j := c\sqrt{\lambda_j}/\ell_\Omega$.

Theorem A.1 (Stability)**.** *The estimates*

$$K\|\boldsymbol{e}\|_\Omega \le \frac{K}{D}\|\boldsymbol{g}\|_\Omega, \qquad \ell_\Omega\|\boldsymbol{\nabla}\times\boldsymbol{e}\|_\Omega \le \frac{K}{D}\|\boldsymbol{g}\|_\Omega \tag{A.5}$$

and

$$\gamma_{\mathrm{s,E}} \le \frac{\omega}{\delta}, \tag{A.6}$$

hold true.

Proof. Since $\boldsymbol{e},\boldsymbol{g}\in\boldsymbol{\mathcal{H}}(\mathrm{div}^0,\Omega)$, we may expand $\boldsymbol{e}$ and $\boldsymbol{g}$ in the basis $\{\boldsymbol{\phi}_j\}_{j\ge0}$ by letting $e_j := (\boldsymbol{e},\boldsymbol{\phi}_j)$ and $g_j := (\boldsymbol{e},\boldsymbol{\phi}_j)$. Then, we see from (A.3) that

$$|e_j| = \frac{K}{|\lambda_j-K^2|}|g_j| \le \frac{1}{D}\frac{K}{\sqrt{\lambda_j}+K}|g_j| \quad\text{and}\quad \left(K+\sqrt{\lambda_j}\right)|e_j| \le \frac{K}{D}|g_j|.$$

Then, (A.5) follows from

$$K^2\|\boldsymbol{e}\|_\Omega^2 + \ell_\Omega^2\|\boldsymbol{\nabla}\times\boldsymbol{e}\|_\Omega^2 = \sum_{j\ge0}(K^2+\lambda_j)|e_j|^2 \le \sum_{j\ge0}\left((K+\sqrt{\lambda_j})|e_j|\right)^2 \le \left(\frac{K}{D}\right)^2\|\boldsymbol{g}\|_\Omega^2.$$

Estimate (A.6) follows by multiplying the above estimate by χ/ℓ_Ω^2. □

A.6. **Basic regularity.** We first establish a basic regularity result for $\boldsymbol{e}$. Notice that while this result would be sufficient to derive sharp estimates when $k=0$, additional work is required for high-order methods.

Lemma A.2 (Basic regularity)**.** *We have*

$$K\|\boldsymbol{e}\|_{\boldsymbol{\mathcal{H}}^1} \le \mathscr{C}_{\mathrm{shift}}\gamma_{\mathrm{s,E}}K\|\boldsymbol{g}\|_{\boldsymbol{\mathcal{H}}^0}, \tag{A.7}$$

and

$$\ell_\Omega\|\boldsymbol{\nabla}\times\boldsymbol{e}\|_{\boldsymbol{\mathcal{H}}^1} \le \mathscr{C}_{\mathrm{shift}}(1+\gamma_{\mathrm{s,E}})K\|\boldsymbol{g}\|_{\boldsymbol{\mathcal{H}}^0}. \tag{A.8}$$

Proof. Shift estimate (A.1) and stability estimate (A.4) imply that

$$\|\boldsymbol{e}\|_{\boldsymbol{\mathcal{H}}^1} \le \mathscr{C}_{\mathrm{shift}}\ell_\Omega\|\boldsymbol{\nabla}\times\boldsymbol{e}\|_{\boldsymbol{\mathcal{H}}^0} \le \mathscr{C}_{\mathrm{shift}}\gamma_{\mathrm{s,E}}\|\boldsymbol{g}\|_{\boldsymbol{\mathcal{H}}^0},$$

and (A.7) follows. On the other hand, we establish (A.8) by

$$\begin{aligned}\ell_\Omega\|\boldsymbol{\nabla}\times\boldsymbol{e}\|_{\boldsymbol{\mathcal{H}}^1} &\le \mathscr{C}_{\mathrm{shift}}\ell_\Omega^2\|\boldsymbol{\nabla}\times\boldsymbol{\nabla}\times\boldsymbol{e}\|_{\boldsymbol{\mathcal{H}}^0}\\ &\le \mathscr{C}_{\mathrm{shift}}\left(K\|\boldsymbol{g}\|_{\boldsymbol{\mathcal{H}}^0} + K^2\|\boldsymbol{e}\|_{\boldsymbol{\mathcal{H}}^0}\right) \le \mathscr{C}_{\mathrm{shift}}(1+\gamma_{\mathrm{s,E}})K\|\boldsymbol{g}\|_{\boldsymbol{\mathcal{H}}^0}.\end{aligned}$$

□

A.7. **Expansion.** As we only have a limited regularity assumption for the right-hand side $\boldsymbol{g}$, we may not expect more regularity than established in Lemma A.2 for the associated solution $\boldsymbol{e}$. As shown in [13, 30] for the Helmholtz equation, the key idea is to introduce a "regularity splitting" of the solution. Here, we shall adapt the approach of [13] to Maxwell's equations, and consider the formal expansion

$$\boldsymbol{e} = \sum_{j\geq 0} K^j \boldsymbol{e}_j. \tag{A.9}$$

After identifying the powers in (A.3), one sees that $\boldsymbol{e}_0 := \boldsymbol{o}$, and that the other elements $\boldsymbol{e}_j \in \boldsymbol{\mathcal{H}}_0(\mathbf{curl},\Omega)\cap\boldsymbol{\mathcal{H}}(\mathrm{div}^0,\Omega)$ are iteratively defined through

$$\ell_\Omega^2 \boldsymbol{\nabla}\times\boldsymbol{\nabla}\times\boldsymbol{e}_1 = \boldsymbol{g}, \qquad \text{and} \qquad \ell_\Omega^2 \boldsymbol{\nabla}\times\boldsymbol{\nabla}\times\boldsymbol{e}_j = \boldsymbol{e}_{j-2} \tag{A.10}$$

for $j \geq 2$. We first show that the iterates in the sequence exhibit increasing regularity.

Lemma A.3 (Increasing regularity of the expansion)**.** *For all $j \geq 0$, we have $\boldsymbol{e}_j \in \boldsymbol{\mathcal{H}}^{j+1}(\Omega)$ and $\boldsymbol{\nabla}\times\boldsymbol{e}_j \in \boldsymbol{\mathcal{H}}^j(\Omega)$ with*

$$\|\boldsymbol{e}_j\|_{\boldsymbol{\mathcal{H}}^{j+1}} \leq \mathscr{C}_{\mathrm{shift}}^{j+1}\|\boldsymbol{g}\|_{\boldsymbol{\mathcal{H}}^0}, \tag{A.11}$$

and

$$\ell_\Omega\|\boldsymbol{\nabla}\times\boldsymbol{e}_j\|_{\boldsymbol{\mathcal{H}}^j} \leq \mathscr{C}_{\mathrm{shift}}^{j}\|\boldsymbol{g}\|_{\boldsymbol{\mathcal{H}}^0}. \tag{A.12}$$

Proof. We start with (A.12). It obviously holds for $j = 0$ as $\boldsymbol{e}_0 := \boldsymbol{o}$. For $j = 1$, recalling (A.10), we have

$$\ell_\Omega\|\boldsymbol{\nabla}\times\boldsymbol{e}_1\|_{\boldsymbol{\mathcal{H}}^1} \leq \mathscr{C}_{\mathrm{shift}}\ell_\Omega^2\|\boldsymbol{\nabla}\times\boldsymbol{\nabla}\times\boldsymbol{e}_1\|_{\boldsymbol{\mathcal{H}}^0} \leq \mathscr{C}_{\mathrm{shift}}\|\boldsymbol{g}\|_{\boldsymbol{\mathcal{H}}^0}.$$

Then, assuming that (A.12) holds up to some j, (A.1) and (A.10) reveal that

$$\ell_\Omega\|\boldsymbol{\nabla}\times\boldsymbol{e}_{j+2}\|_{\boldsymbol{\mathcal{H}}^{j+2}} \leq \mathscr{C}_{\mathrm{shift}}\ell_\Omega^2\|\boldsymbol{\nabla}\times\boldsymbol{\nabla}\times\boldsymbol{e}_{j+2}\|_{\boldsymbol{\mathcal{H}}^{j+1}} \leq \mathscr{C}_{\mathrm{shift}}^2\ell_\Omega\|\boldsymbol{\nabla}\times\boldsymbol{e}_j\|_{\boldsymbol{\mathcal{H}}^j} \leq \mathscr{C}_{\mathrm{shift}}^{j+2}\|\boldsymbol{g}\|_{\boldsymbol{\mathcal{H}}^0},$$

and (A.12) follows by induction.

On the other hand, (A.11) is a direct consequence of (A.12), since (A.1) shows that

$$\|\boldsymbol{e}_j\|_{\boldsymbol{\mathcal{H}}^{j+1}} \leq \mathscr{C}_{\mathrm{shift}}\ell_\Omega\|\boldsymbol{\nabla}\times\boldsymbol{e}_j\|_{\boldsymbol{\mathcal{H}}^j} \leq \mathscr{C}_{\mathrm{shift}}\left(\mathscr{C}_{\mathrm{shift}}^{j}\|\boldsymbol{g}\|_{\boldsymbol{\mathcal{H}}^0}\right).$$

□

So far, expansion (A.9) is only formal, and we need to cut the expansion into a finite sum. To do so, we introduce, for $\ell \geq 0$, the "residual" term

$$\boldsymbol{r}_\ell := \boldsymbol{e} - \sum_{j=0}^{\ell}\omega^j\boldsymbol{e}_j \in \boldsymbol{\mathcal{H}}_0(\mathbf{curl},\Omega)\cap\boldsymbol{\mathcal{H}}(\mathrm{div}^0,\Omega),$$

so that $\boldsymbol{e} = \sum_{j=0}^{\ell} K^j\boldsymbol{e}_j + \boldsymbol{r}_\ell$.

As we show next, these residuals have increasing regularity.

Lemma A.4 (Regularity of residual terms)**.** *We have*

$$K\|\boldsymbol{r}_\ell\|_{\boldsymbol{\mathcal{H}}^{\ell+1}} \leq \gamma_{\mathrm{s,E}}(\mathscr{C}_{\mathrm{shift}}K)^{\ell+1}\|\boldsymbol{g}\|_{\boldsymbol{\mathcal{H}}^0}, \tag{A.13}$$

and

$$\ell_\Omega\|\boldsymbol{\nabla}\times\boldsymbol{r}_\ell\|_{\boldsymbol{\mathcal{H}}^{\ell+1}} \leq (1+\gamma_{\mathrm{s,E}})(\mathscr{C}_{\mathrm{shift}}K)^{\ell+1}\|\boldsymbol{g}\|_{\boldsymbol{\mathcal{H}}^0}. \tag{A.14}$$

Proof. We have $\boldsymbol{r}_0 := \boldsymbol{e}$, so that (A.13) and (A.14) holds for $\ell = 0$ as a direct consequence of (A.7) and (A.8).

For the case $\ell = 1$, simple computations show that $\ell_\Omega^2\boldsymbol{\nabla}\times\boldsymbol{\nabla}\times\boldsymbol{r}_1 = K^2\boldsymbol{e}$. It then follows from (A.7) that

$$K\|\boldsymbol{r}_1\|_{\boldsymbol{\mathcal{H}}^2} \leq K\mathscr{C}_{\mathrm{shift}}^2\ell_\Omega^2\|\boldsymbol{\nabla}\times\boldsymbol{\nabla}\times\boldsymbol{r}_1\|_{\boldsymbol{\mathcal{H}}^0} \leq \mathscr{C}_{\mathrm{shift}}^2K^3\|\boldsymbol{e}\|_{\boldsymbol{\mathcal{H}}^0} \leq \gamma_{\mathrm{s,E}}\mathscr{C}_{\mathrm{shift}}^2K^2\|\boldsymbol{g}\|_{\boldsymbol{\mathcal{H}}^0},$$

and

$$\ell_\Omega\|\boldsymbol{\nabla}\times\boldsymbol{r}_1\|_{\boldsymbol{\mathcal{H}}^2} \leq \mathscr{C}_{\mathrm{shift}}\ell_\Omega^2\|\boldsymbol{\nabla}\times\boldsymbol{\nabla}\times\boldsymbol{r}_1\|_{\boldsymbol{\mathcal{H}}^1} \leq \mathscr{C}_{\mathrm{shift}}K^2\|\boldsymbol{e}\|_{\boldsymbol{\mathcal{H}}^1} \leq \gamma_{\mathrm{s,E}}\mathscr{C}_{\mathrm{shift}}^2K^2\|\boldsymbol{g}\|_{\boldsymbol{\mathcal{H}}^0},$$

so that (A.13) and (A.14) are also valid when $\ell = 1$.

For the general case, we first observe that $\ell_\Omega^2 \boldsymbol{\nabla} \times \boldsymbol{\nabla} \times \boldsymbol{r}_{\ell+2} = K^2 \boldsymbol{r}_\ell$. Therefore, using (A.1) and (A.2), we have

$$\|\boldsymbol{r}_{\ell+2}\|_{\boldsymbol{\mathcal{H}}^{\ell+3}} \leq \mathscr{C}_{\rm shift}^2 K^2 \|\boldsymbol{r}_\ell\|_{\boldsymbol{\mathcal{H}}^{\ell+1}},$$

and

$$\begin{aligned}\ell_\Omega \|\boldsymbol{\nabla} \times \boldsymbol{r}_{\ell+2}\|_{\boldsymbol{\mathcal{H}}^{\ell+3}} &\leq \mathscr{C}_{\rm shift} \ell_\Omega^2 \|\boldsymbol{\nabla} \times \boldsymbol{\nabla} \times \boldsymbol{r}_{\ell+2}\|_{\boldsymbol{\mathcal{H}}^{\ell+2}} \\ &\leq \mathscr{C}_{\rm shift} K^2 \|\boldsymbol{r}_\ell\|_{\boldsymbol{\mathcal{H}}^{\ell+2}} \leq \mathscr{C}_{\rm shift}^2 K^2 \ell_\Omega \|\boldsymbol{\nabla} \times \boldsymbol{r}_\ell\|_{\boldsymbol{\mathcal{H}}^{\ell+1}},\end{aligned}$$

and the general case follows by induction. □

A.8. **Approximation factor.** We are now ready to provide an upper bound for the approximation factor $\gamma_{\rm ba,E}$.

Theorem A.5 (Approximation factor)**.** *Assume that $\mathscr{C}_{\rm shift}(\omega h/c) \leq 1/2$, then the following estimate holds true*

$$\gamma_{\rm ba,E} \leq \mathscr{C}_{\rm i} \left(2\sqrt{2} \mathscr{C}_{\rm shift} \frac{\omega h}{c} + \sqrt{1 + 2\gamma_{\rm s,E}^2} \left(\mathscr{C}_{\rm shift} \frac{\omega h}{c} \right)^{k+1} \right).$$

Proof. Let be $\ell \geq 1$ and $j = 1, \ldots, \ell$. Recalling (2.13a) and the finite expansion for $\boldsymbol{e}$, it is sufficient to provite upper bounds for the high order interpolation error of $\boldsymbol{e}_j$ and $\boldsymbol{r}_\ell$. For $\boldsymbol{e}_j$, the definition of K and (A.10) imply that

$$K^{j+1} \|\boldsymbol{e}_j - \mathcal{R}_h \boldsymbol{e}_j\|_{\boldsymbol{\mathcal{H}}^0} \leq \mathscr{C}_{\rm i} K^{j+1} \frac{h^{j+1}}{\ell_\Omega^{j+1}} \|\boldsymbol{e}_j\|_{\boldsymbol{\mathcal{H}}^{j+1}} = \mathscr{C}_{\rm i} \left(\frac{\omega h}{c} \right)^{j+1} \|\boldsymbol{e}_j\|_{\boldsymbol{\mathcal{H}}^{j+1}} \leq \mathscr{C}_{\rm i} \left(\mathscr{C}_{\rm shift} \frac{\omega h}{c} \right)^{j+1} \|\boldsymbol{g}\|_{\boldsymbol{\mathcal{H}}^0},$$

and

$$\ell_\Omega K^j \|\boldsymbol{\nabla} \times (\boldsymbol{e}_j - \mathcal{R}_h \boldsymbol{e}_j)\|_{\boldsymbol{\mathcal{H}}^0} \leq \mathscr{C}_{\rm i} K^j \frac{h^j}{\ell_\Omega^j} \ell_\Omega \|\boldsymbol{\nabla} \times \boldsymbol{e}_j\|_{\boldsymbol{\mathcal{H}}^j} \leq \mathscr{C}_{\rm i} \left(\mathscr{C}_{\rm shift} \frac{\omega h}{c} \right)^j \|\boldsymbol{g}\|_{\boldsymbol{\mathcal{H}}^0},$$

and since $\mathscr{C}_{\rm shift}(\omega h/c) \leq 1$, we get

$$K^j \left(K^2 \|\boldsymbol{e}_j - \mathcal{R}_h \boldsymbol{e}_j\|_{\boldsymbol{\mathcal{H}}^0}^2 + \ell_\Omega^2 \|\boldsymbol{\nabla} \times (\boldsymbol{e}_j - \mathcal{R}_h \boldsymbol{e}_j)\|_{\boldsymbol{\mathcal{H}}^0}^2 \right)^{1/2} \leq \mathscr{C}_{\rm i} \sqrt{2} \left(\mathscr{C}_{\rm shift} \frac{\omega h}{c} \right)^j \|\boldsymbol{g}\|_{\boldsymbol{\mathcal{H}}^0}.$$

Similarly, for the residual $\boldsymbol{r}_\ell$, we have

$$K \|\boldsymbol{r}_k - \mathcal{R}_h \boldsymbol{r}_k\|_{\boldsymbol{\mathcal{H}}^0} \leq \mathscr{C}_{\rm i} \left(\frac{h}{\ell_\Omega} \right)^{k+1} K \|\boldsymbol{r}_k\|_{\boldsymbol{\mathcal{H}}^{k+1}} \leq \mathscr{C}_{\rm i} \gamma_{\rm s,E} \left(\mathscr{C}_{\rm shift} \frac{\omega h}{c} \right)^{k+1} \|\boldsymbol{g}\|_{\boldsymbol{\mathcal{H}}^0}$$

and

$$\ell_\Omega \|\boldsymbol{\nabla} \times (\boldsymbol{r}_k - \mathcal{R}_h \boldsymbol{r}_k)\|_{\boldsymbol{\mathcal{H}}^0} \leq \mathscr{C}_{\rm i} \left(\frac{h}{\ell_\Omega} \right)^{k+1} \ell_\Omega \|\boldsymbol{\nabla} \times \boldsymbol{r}_k\|_{\boldsymbol{\mathcal{H}}^{k+1}} \leq \mathscr{C}_{\rm i} (1 + \gamma_{\rm s,E}) \left(\mathscr{C}_{\rm shift} \frac{\omega h}{c} \right)^{k+1} \|\boldsymbol{g}\|_{\boldsymbol{\mathcal{H}}^0},$$

and hence

$$K^2 \|\boldsymbol{r}_k - \mathcal{R}_h \boldsymbol{r}_k\|_{\boldsymbol{\mathcal{H}}^0}^2 + \ell_\Omega^2 \|\boldsymbol{\nabla} \times (\boldsymbol{r}_k - \mathcal{R}_h \boldsymbol{r}_k)\|_{\boldsymbol{\mathcal{H}}^0}^2 \leq \mathscr{C}_{\rm i} \sqrt{1 + 2\gamma_{\rm s,E}^2} \left(\mathscr{C}_{\rm shift} \frac{\omega h}{c} \right)^{k+1} \|\boldsymbol{g}\|_{\boldsymbol{\mathcal{H}}^0}.$$

Then, since $\boldsymbol{e} = \sum_{j=1}^k K^j \boldsymbol{e}_j + \boldsymbol{r}_k$ and the above estimates, we obtain

$$\begin{aligned}&K^2 \|\boldsymbol{e} - \mathcal{R}_h \boldsymbol{e}\|_{\boldsymbol{\mathcal{H}}^0}^2 + \ell_\Omega^2 \|\boldsymbol{\nabla} \times (\boldsymbol{e} - \mathcal{R}_h \boldsymbol{e})\|_{\boldsymbol{\mathcal{H}}^0}^2 \\ &\qquad \leq \mathscr{C}_{\rm i} \left(\sqrt{2} \sum_{j=1}^k \left(\mathscr{C}_{\rm shift} \frac{\omega h}{c} \right)^j + \sqrt{1 + 2\gamma_{\rm s,E}^2} \left(\mathscr{C}_{\rm shift} \frac{\omega h}{c} \right)^{k+1} \right) \|\boldsymbol{g}\|_{\boldsymbol{\mathcal{H}}^0}.\end{aligned}$$

Finally, the result follows by

$$\sum_{j=1}^k \left(\mathscr{C}_{\rm shift} \frac{\omega h}{c} \right)^j = \left(\mathscr{C}_{\rm shift} \frac{\omega h}{c} \right) \sum_{j=0}^{k-1} \left(\mathscr{C}_{\rm shift} \frac{\omega h}{c} \right)^j = \left(\mathscr{C}_{\rm shift} \frac{\omega h}{c} \right) \frac{1 - \left(\mathscr{C}_{\rm shift} \frac{\omega h}{c} \right)^k}{1 - \left(\mathscr{C}_{\rm shift} \frac{\omega h}{c} \right)} \leq 2 \mathscr{C}_{\rm shift} \frac{\omega h}{c}.$$

□

Corollary A.6 (Simplified estimate)**.** *Assume that* $\mathscr{C}_{\rm shift}(\omega h/c) \le 1/2$ *and* $\omega \ge \delta$*, then*

$$\gamma_{\rm ba,E} \le C(\Omega,k)\left(\frac{\omega h}{c} + \frac{\omega}{\delta}\left(\frac{\omega h}{c}\right)^{k+1}\right). \tag{A.15}$$

Appendix B. Gradient extraction

Theorem B.1 (Gradient extraction with boundary conditions)**.** *For all* $\boldsymbol{\theta} \in \boldsymbol{\mathcal{H}}_0(\mathbf{curl},\Omega)$*, there exist* $\boldsymbol{\phi} \in \boldsymbol{\mathcal{H}}^1(\Omega) \cap \boldsymbol{\mathcal{H}}_0(\mathbf{curl},\Omega)$ *and* $p \in \mathcal{H}^1_0(\Omega)$ *such that* $\boldsymbol{\theta} = \boldsymbol{\phi} + \boldsymbol{\nabla} p$*, and*

$$\|\boldsymbol{\nabla}\boldsymbol{\phi}\|_\Omega \le \mathscr{C}_{\rm e,\Omega}\|\boldsymbol{\nabla}\times\boldsymbol{\theta}\|_\Omega, \qquad \|\boldsymbol{\nabla} p\|_\Omega \le \mathscr{C}_{\rm e,\Omega}\|\boldsymbol{\theta}\|_\Omega,$$

where $\mathscr{C}_{\rm e,\Omega} := 2 + \inf_{\mathcal{B}} \mathscr{C}_{\rm e,\mathcal{B}}$ *with the infinimum is taken over all open balls* $\mathcal{B} \supset \overline{\Omega}$*, and*

$$\mathscr{C}_{\rm e,\mathcal{B}} := \sup_{\substack{r\in H^2(\mathcal{B}\setminus\overline{\Omega}) \\ \|\boldsymbol{\nabla}^2 r\|_\Omega = 1}} \inf_{\substack{q\in H^2(\mathcal{B}) \\ q|_{\mathcal{B}\setminus\overline{\Omega}} = r|_{\mathcal{B}\setminus\overline{\Omega}}}} \|\boldsymbol{\nabla}^2 q\|_\Omega.$$

Proof. Let $\mathcal{B} \supset \overline{\Omega}$ be an open ball containing the computational domain. For the sake of simplicity, we also introduce $G := \mathcal{B}\setminus\overline{\Omega}$. Consider $\boldsymbol{\theta}_\Omega \in \boldsymbol{\mathcal{H}}_0(\mathbf{curl},\Omega)$ and set $\boldsymbol{\vartheta}_\Omega := \boldsymbol{\nabla}\times\boldsymbol{\theta}_\Omega \in \boldsymbol{\mathcal{H}}_0(\mathrm{div}^0,\Omega)$. Because of the boundary conditions satisfied by $\boldsymbol{\vartheta}_\mathcal{B}$, the extension of $\boldsymbol{\vartheta}_\Omega$ by $\boldsymbol{o}$ to $\mathcal{B}$ belongs to $\boldsymbol{\mathcal{H}}_0(\mathrm{div}^0,\mathcal{B})$. As a result, there exists a unique element $\boldsymbol{\Theta}_\mathcal{B} \in \boldsymbol{\mathcal{H}}_0(\mathbf{curl},\mathcal{B}) \cap \boldsymbol{\mathcal{H}}(\mathrm{div}^0,\mathcal{B})$ such that

$$(\boldsymbol{\nabla}\times\boldsymbol{\Theta}_\mathcal{B}, \boldsymbol{\nabla}\times\boldsymbol{v}_\mathcal{B})_\mathcal{B} = (\boldsymbol{\vartheta}_\mathcal{B}, \boldsymbol{v}_\mathcal{B})_\mathcal{B} \tag{B.1}$$

for all $\boldsymbol{v}_\mathcal{B} \in \boldsymbol{\mathcal{H}}_0(\mathbf{curl},\mathcal{B}) \cap \boldsymbol{\mathcal{H}}(\mathrm{div}^0,\mathcal{B})$. The existence and uniqueness of $\boldsymbol{\Theta}$ follows from Weber's inequality [26, Lemma 3.4], which ensures that the sesquilinear form in the left-hand side is coercive (observe that $\mathcal{B}$ is in particular simply connected). We now define $\boldsymbol{\psi}_\mathcal{B} := \boldsymbol{\nabla}\times\boldsymbol{\Theta}_\mathcal{B} \in \boldsymbol{\mathcal{H}}(\mathbf{curl},\Omega)$. Observe that then (B.1) actually defines the weak rotation of $\boldsymbol{\psi}_\mathcal{B}$, so that

$$\boldsymbol{\nabla}\times\boldsymbol{\psi}_\mathcal{B} = \boldsymbol{\vartheta}_\mathcal{B}. \tag{B.2}$$

Selecting the test function $\boldsymbol{v}_\mathcal{B} := \boldsymbol{\Theta}_\mathcal{B}$ in (B.1), we have

$$\|\boldsymbol{\psi}_\mathcal{B}\|^2_\mathcal{B} = \|\boldsymbol{\nabla}\times\boldsymbol{\Theta}_\mathcal{B}\|^2_\mathcal{B} = (\boldsymbol{\vartheta}_\mathcal{B}, \boldsymbol{\Theta}_\mathcal{B})_\mathcal{B} = (\boldsymbol{\nabla}\times\boldsymbol{\theta}_\Omega, \boldsymbol{\Theta}_\mathcal{B})_\Omega.$$

Since $\boldsymbol{\theta}_\mathcal{B} \in \boldsymbol{\mathcal{H}}_0(\mathbf{curl},\Omega)$, integration by parts shows that

$$\|\boldsymbol{\psi}_\mathcal{B}\|^2_\mathcal{B} = (\boldsymbol{\theta}_\Omega, \boldsymbol{\nabla}\times\boldsymbol{\Theta}_\mathcal{B})_\Omega = (\boldsymbol{\theta}_\Omega, \boldsymbol{\psi}_\mathcal{B})_\Omega,$$

from which we conclude that

$$\|\boldsymbol{\psi}_\mathcal{B}\|_\mathcal{B} \le \|\boldsymbol{\theta}_\Omega\|_\Omega. \tag{B.3}$$

Now, we have $\boldsymbol{\psi}_\mathcal{B} \in \boldsymbol{\mathcal{H}}(\mathbf{curl},\mathcal{B}) \cap \boldsymbol{\mathcal{H}}_0(\mathrm{div},\mathcal{B})$, and Corollary 3.6 of [26] shows that $\boldsymbol{\psi}_\mathcal{B} \in \boldsymbol{\mathcal{H}}^1(\Omega)$ with

$$\|\boldsymbol{\nabla}\boldsymbol{\psi}_\mathcal{B}\|_\mathcal{B} = \|\boldsymbol{\nabla}\times\boldsymbol{\psi}_\mathcal{B}\|_\mathcal{B} = \|\boldsymbol{\vartheta}_\mathcal{B}\|_\mathcal{B} = \|\boldsymbol{\nabla}\times\boldsymbol{\theta}_\mathcal{B}\|_\Omega. \tag{B.4}$$

Let us respectively denote by $\boldsymbol{\vartheta}_G$ and $\boldsymbol{\psi}_G$ the restrictions of $\boldsymbol{\vartheta}_\mathcal{B}$ and $\boldsymbol{\psi}_\mathcal{B}$ to G. We observe that $\boldsymbol{\vartheta}_\mathcal{B}$ being the extension of $\boldsymbol{\vartheta}_\Omega$ by $\boldsymbol{o}$, we have $\boldsymbol{\vartheta}_G = \boldsymbol{o}$. It follows that $\boldsymbol{\nabla}\times\boldsymbol{\psi}_G = \boldsymbol{\nabla}\times\boldsymbol{\theta}_G = \boldsymbol{o}$, and therefore $\boldsymbol{\psi}_G = \boldsymbol{\nabla} p_G$ for some $q_G \in H^1(G)$. Let us further remark that since $\boldsymbol{\psi}_G \in \boldsymbol{\mathcal{H}}^1(G)$, we also have $q_G \in H^2(G)$, with $|q_G|_{H^2(G)} \le \|\boldsymbol{\nabla}\times\boldsymbol{\theta}_\mathcal{B}\|_\Omega$. We then select $q_\mathcal{B} \in \mathcal{H}^2(\mathcal{B})$ such that $q_\mathcal{B} = q_G$ on G and

$$\|\boldsymbol{\nabla}(\boldsymbol{\nabla} q_\mathcal{B})\|_\mathcal{B} \le \mathscr{C}_{\rm e,\mathcal{B}}|q_G|_{H^2(G)} \le \mathscr{C}_{\rm e,\mathcal{B}}\|\boldsymbol{\nabla}\times\boldsymbol{\theta}_\Omega\|_\Omega. \tag{B.5}$$

We then define $\boldsymbol{\phi}_\Omega := \boldsymbol{\psi}_\Omega - \boldsymbol{\nabla} q_\Omega$, where $\boldsymbol{\psi}_\Omega$ and q_Ω are the respective restrictions of $\boldsymbol{\psi}_\mathcal{B}$ and $q_\mathcal{B}$ to Ω. Since both $\psi_\mathcal{B}, \boldsymbol{\nabla} q_\mathcal{B} \in \boldsymbol{\mathcal{H}}(\mathbf{curl},\mathcal{B})$, continuity of the tangential trace implies that

$$\boldsymbol{\phi}_\Omega \times \boldsymbol{n}_\Omega = (\boldsymbol{\psi}_\Omega - \boldsymbol{\nabla} q_\Omega)\times\boldsymbol{n}_\Omega = (\boldsymbol{\psi}_G - \boldsymbol{\nabla} q_G)\times\boldsymbol{n}_\Omega = \boldsymbol{o},$$

so that $\boldsymbol{\phi}_\Omega \in \boldsymbol{\mathcal{H}}_0(\mathbf{curl},\Omega)$. In addition, recalling (B.4) and (B.5), we have $\boldsymbol{\phi}_\Omega \in \mathcal{H}^1(\Omega)$ with

$$\|\boldsymbol{\nabla}\boldsymbol{\phi}_\Omega\|_\Omega \le \|\boldsymbol{\nabla}\boldsymbol{\psi}_\mathcal{B}\|_\Omega + \|\boldsymbol{\nabla}(\boldsymbol{\nabla} q_\mathcal{B})\|_\Omega \le (1 + \mathscr{C}_{\rm e,\mathcal{B}})\,\|\boldsymbol{\nabla}\times\boldsymbol{\theta}\|_\Omega. \tag{B.6}$$

Finally, recalling (B.2), we have $\boldsymbol{\nabla}\times\boldsymbol{\phi}_\Omega = \boldsymbol{\nabla}\times\boldsymbol{\psi}_\Omega = \boldsymbol{\nabla}\times\boldsymbol{\theta}_\Omega$, and it follows that

$$\boldsymbol{\theta}_\Omega - \boldsymbol{\phi}_\Omega = \boldsymbol{\nabla} p_\Omega \tag{B.7}$$

for some $p_\Omega \in H^1_0(\Omega)$. But then, we have

$$\|\boldsymbol{\nabla} p_\Omega\| \leq \|\boldsymbol{\theta}_\Omega\|_\Omega + \|\boldsymbol{\psi}_\Omega\|_\Omega \leq (2 + \mathscr{C}_{\mathrm{e},\mathcal{B}})\, \|\boldsymbol{\theta}_\Omega\|_\Omega, \tag{B.8}$$

where we employed (B.3). The proof now follows from (B.6), (B.7) and (B.8). □

Since Ω is assumed to be Lipschitz, there exists an extension operator $E : \boldsymbol{\mathcal{H}}(\mathbf{curl}, \Omega) \to \boldsymbol{\mathcal{H}}(\mathbf{curl}, \mathbb{R}^3)$ such that $E(\boldsymbol{v})|_\Omega = \boldsymbol{v}$ and

$$\|E(\boldsymbol{v})\|_{\mathbb{R}^3} \leq \widetilde{\mathscr{C}}_{\mathrm{e},\Omega} \|\boldsymbol{v}\|_\Omega, \qquad \|\boldsymbol{\nabla} \times E(\boldsymbol{v})\|_{\mathbb{R}^3} \leq \widetilde{\mathscr{C}}_{\mathrm{e},\Omega} \|\boldsymbol{\nabla} \times \boldsymbol{v}\|_\Omega,$$

for all $\boldsymbol{v} \in \boldsymbol{\mathcal{H}}(\mathbf{curl}, \Omega)$, where $\widetilde{\mathscr{C}}_{\mathrm{e},\Omega}$ only depends on the Lipschitz constant of Ω. Such extension operator may be constructed using a partition of unity argument, local flattening of the boundary, reflections, cutoff functions and Piola mappings.

Theorem B.2 (Gradient extraction without boundary conditions)**.** *For all $\boldsymbol{\theta} \in \boldsymbol{\mathcal{H}}(\mathbf{curl}, \Omega)$, there exist $\boldsymbol{\phi} \in \boldsymbol{\mathcal{H}}^1(\Omega)$ and $p \in \mathcal{H}^1(\Omega)$ such that $\boldsymbol{\theta} = \boldsymbol{\phi} + \boldsymbol{\nabla} p$, and*

$$\|\boldsymbol{\nabla} \boldsymbol{\phi}\|_\Omega \leq \widetilde{\mathscr{C}}_{\mathrm{e},\Omega} \|\boldsymbol{\nabla} \times \boldsymbol{\theta}\|_\Omega, \qquad \|\boldsymbol{\nabla} p\|_\Omega \leq \widetilde{\mathscr{C}}_{\mathrm{e},\Omega} \|\boldsymbol{\theta}\|_\Omega.$$

Proof. Let $\boldsymbol{\theta} \in \boldsymbol{\mathcal{H}}(\mathbf{curl}, \Omega)$. We introduce p as the unique element of $H^1(\mathbb{R}^3)$ such that

$$(\boldsymbol{\nabla} p, \boldsymbol{\nabla} q)_{\mathbb{R}^3} = (E(\boldsymbol{\theta}), \boldsymbol{\nabla} q)_{\mathbb{R}^3}$$

for all $q \in H^1(\mathbb{R}^3)$. Then, it is clear that $\boldsymbol{\phi} := E(\boldsymbol{\theta}) - \boldsymbol{\nabla} p \in \boldsymbol{\mathcal{H}}(\mathbf{curl}, \mathbb{R}^3) \cap \boldsymbol{\mathcal{H}}(\mathrm{div}^0, \mathbb{R}^3)$. Standard Fourier transform arguments then show that $\boldsymbol{\phi} \in \boldsymbol{\mathcal{H}}^1(\mathbb{R}^3)$ with

$$\|\boldsymbol{\nabla} \boldsymbol{\phi}\|_{\mathbb{R}^3} = \|\boldsymbol{\nabla} \times \boldsymbol{\phi}\|_{\mathbb{R}^3} = \|\boldsymbol{\nabla} \times E(\boldsymbol{\theta})\|_{\mathbb{R}^3} \leq \widetilde{\mathscr{C}}_{\mathrm{e},\Omega} \|\boldsymbol{\nabla} \times \boldsymbol{\theta}\|_\Omega.$$

On the other hand, we have $\|\boldsymbol{\nabla} p\|_{\mathbb{R}^3} \leq \|E(\boldsymbol{\theta})\|_{\mathbb{R}^3} \leq \widetilde{\mathscr{C}}_{\mathrm{e},\Omega} \|\boldsymbol{\theta}\|_\Omega$, and we infer that the decomposition $\boldsymbol{\theta} = \boldsymbol{\phi}|_\Omega + \boldsymbol{\nabla}(p|_\Omega)$, fulfils the requirements of the theorem. □

References

1. R. Adams and J. Fournier, Sobolev spaces, Academic Press, 2003.
2. M. Ainsworth and J. T. Oden, A posteriori error estimation in finite element analysis, Wiley, 2000.
3. D. N. Arnold, F. Brezzi, B. Cockburn, and L. D. Marini, Unified analysis of discontinuous Galerkin, methods for elliptic problems, SIAM J. Numer. Anal. **39** (2002), no. 5, 1749–1779.
4. R. Beck, R. Hiptmair, R. H. W. Hoppe, and B. Wohlmuth, Residual based a posteriori error estimators for eddy current computation, ESAIM Math. Model. Numer. Anal. **34** (2000), 159–182.
5. A. Bendali, Numerical analysis of the exterior boundary value problem for the time-harmonic Maxwell equations by a boundary finite element method. Part 2: the discrete problem, Math. Comp. **43** (1984), no. 127, 47–68.
6. J. P. Bérenger, A perfectly matched layer for the absortion of electromagnetics waves, J. Comput. Phys. **114** (1994), 185–200.
7. ———, Three-dimensional perfectly matched layer for the absorption of electromagnetic waves, J. Comput. Phys. **127** (1996), 363–379.
8. A. Bonito, J.-L. Guermond, and F. Luddens, Regularity of the Maxwell equations in heterogeneous media and Lipschitz domains, J. Math. Anal. Appl. **408** (2013), 498–512.
9. A. Bonito and R. H. Nochetto, Quasi-optimal convergence rate of an adaptive discontinuous Galerkin method, SIAM J. Numer. Anal. **48** (2010), no. 2, 734–771.
10. T. Chaumont-Frelet, Mixed finite element discretization of acoustic Helmholtz problems with high wavenumbers, Calcolo **56** (2019), no. 46.
11. T. Chaumont-Frelet, A. Ern, and M. Vohralík, On the derivation of guaranteed and p-robust a posteriori error estimates for the Helmholtz equation, submitted, preprint hal-02202233, 2019.
12. T. Chaumont-Frelet and S. Nicaise, High-frequency behaviour of corner singularities in Helmholtz problems, ESAIM Math. Model. Numer. Anal. **5** (2018), 1803–1845.
13. ———, Wavenumber explicit convergence analysis for finite element discretizations of general wave propagation problems, IMA J. Numer. Anal. **40** (2020), 1503–1543.
14. T. Chaumont-Frelet, S. Nicaise, and D. Pardo, Finite element approximation of electromagnetic fields using nonfitting meshes for Geophysics, SIAM J. Numer. Anal. **56** (2018), 2288–2321.
15. P. G. Ciarlet, The finite element method for elliptic problems, SIAM, 2002.
16. M. Costabel, M. Dauge, and S. Nicaise, Singularities of Maxwell interface problems, ESAIM Math. Model. Numer. Anal. **33** (1999), no. 3, 627–649.
17. L. Demkowicz, Computing with *hp*-adaptive finite elements, vol. 1, Wiley, 2006.
18. C. Dobrzynski, MMG3D: User guide, Tech. Report 422, Inria, 2012.
19. R. C. Dorf, Electronics, power electronics, optoelectronics, microwaves, electromagnetics and radar, Taylor & Francis, 2006.

20. W. Dörfler, A convergent adaptive algorithm for Poisson's equation, SIAM J. Numer. Anal. **33** (1996), no. 3, 1106–1124.
21. W. Dörfler and S. Sauter, A posteriori error estimation for highly indefinite Helmholtz problems, Comput. Meth. Appl. Math. **13** (2013), 333–347.
22. A. Ern and J.-L. Guermond, Finite element quasi-interpolation and best approximation, ESAIM Math. Model. Numer. Anal. **51** (2017), 1367–1385.
23. ———, Analysis of the edge finite element approximation of the maxwell equations with low regularity solutions, Comp. Math. Appl. **75** (2018), 918–932.
24. X. Feng, P. Lu, and X. Xu, A hybridizable discontinuous Galerkin method for the time-harmonic Maxwell equations with high wave number, Comput. Methods Appl. Math. **16** (2016), no. 3, 429–445.
25. S. V. Gaponenko, Introduction to nanophotonics, Cambridge University Press, 2010.
26. V. Girault and P. A. Raviart, Finite element methods for Navier-Stokes equations: theory and algorithms, Springer-Verlag, 1986.
27. D. J. Griffiths, Introduction to Electrodynamics, Prentice Hall, 1999.
28. J. S. Hesthaven and T. Warburton, Nodal high-order methods on unstructured grids. Part I. Time-domain solution of Maxwell's equations, J. Comput. Phys. **181** (2002), 1266–1288.
29. L. Li, S. Lanteri, and R. Perrussel, A hybridizable discontinuous Galerkin method combined to a schwarz algorithm for the solution of 3d time-harmonic Maxwell's equations, J. Comput. Phys. **256** (2014), 563–581.
30. J. M. Melenk and S. Sauter, Wavenumber explicit convergence analysis for Galerkin discretizations of the Helmholtz equation, SIAM J. Numer. Anal. **49** (2011), no. 3, 1210–1243.
31. J. M. Melenk and S. A. Sauter, Wavenumber-explicit *hp*-FEM analysis for Maxwell's equations with transparent boundary conditions, Found. Comp. Math., in press (2020).
32. P. Monk, A posteriori error indicators for Maxwell's equations, J. Comput. Appl. Math. **100** (1998), 173–190.
33. P. Monk, Finite element methods for Maxwell's equations, Oxford science publications, 2003.
34. J. C. Nédélec, Mixed finite elements in $\mathbb{R}^3$, Numer. Math. **35** (1980), 315–341.
35. ———, A new family of mixed finite elements in $\mathbb{R}^3$, Numer. Math. **50** (1986), 57–81.
36. N. C. Nguyen, J. Peraire, and B. Cockburn, Hybridizable discontinuous Galerkin methods for the time-harmonic Maxwell's equations, J. Comput. Phy. **230** (2011), 7151–7175.
37. S. Nicaise and E. Creusé, A posteriori error estimation for the heterogeneous Maxwell equations on isotropic and anisotropic meshes, Calcolo **40** (2003), 249–271.
38. S. Nicaise and J. Tomezyk, Convergence analysis of a *hp*-finite element approximation of the time-harmonic Maxwell equations with impedance boundary conditions in domains with an analytic boundary, submitted, preprint hal-02063271, 2019.
39. I. Perugia and D. Schötzau, The *hp*-local discontinuous galerkin method for low-frequency time-harmonic Maxwell equations, Math. Comp. **72** (2003), 1179–1214.
40. P. Russer, Electromagnetics, microwave circuit and antenna design for communications engineering, Artech house, 2006.
41. S. Sauter and J. Zech, A posteriori error estimation of *hp*-dg finite element methods for highly indefinite Helmholtz problems, SIAM J. Numer. Anal. **53** (2015), 2414–2440.
42. R. Verfürth, A posteriori error estimation and adaptive mesh-refinement techniques, J. Comput. Appl. Math. **50** (1994), 67–83.
43. J. Viquerat, Simulation of electromagnetic waves propagation in nano-optics with a high-order discontinuous Galerkin time-domain method, Ph.D. thesis, Université Nice Sophia-Antipolis and Inria project-team Nachos, 2015.
44. K. Yee, Numerical solution of initial boundary value problems involving Maxwell's equations in isotropic media, IEEE Trans. Antennas Propag. **16** (1966), 302–307.
45. L. Zhong, L. Chen, S. Shu, G. Wittum, and J. Xu, Convergence and optimality of adaptive edge finite element methods for time-harmonic Maxwell equations, Math. Comp. **81** (2012), 623–642.
46. L. Zhong, S. Shu, G. Wittum, and J. Xu, Optimal error estimates for Nédélec edge elements for time-harmonic Maxwell's equations, J. Comp. Math. **27** (2009), no. 5, 563–572.